SHAPE OPTIMIZATION

FOR

BEAM STRUCTURAL DESIGN

A Dissertation
Presented To
the Faculty of the Graduate School
University of Missouri-Columbia

In Partial Fulfillment
Of The Requirements For
The Degree Of
Doctor Of Philosophy

---

by

HSIENDER LEE

Dr. Eric Sandgren Dissertation Supervisor

August, 1988

DEDICATION

To my parents

ACKNOWLEDGEMENTS

There are many people who has contributed significantly to this rearch and who have been very supportive throughout my years at the University of Missouri. I should like to express my sincere gratitude and appreciation to them.

First, and certainly most important, must be my advisor, Dr. Eric Sandgren, without whom I would not have had the opportunity to pursue this project. His guidance, counseling, and support throughout my entire graduate program were very essential.

My committee members, Dr. Paul Braisted, Dr. Uee Wan Cho, Dr. Mohamed El-sayed, and especially my second and third readers, Dr. Roger Duffield and Dr. Harold Salane have given me guidance and inspiration during the research and through the completion of this dissertation.

Finally, I would like to express my deep appreciation to my wife, Sheng-Mei for her understanding, sacrifice and support in helping achieve my goals. Also, I would like to express my gratitude to my parents for their high expectations and moral support motivated me to accomplish this work.

TABLE OF CONTENTS

LIST OF FIGURES

FIGURE

LIST OF TABLES

TABLES

CHAPTER I

INTRODUCTION

1.1 Introduction

Optimization is concerned with achieving the best outcome of a given objective while satisfying certain restrictions. The central purpose of structural analysis is to predict the behavior of known structural configurations which are subject to known distributions of specified loads, displacements, and temperatures. As the engineers were able to perform structural design, it was natural to introduce optimization schemes into structural analysis. Design optimization provides not only savings in structural weight and cost but also allows sensitivity studies which provide valuable information about the design.

Engineering design optimization is a fundamental objective of virtually every engineer who strives to create a component, device, or system to meet a need. To fulfill this objective, engineers must have organized methods tailored to the special features and needs of these fields of engineering design. Thus, an applicable method of optimal design for finite dimensional optimization and a nonlinear mathematical programming method will be presented in this

dissertation. Also because the finite element method is the principal modeling method, it is incorporated as an integral part of optimal design method. This is difficult to accomplish with a commercially available finite element code.

It is very important to realize that engineering design optimization and engineering analysis are fundamentally different in nature. In analysis, one is generally assured that a solution exists and the numerical methods used are stable. In optimal design, on the other hand, existence of even a nominal design satisfying the constraints is not assured, much less the existence of an optimum design. Even when an optimum design exists, numerical methods for its solution are often quite sensitive to initial estimates and require considerable computational art to achieve iterative convergence. These properties will be observed again and again in this dissertation.

In the structural optimization of discrete structures, much of the work has been concerned with truss problems [1,2,3,4,5,6,7,8,9]. Some work has also been reported for frame structures[10,11,12]. However, the vast majority of this effort was almost exclusively focused on member sizing(fixed-shape) problems where the design variables are the cross sectional area of the truss members. Relatively little effort has been devoted to the configuration problem where the node positions in the finite element structure are treated as design variables, and virtually no effort has

been devoted to the topological problem of choosing the number of members and their connectivity in the structure.

The beam member is the most common and an important structural system for a variety of industrial applications. In this dissertation, applications of the finite element method and nonlinear mathematical programming techniques for the optimum design of beam frame structures subject to sizing changes, configurational changes and topological changes is presented. These features are required in order to produce a "true" structural design/optimization tool. Anything less will simply allow the user to "fine tune" an existing design.

In the context of shape optimization, the geometric design variables in discrete structures are the coordinates of node locations(joints) in the structure. The shape geometry can be optimized through the coordinate change or use of parametric cubic curves. For beam-type frames, this means node locations are allowed to vary. Commercial general purpose finite element codes do not appear to be particular useful in configuration design because of rigid input and output formats and no way to access intermediate information. This creates a need for a special purpose code for beam finite elements to calculate the static response. The developed beam elements will meet the particular requirements in configuration design and do not have the tradeoffs associated with a commercial general purpose finite element package.

For this research project, it was decided to develop a finite element code including tubular circular, tubular rectangular and symmetric open channel cross sections for sizing, configurational and topological design for three dimensional beam frame structures; and to also develop an efficient algorithm based on combining a finite element analysis method and a nonlinear mathematical programming approach subject to multiple loading conditions and displacement and stress constraints.

In Chapter 2, an overview of structural optimization will be presented as well as a literature review covering the development and application of structural optimization. The potential for growth in the area of structural optimization is also discussed.

In Chapter 3 some general topics related to the optimization of beam frame structural systems are discussed. Approaches for finite element analysis and optimization algorithms are presented.

In Chapter 4 the gradient computations required for the development of structural optimization are presented. The calculation of sensitivities with respect to static response is reviewed.

Chapter 5 introduces the topic of geometric modeling for structural optimization and topological design, and presents the shape optimization for beam frame design.

Chapter 6 contains the research results regarding the application to beam structures subject to sizing, shape

geometry and topological changes.

Chapter 7 presents the conclusions of the research and recommendations for future studies.

1.2 Objective and Scope of This Research

Schmit[13] pointed out the scope of the structural optimization field is so broad that there are, unfortunately, many important topics and associated key ideas that have not been touched. This dissertation will address several of the untouched areas required for the development of a useful modern structural optimization methodology. The objective of this research is to investigate the applicability of geometric optimization and topological optimization in the beam structure by developing innovative ways of merging finite element analysis and mathematical programming algorithms.

The basic methodology of this research is to develop a beam finite element program, provide for an analysis capability for beam type structures using the finite element procedure, and couple this procedure with a design optimization algorithm to search for the optimum design. The major goal is to design, implement and test a structural optimization algorithm subject to sizing, shape geometry and topological design for specific application to three-dimensional frame structures using a beam finite element.

The focus of the structural optimization developments in this research is to create an interface between the structural analysis and optimization algorithms in a very effective way. This includes the development of strategies for enhancing the efficiency of the optimization algorithms and providing the rational heuristic search technique to guide the optimization process at different levels to progress toward the topological optimum. The approach to geometric modeling and topologic design will be addressed in this dissertation. The end result will be a structural optimization code which extends the capabilities of existing codes. The algorithm will also serve as a base for future research in the area.

1.3 REFERENCES

[1]Kirth, U. and D. Benardout, "Optimal Design of Elastic Trusses by Approximate Equilibrium," Comput. Meth. Appl. Mech. Eng., Vol. 22, No. 3, June 1980, pp.347-359.

[2]Lapay, W. S. and G. G. Goble, "Optimum Design of Trusses for Ultimate Loads," J. Struct. Div. ASCE, Vol. 97, No.ST1, January 1971, pp.157-174.

[3]Sheu, C. Y. and L. A. Schmit, "Minimum Weight Design of Elastic Redundant Trusses Under Multiple Static Loading Conditions," AIAA J., Vol. 10, No. 2, February 1972, pp.155-162.

[4]Farshi, B. and L. A. Schmit, "Minimum Weight Design of Stress Limited Trusses," J. Struct. Div. ASCE, Vol. 100, No. ST1, January 1974, pp.97-107.

[5]Dobbs, M. W. and R. B. Nelson, "Application of Optimality Criteria to Automated Structural Design," AIAA J., Vol. 14, No. 10, 1976, pp.1435-1443.

[6]Venkayya, V. B., "Design of Optimum Structures," Computers and Structures, Vol. 1, No.1-2, 1971, pp.265-309.

[7]Schmit, L. A. and B. Farshi, "Some Approximation Concepts for Structural Synthesis," AIAA Journal, Vol. 12, No. 5, 1974, pp. 692-699.

[8]Fox, R. L. and M. Miura, "An Approximate Analysis Technique for Design Calculation, "AIAA J., Vol. 9, No. 1, 1971, pp.177-179.

[9]Lipson, S. L. and L. B. Gwinn, "Discrete Sizing of Trusses for Optimal Geometry," Proc. Am. Soc. of Civil Engineers, 103(ST5), 1977, pp.1031-1046.

[10]Horne, M. R. and L. J. Morris, "Optimum Design of Multistory Rigid Frames," Optimum Structure Design, Edited by R. H. Gallagher and O. C. Zienkiewicz, John Wiley & Sons, 1973.

[11]Kavlie, D. and J. Moe, "Automated Design of Frame Structures," J. Struct. Div., ASCE, VOL. 97, No. ST1, January 1971, pp.33-62.

[12]Govil, A. K., J. S. Arora and E. J. Haug, "Optimal Design of Frames with Substructuring," Computers and Structures, Vol. 12, 1980, pp.1-10.

[13]Schmit, L. A. Jr, "Structural optimization -- Some Key Ideas and Insights", New Direction in Optimum Structural Design, Edited by E. Atrek, R. H. Gallagher, K. M. Ragsdell, and O. C. Zienkiewicz, John Wiley & Sons Ltd., 1984, pp.1-46.

CHAPTER II

LITERATURE REVIEW

2.1 An Overview of Structural Optimization

Structural optimization began about twenty years ago with weight minimization. The importance of the minimum weight design of structures was first recognized in the aerospace industry where aircraft structural designs are controlled more by weight than by cost considerations. In ship design, the reduction of structural weight directly influences not only the cost of the construction but also the cost of the fuel required to power them. In other industries dealing with civil, mechanical and automotive engineering systems, cost may be the primary consideration although the weight of the system does directly affect the cost.

A growing realization of the scarcity of raw materials and a rapid depletion of our conventional sources of energy is being translated into a demand which emphasizes the need for the engineers of today to be cognizant of the techniques for weight and cost optimization of structures. In addition to the objectives of cost and weight, there are

objectives still to be developed in areas of efficiency, reliability, performance, or a combination of these.

During the late 40's and early 50's the development of mathematical programming techniques provided the impetus to the application of optimization methods in engineering design. In the late fifties and early sixties the advent of high speed electronic computers had a profound effect on structural analysis solution procedures. Of particular importance is the emergence of the finite element method for the solution of continuum mechanics problems.

In 1960 Schmit[1] was the first to offer a comprehensive statement of the use of mathematical programming techniques to solve the nonlinear inequality constrained problem of designing elastic structures under a multiplicity of loading conditions. Also he proposed coupling finite element analysis and mathematical programming methods for structural design optimization. This work is significant, not only in that it ushered in the era of structural optimization, but also because it offered a new philosophy of engineering design which is only now beginning to be broadly applied. In [2] Schmit provides an excellent historical review of the development of this concept.

However, as the applications became more and more ambitious, the limitations of the mathematical programming methods proved to be too restrictive for practical applications. The elaborate mathematical transformations for

determining travel direction, the sensitivity of the algorithms to step size and the effect of the initial starting point on the solution are only a few of the difficulties encountered in applying mathematical programming methods to practical structural optimization problems. To offset some of these difficulties an intense effort to revive the optimality criteria approach was conducted in 1968. The approach was presented in analytical form by Prager and coworkers[3,4] and in numerical form by Venkayya, Khot, and Reddy[5]. These efforts paid off well as evidenced by the renewed interest in structural optimization and subsequently resulted in very successful optimization schemes.

In 1971 Pope and Schmit[6] made an assessment of mathematical programming methods for structural design. Venkayya[7] derived optimality criteria for generalized stiffness, prescribed displacements, dynamic stiffness and static stability requirements and used the optimality criteria approach for the optimization of structures. In 1973 Gallagher[8] used the fully stressed design(FSD) concept, which was one of the early optimality criteria, to design a minimum weight structure.

In 1974 Berke and Venkayya[9] reviewed the optimality criteria approaches and pointed out the advantages and shortcoming of these approaches. It was also noted that the computational aspects of optimality criteria approaches are more in tune with the requirements of large scale structural

optimization. Moses[10] gave an update of the development in mathematical programming methods for structural optimization. Stroud[11] presented a comprehensive state of the art survey of automated structural design with aeroelastic constraints.

During the late 1970's, development continued in both optimality criteria and mathematical programming approaches to structural optimization. In terms of understanding the automated design process, perhaps the most significant work was in the area of reconciling the mathematics of the two basic concepts. The definitive work of Fleury[12,13] and Fleury and Sander[14] offers fundamental insight into the mathematical basis of both approaches and, in fact, shows a common basis in the duality of the original problem statement. This work principally shows that optimality criteria are valid for a mathematically separable problem and, as such, may be viewed as a special case of mathematical programming.

During the early 1980's approximation concepts were combined with the dual method formulation to create a powerful new method for minimum weight design of structural systems[15,16]. This combination has led to a new perspective from which it can be seen that the generalized optimality criteria and mathematical programming approaches have coalesced to the same method. As Fleury[18] shows, "the mathematical programming and optimality criteria approaches are far from being ineluctably opposed, and in fact have

converged to the same method". The inherent difficulties associated with conventional optimality criteria have been resolved by combining approximation concepts and dual methods.

A significant contribution to advancing the state-of-art of structural optimization is design sensitivity analysis. It plays an important role in structural analysis and optimization, since virtually all optimization methods require computation of derivatives of structural response quantities with respect to design variables. In 1979 Arora and Haug[18] presented three fundamentally different approaches to design sensitivity analysis. These approaches have been used extensively in the structural optimization literature. In 1982 Sobieszczanski-Sobieski[19] further extended design sensitivity analysis to provide the necessary coupling between the subsystems of multilevel structural optimization.

2.2 Development and Application of Structural Optimization

The objective of structural optimization is to find values for the design variables of a system that minimize a cost function and satisfy various performance requirements. The quantities describing a structural system that are varied during the optimization procedure are called design variables. The simplest design variables are the cross-sectional dimensions, for example, the cross sectional area

of a structural member, widths, thickness, and the area moments of inertia. Configurational or geometric layout variables can be included during the optimization process, such as the coordinate position of joints in a frame, and the location of the support for a beam. Other design variables considered in a structural system include topology and material selection.

Two philosophically different approaches to structural optimization have been followed in the literature. The first technique is called the numerical optimality criterion method, or indirect method. Most recent optimality criteria methods are based on solving the nonlinear set of equations obtained by applying the Kuhn-Tucker necessary conditions to the original design problem. These equations are solved numerically in an iterative manner until the predetermined optimality criteria are satisfied. Traditionally, the following recurrence formula for calculating optimum values of design variables has been used in these methods:

$$X_j^{(v+1)} = c_j^{(v)} \, X_j^{(v)} \qquad (2\text{-}1)$$

where X_j = jth design variable(1,2,....m)

$c_j^{(v)}$ = multiplier

v = iteration step number

= 0,1,2,.....v

$X^{(0)}$ = starting point

The second basic approach is called the mathematical programming method, and is more direct in nature. In this approach, one starts with a design estimate X and finds a search direction based on the local behavior of cost and constraint functions. A small move in this direction gives an improved design. Thus, a sequence of design modifications is generated that reduces the cost function, while simultaneously satisfying design constraints. Traditionally, the following iterative formula has been used for design improvement in these methods:

$$X^{(v+1)} = X^{(v)} + \delta X^{(v)} \qquad (2\text{-}2)$$

where $\delta X^{(v)}$ is a small change in the design at the vth iteration. There are several procedures for calculating the optimum design change $\delta X^{(v)}$ at each iteration.

The fundamental difference between the two approaches is that in the optimality criteria approach, the Kuhn-Tucker necessary conditions are applied to the original nonlinear optimal design problem, whereas in the mathematical programming approach, a change in the design is computed by applying the Kuhn-Tucker necessary conditions to a reduced problem that is obtained by linearlization of the various functions about the current design point.

In the indirect approach, different numerical methods for solving the nonlinear set of necessary conditions give a variety of optimality criteria methods[8,9,12]. Haug and Arora[20] show that many calculations in the two approaches

are identical and methods of both approaches may be generated from the same information by a very simple modification of logic in the gradient projection algorithm.

In general, different types of constraints require different redesign schemes. Over the past few years there have been developments in both mathematical programming and optimality methods resulting in computer programs which from a solution-time standpoint are equivalent. However, each type of approach retains its advantages for certain types of problems. In addition, recent research has shown that in some cases the methods are essentially identical[13].

Because of its basic generality, we chose to discuss in greater detail the mathematical programming approach. Using this approach, a structural optimization problem can be easily cast in the form which can be handled by a general nonlinear constrained optimization method.

However, any of these methods require many evaluations of the constraints. Each constraint evaluation will require the solution of the finite element problem for displacements, stresses, and natural frequencies. Therefore, when possible it is wise to employ techniques which reduce the number of finite element solutions required.

The literature on the application of structural optimization is so voluminous that is difficult to cite all available references. Structural optimization is reviewed in [21]. Some of the structural optimization papers consider only static cases while others treat both the static and

dynamic case. The type of structures optimized are trusses, frames, plates or a combination. Most of the numerical structural optimization research was almost exclusively focused on sizing design variables. These sizing variables do not require a change in the finite element model of the structure as they are modified. The structural optimization shape design variables which control the geometry of the structure are more complex than sizing design variables.

One of the first treatments of the general problem of selection of the shape of a structure by using the design variables was presented by Zienkiewicz and Campbell[22]. They formulated the shape optimal design problem using a finite element model and treated the location of the nodal points of the finite element model as design variables. They then calculated derivatives of stiffness and load matrices with respect to design parameters, obtained derivatives of structural response measures, and employed sequential linear programming for numerical solution. They presented examples associated with dams and rotating turbine machinery. Ramakrishnan and Francarilla[23] employed a similar finite element formulation, but they used a penalty function method for numerical optimization. Francarilla, Ramakrishnan, and Zienkiewicz[24] employed the finite element method for fillet optimization in order to minimize stress concentration.

The most direct approach in discrete structure shape optimization would be to include both member sizing and

geometric variables in the design variable set. Pedersen[25] used this approach to solve plannar truss structure problems subject to single load condition and stress constraints. Sheppard and Palmer[26] used dynamic programming to design towers of practicable size and complexity. Lipson and Gwin [27] used Box's complex method to design truss structures. The recent work of Imai and Schmit[28] used the Augmented Lagrange Multiplier method to solve the shape optimization problem.

2.3 REFERENCES

[1]Schmit, L. A., "Structural Design by Systematic Synthesis," Proceedings of the 2nd Conference on Electronic Computation, ASCE, 1960, pp.105-122.

[2]Schmit, L. A., "Structural Synthesis-Its Genesis and Development," AIAA Journal, Vol. 19, Oct. 1981, pp. 1249-1263.

[3]Prager, W. and Taylor, J. E., "Problems of Optimal Structural Design", Journal of Applied Mechanics, Vol. 35, No. 1, 1968, pp.102-106.

[4]Prager, W. and Shield, R. T., "Optimal Design of Multi-Purpose Structures", International Journal of Solids and Structures, Vol.4, 1968, pp.469-475.

[5]Venkayya, V.B., Khot,N.S., and Reddy, V.S., "Optimization of Structures Based on the Study of Strain Energy Distribution", AFFDL-TR-68-150, 1968.

[6]Pope, G. G. and Schmit, L. EA.(Eds), "Structural Design Applications of Mathematical Programming Methods", AGARDograph No. 149, 1971.

[7]Venkayya, V. B., "Design of Optimum Structures", Computer & Structure, 1, No. 1-2, pp.265-309.

[8]Gallagher, R. H., "Fully-Stressed Design", Optimum Structural Design, Theory and Applications, Edited by R. H. Gallagher and O. C. Zienkiewicz., John Wiley & Sons Ltd., 1973.

[9]Berke, L. and Venkayya,V. B., "Review of Optimality Criteria Approaches to Structural Optimization", Struc. Opt. Symp., (Ed. L. A. Schmit), ASME Winter Annual Meeting, 1974.

[10]Moses, F., "Mathematical Programming Methods for Structural Optimization", idib.

[11]Stroud, W.J., "Automated Structural Design with Aeroelastic Constraints: A Review and Assessment of the State of the Art", ibid.

[12]Fleury, C., "An Efficient Optimality Criteria Approach in Minimum Weight Design of Elastic Structures", Journal of Computers and Structures, Vol. 11, 1980, pp.163-173.

[13]Fleury, C., "A Unified Approach to Structural Weight Minimization", Computer Methods in Applied Mechanics in Engineering, Vol.20, No.1, 1979, pp.17-38.

[14]Fleury, C. and Sander, G., "Relations Between Optimality Criteria and Mathematical Programming in Structural Optimization", Proceedings of the Symposium on Application Computer Methods in Engineer, University of Southern California, Los Angeles, Aug. 1977, pp.507-520.

[15]Schmit, L. A. and C. Fleury, "Structural Synthesis by Combining Approximation Concepts and Dual Methods", AIAA Journal, 18, pp.1252-1260.

[16]Schmit, L.A. and C. Fleury,"Discrete-Continuous Variable Structural Synthesis Using Dual Methods", AIAA Journal, 18, pp.1515-1524.

[17]Fleury, C., "Reconciliation of Mathematical Programming and Optimality Criteria Approach to Structural Optimization", Foundations of Structural Optimization: A Unified Approach, Edited by A. J. Morris, John Wiley & Sons Ltd., 1982.

[18]Arora, S. J. and Haug E. J., "Methods of Design Sensitivity Analysis in Structural Optimization", AIAA Journal, Vol. 17, No. 9, 1979, pp.970-974.

[19]Sibieszczanski-Sobieski,J., J. F. Barthelemy and K. M. Riley, "Sensitivity of Optimum Design Solutions to Problem Parameters.", AIAA Journal 20, 1982, pp.1291-1299.

[20]Haug, Edward J. and Jasbir S. Arora,"Applied Optimal Design", John Wiley & Sons Ltd., 1979.

[21]Venkayya, Vipperla B.,"Structural Optimization: A Review and Some Recommendations", International Journal for Numerical Methods in Engineer, Vol. 13, pp.203-228, 1978.

[22]Zienkiewicz, O.C. and J.S. Campbell, "Shape Optimization and Sequential Linear Programming", in Optimum Structural Design, Edited by R.H. Gallagher and O.C. Zienkiewicz, John Wiley & Sons Ltd., N.Y., 1973, PP.109-126.

[23]Ramakrishnan, C.V. and A. Francarilla, "Structural Shape Optimization Using Penalty Function", Journal of Structure Mechanics, 3(4), pp.403-432, 1975.

[24]Francarilla,A., C.V. Ramakrishnan and O.C. Zienkiewicz, "Optimization of Shape to Minimum Stress Concentration", Journal of Strain Analysis, 10, pp.63-70, 1975.

[25]Pedersen, P., "On the Minimum Mass Layout of Multi-purpose trusses", Computer & Structures, 2, 4., 1971.

[26]Sheppard, K.H. and A. C. Palmer, "Optimal design of Transmission Tower by Dynamic Programming", Computer & Structure, 2, pp.445-468, 4, 1972.

[27]Lipson, S. L. and L. B. Gwin, "The Complex Method Applied to Optimal Truss Configuration", Computer & Structure, 7, pp.1031-1046, 4, 1977.

[28]Imai, K. and L. A. Schmit, "Configuration Optimization of Trusses", Proc. ASCE, 107, No. ST5, 745-756, 4, 6, 1981.

CHAPTER III

SOME CONSIDERATIONS IN STRUCTURAL OPTIMIZATION

3.1 Introduction

In this chapter, some general topics related to the optimization of beam structural systems are discussed. The general formulation for structural optimization in mathematical form is presented in Sec. 3-2. The method to convert the continuum into equivalent finite elements is described in Sec. 3-3. The combined stress calculation and Von Mises failure criteria is discussed in Sec. 3-4. The optimization technique for structural design is presented in Sec. 3-5.

3.2 The Design Problem

The structural optimization task is presented with basic definitions to provide a common terminology for discussion. The problem sis stated in the context of mathematical programming because this provides the most general form for design.

Mathematically, the design task is to find the set of n

design variables contained in the vector X that will minimize

$$F(X)$$

Subject to

$$g_j(X) \geq 0 \qquad j=1,....m \qquad (3\text{-}1)$$

$$h_k(X) = 0 \qquad k=1,....l \qquad (3\text{-}2)$$

$$X_i^L \leq X_i \leq X_i^U \qquad i=1,.....n \qquad (3\text{-}3)$$

The components X_i of X are referred to as design variables. All of the design parameters which can uniquely determine an engineering design will be written as a function of X according to a specified practical problem. The designer is free to change their values to improve the design. In structural optimization the design variables are typically member cross sectional dimensions and joint coordinates.

The function F(X) is called the objective. While F(X) may be cost, or some measure of performance, it is commonly the weight or volume of the structure.

The functions $g_j(X)$ and $h_k(X)$ represent inequality and equality constraints respectively. Collectively they will determine a feasible region in the N-dimensional design space. Inequality constraints $g_j(X)$ are the response limits imposed on the design. Common inequality constraints include limits on deflection and stress. These are one-sided limits that need not be satisfied with precise equality.

Lower and upper bounds on the design variables are imposed in the form of side constraints, X_i^U and X_i^L, respectively. These could be included in the general inequality constraint set $g_j(X)$ but are usually treated separately because they directly limit the region of search for the optimum.

The parameters n, m, and l correspond to the number of design variables, the number of inequality constraints, and the number of equality constraints respectively.

The above problem statement is quite general and provides a logical format for automated design. However, in order to avoid being unnecessarily abstract, we can, without loss of generality, specialize this to a more common example of structural optimization defined as follows:

$$\text{Minimize} \qquad W = \sum_{i=1}^{NE} P_i A_i L_i \tag{3-4}$$

Subject to

$$1 - \frac{\sigma_{ij}}{\sigma_{allow}} \geq 0 \qquad \begin{matrix} i=1,...NE \\ j=1,.. NLC \end{matrix} \tag{3-5}$$

$$1 - \frac{r_{ijk}}{r_{allow}} \geq 0 \qquad \begin{matrix} i=1,...NJ \\ j=1,...NLC \\ k=1,2,3 \end{matrix} \tag{3-6}$$

$$X_i^L \leq X_i \qquad i=1,..n \tag{3-7}$$

where NE = number of finite element

NJ = number of nodes(joints)

NLC = number of loading condition

K = coordinate direction

n = design variables

Here W is the weight of the structure. The parameters P_i, A_i, and L_i represent the material density, area, and length of the ith finite element in the structural model respectively. For simplicity, only stress and displacement constraints are included in addition to the usual side constraints.

Here σ_{ij} is a computed stress in element i under loading condition j and r_{ijk} is the displacement at joint i under loading condition j in the coordinate direction k. If both upper and lower bounds are imposed on stress and displacement, two constraints result, with the appropriate sign on σ_{allow} and r_{allow}.

Depending on the structural model, we may wish to calculate several stresses per element, in which case an additional subscript would be used on σ. The bounds on σ and r are given as σ_{allow} and r_{allow}, respectively. Conceptually, stress limits may be viewed as local or element level constraints, while displacement(stiffness) limits may be viewed as global or system level constraints. Thus, by including the two types of common design constraints, we retain the salient features of the general structural optimization problem.

The objective function, W, is easily evaluated as the sum of the individual element weights. In order to evaluate the constraints on stress and displacement, we assume that the finite element approach using the displacement method will be used for analysis. Therefore, whenever the constraint functions must be evaluated, an analysis of the structure is required. This entails the solution of the stiffness equation as a subproblem during the optimization process. Note that this actually involves the solution of a set of equality constraints but we treat the analysis as a subproblem for computational convenience.

Having stated the design task in mathematical form, and given the ability via the finite element method to evaluate the objective and constraint functions, it is now necessary to devise a rational numerical search technique to progress toward the optimum. The most common mathematical programming approach is to iteratively update the design by the equation:

$$X^i = X^{i-1} + q * S^i \qquad (3\text{-}8)$$

Where i is the iteration number, S is a vector search direction in the design space, and q is a scalar move parameter determining the amount of design change possible in this direction.

A multitude of algorithms are available for determining the search direction, S, and the scalar parameter, q, each

with its own unique features. For purpose of this discussion, the actual algorithm is not of particular importance, except as it impacts the efficiency of the overall optimization.

Most state-of-the-art methods in non-linear programming require that gradient information be available. Finite element analysis lends itself well to this. Because, for linearly elastic structures, sensitivity of the structural response to the design variables may be efficiently obtained in most cases. In the following section the essential features of the finite element method are discussed, as they relate to both fixed-shape and variable-shape design.

3.3 Finite Element Analysis

The finite element technique was developed in the 1950s by structural engineers for analysis of structural systems. It is a mathematical technique for constructing approximate solutions to boundary value and eigenvalue problems. The method involves dividing the mathematical domain(structure) associated with the solution into a finite number of subdomains called finite elements. Generally, variational or weighted residual concepts are used to construct an approximate of the solution over the collection of finite elements.

The finite element method is widely used as an

approximate method of solution for structural mechanics problems. Although intially developed by researchers in structural mechanics, the finite element method has become useful in many other areas including fluid mechanics, heat transfer, electric and magnetic fields. In this section, the finite element method[1,2] is presented as an analysis technique for complex structural systems.

Most practical structures are modeled by subdivision into elements, for purposes of analysis, with the finite element method. The displacement method is the most popular form of the finite element method in structural mechanics, and the equilibrium equation to be solved in terms of displacements is:

$$[K]\ \{r\} = \{R\} \tag{3-9}$$

where [K] is the master stiffness matrix, formed by assembling all element stiffness matrices $[K]_i$

$$[K] = \sum_{i=1}^{NE} [K]_i \tag{3-10}$$

{r} is the global nodal generalized displacement vector, and {R} is the vector of structural generalized forces. Using the Choleski decomposition method[3,4], {r} can be solved by

$$\{r\} = [K]^{-1}\{R\} \tag{3-11}$$

Once the necessary nodal displacements are determined, all other structural responses can be sequentially calculated. We can calculated the member stresses using the displacement associated with the element together with the element stiffness matrix or the local interpolation functions associated with the element.

The beam member is a common structural element in many important structural systems used for a variety of industrial applications. Framed Structures are used in many building, transmission towers, airplane wing structures, and vehicle uniframe and seat frame structures. Members of a Frame structure are usually subjected to bending moment, axial load, shear load, and twisting moment. In this dissertation, optimal design of general three dimensional framed structures using hollow rectangular, hollow circular and symmetric open channel cross sections is considered.

In this chapter, it is assumed that the material is elastic, homogeneous(that is, it has the same elastic properties everywhere in the bar), and isotropic(that is, the elastic properties are the same in every direction). Furthermore, we assume that the strains and deformations are relatively small. These are the usual assumptions of the theory of elasticity[5].

For the frame element shown in Fig.3-1, The beam element includes extension, torsion and bending in two perpendicular planes and associated shears. The stiffness matrix of the beam element is a 12x12 matrix of coefficients

expressing the forces and moments acting on the degrees of freedom at its ends. Fig.3-2 shows the node at one end of an beam element and the forces and moments that are present with respect to a local coordinate system. The force and moment resultants are as indicated in Fig.3-2. The components of this force and moment vector are defined as:

F_x = Axial force in direction of local x axis

F_y = Axial force in direction of local y axis

F_z = Axial force in direction of local z axis

M_x = Moment about the local x axis

M_y = Moment about the local y axis

M_z = Moment about the local z axis

3.4 Combined Stress Calculation

Through the finite element method presented in the previous section, the stresses and deformations resulting from the separate effects of bending moment, axial force, shear force, and twisting moment will be calculated. In this section, the individual effects of axial force, shear force, bending moment, and twisting moment are discussed. The combination of the normal stresses and shear stresses is presented. Also the stress sampling points are defined for the different cross sections, and the failure criteria applied for this work is defined.

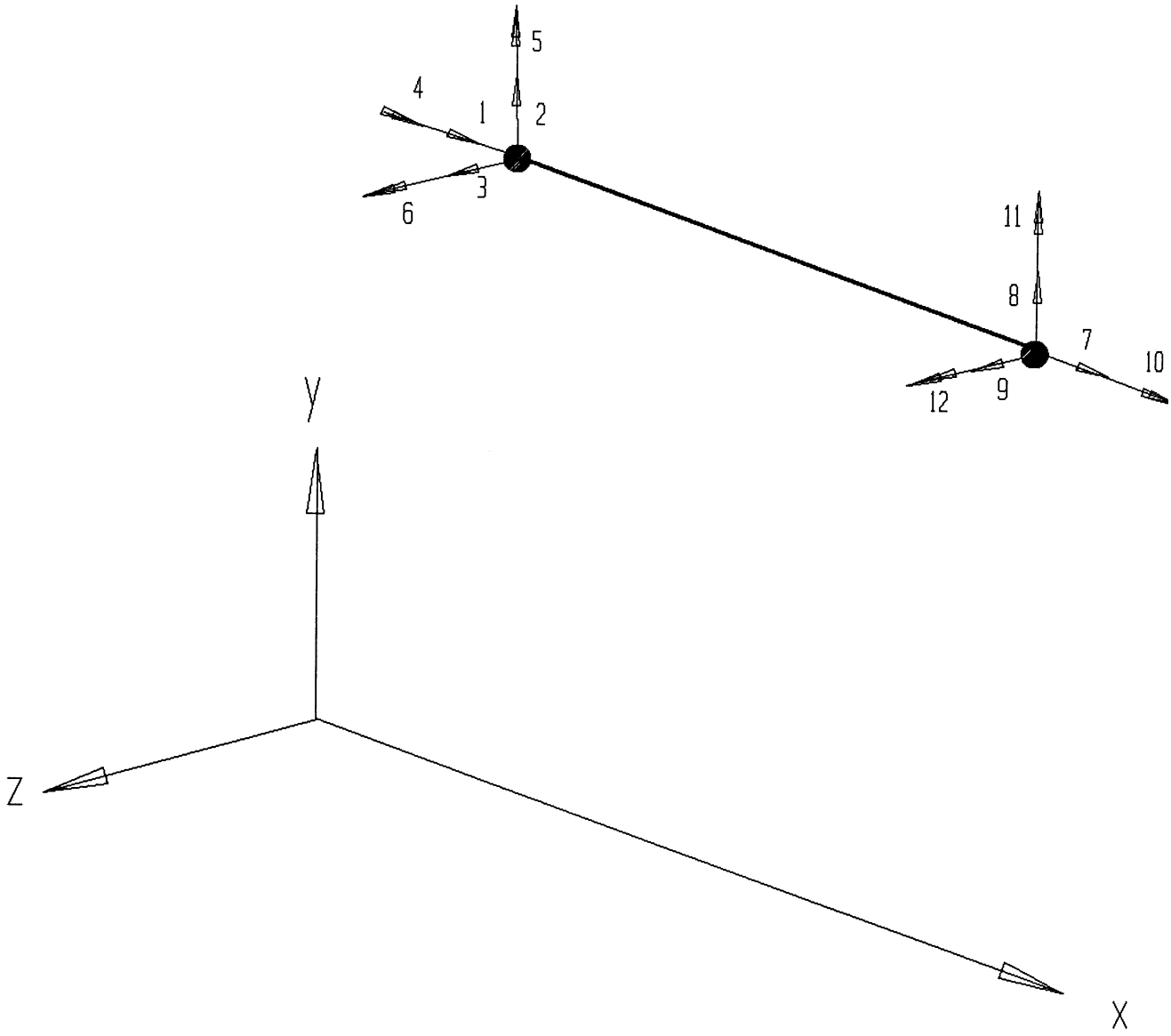

Fig. 3-1 A Frame Element

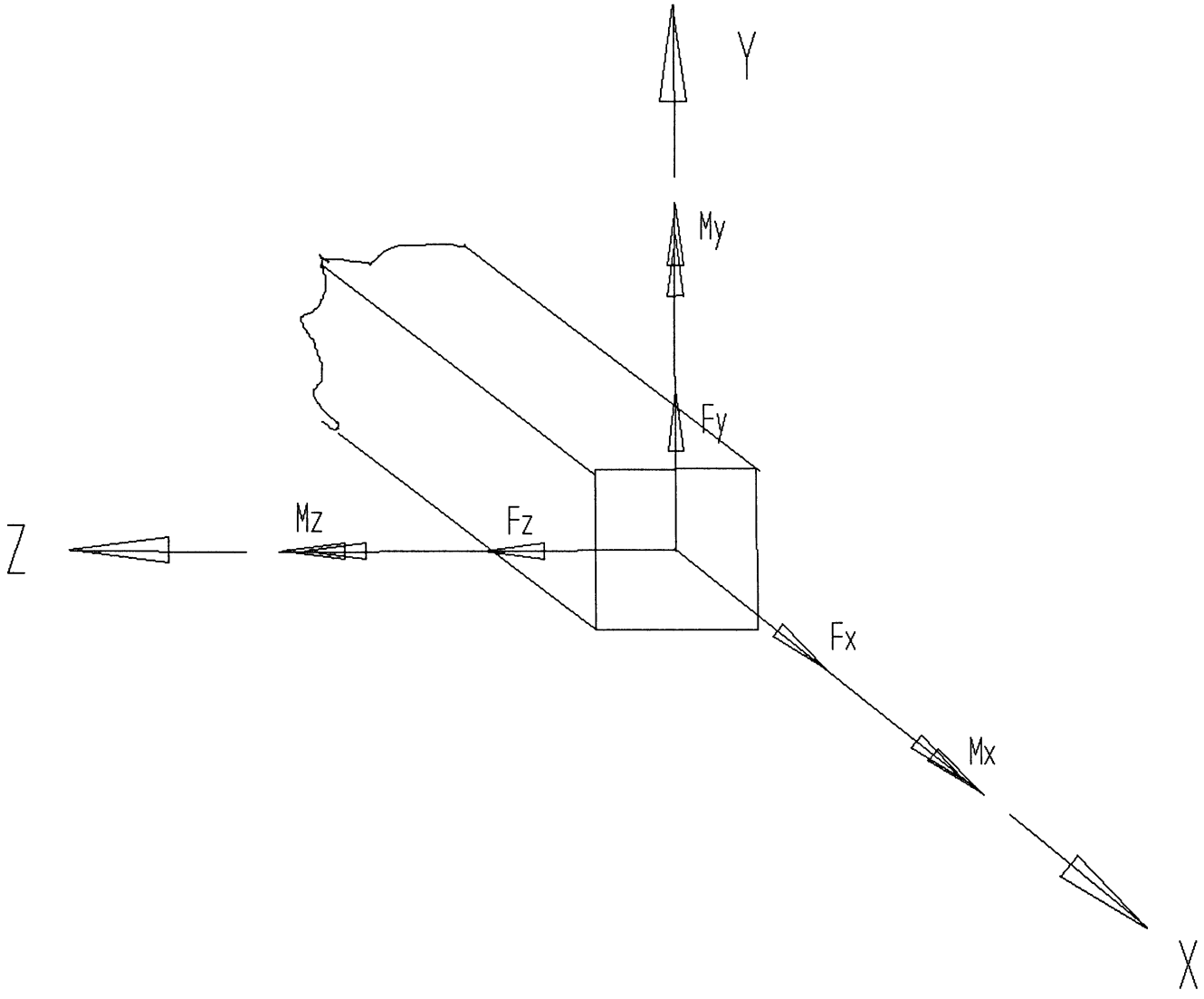

Fig. 3-2 Forces and Moments at a Node

The normal stress due to axial force and normal stress due to bending moment are computed individually. The normal stresses may be obtained by superimposing the stresses from the bending moments on the stress from the axial load by simple algebraic addition. The shear stress due to torsion and shear stresses due to bending are computed independently and then combined to determined the resultant shear stress.

First of all, the normal stress calculation is obtained using the element theory of mechanics of deformable bodies. We consider the cross section of a bar, as shown in Fig.3-2, to be undergoing an axial load and bending moments. This bar is of an arbitary uniform cross sectional shape. A cross section can be located along the longitudinal axis by the local coordinate distance x. Any point in a cross section can be identified using the y-z local coordinate axes. The cross section is assumed to remain plannar and normal to the centroidal axis of deformation. If the y-z axis system has an origin at the centroid and is a principal axis system, then the normal stress is equal to

$$\sigma = \frac{F_x}{A} - \frac{M_z\, y}{I_z} + \frac{M_y\, z}{I_y} \qquad (3\text{-}12)$$

Where F_x = axial force in the direction of local x axis

M_z = moment about the local z axis

M_y = moment about the local y axis

I_z = area moments of inertia about z axis

I_y = area moments of inertia about y axis

A = cross sectional area

y = y distance for stress calculation

z = z distance for stress calculation

Next, the torsional shear stresses are determined assuming the cross secton is thin walled. The torsional shear stresses vary linearly across the thickness of an element of the open channel cross section and act in a direction parallel to the edge of the element. They are maximum and equal, but of opposite direction at the two opposite edges. The stress at the edge of the element is determined by the formula[6]:

$$T_{max} = \frac{M_x \, t_{max}}{J} \qquad (3\text{-}13)$$

The torsional shear stress will be largest in the thickest element of the cross section. Where t_{max} is the maximum thickness and J is expressed in Eq.(3-14). M_x is the moment about the local x axis. The torsional constant for thin walled open section is given by

$$J = 2/3 \; bt^3 + 1/3 \; ht^3 \qquad (3\text{-}14)$$

Where b is the width of the flange and h is the height of the web. The cross sectional dimensions of the open

channel section are shown in Fig.(3-3).

For points that are located at reentrant corners, such as that shown in Fig.(3-3), high stress concentrations can occur which are not accounted for by the approximate formula shown in Eq.(3-13). Because of this, such corners are rounded by fillets, in practice, to allow a smooth flow of stress from one element to another. To evaluate the maximum torsional shear stress at the fillet T_f, we use the empirical formula presented by Trefftz[6].

$$T_f = T_{max}\ 1.74\left(\frac{t}{r}\right)^{1/3} \qquad (3\text{-}15)$$

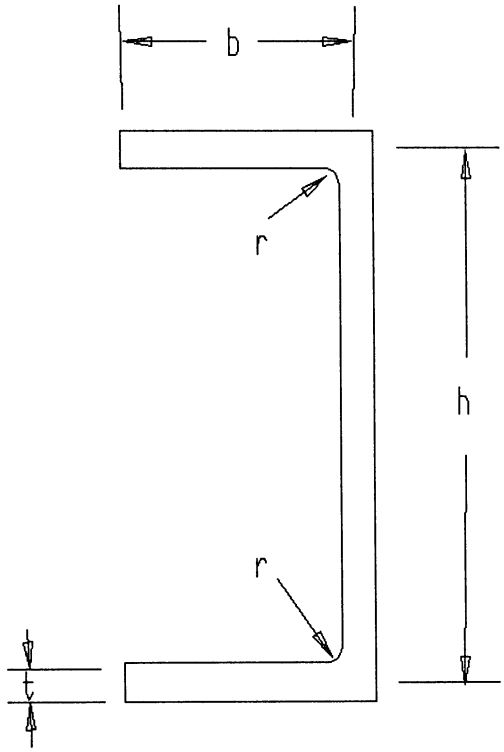

Fig. 3-3 Reentrant Corners and Cross Sectional Dimension of Open Channel Section

Where r is the radius of the fillet, t is the thickness of the element and T_{max} is given by Eq.(3-13). It is shown that the stresses at the reentrant corner are higher, depending on the magnitude of the radius. The effect of the reentrant corner is a stress concentration. If t/r=1, for example, Eq.(3-15) yields a value for T_f which is 74 percent greater than that given by Eq.(3-13). These concentrations become less severe when the angle of intersection of the elements is greater than a right angle.

Bars with thin walled closed cross sections, such as circular or rectangular cross sections, are called tubes. The formula shown in Eq.(3-13) for the analysis of open section cannot be used when the sections are closed. This is fundamentally due to the way that the member must develop shearing stress to resist applied torques. The shear stress due to torsion at any point in the close section is clearly

$$T = \frac{M_x}{2 A_m t} \qquad (3\text{-}16)$$

Where A_m is the total area enclosed by the center line of the tube wall and t is the thickness on the wall. It can be seen from Eq.(3-16), in contrast with the thin walled open section, that it acquires a maximum value at the point of smallest thickness.

Thus far we have considered the response of the beam to the internal resultants F_x, M_y, M_z, and M_x. Therefore, it

remains to determine the response of beams to the internal shear resultants F_y, and F_z. Often in structural analysis procedures it is customary to neglect the shearing stresses in beams. However, this assumption is not always a wise one in the analysis and design of beams for the reason that components of the beam may be very thin so that they are required to carry very large shearing stress. For this reason it is important to construct accurate, but simplified techniques for analysis of beams in shear.

When the cross section is composed of open thin walled elements, the shear stress is essentially uniform over the thickness and is negligible in the direction perpendicular to the center line of the walls. The shear stress is given by Eq.(3-17)

$$T = - \frac{Q_z F_y}{I_z t} - \frac{Q_y F_z}{I_y t} \qquad (3\text{-}17)$$

Where Q_z and Q_y are moments of the area A_s about the z and y axes respectively and t is the thickness of the element at the point (y,z), shown in Fig. 3-4. F_y and F_z are the y and z components of the resultant shear force respectively.

The evaluation of shear stress in thin walled closed sections is more involved than for a thin walled open section. Equation (3-17) is not directly applicable in this case because the quantities Q_y and Q_z have meaning only for open sections. To resolve this situation, then, the section

is imagined to be cut open at an arbitrarily selected point A on the periphery of the tube. We choose this reference point A on the wall as the origin of the perimetric coordinate s, shown in Fig. 3-5. Then the total shear flow is equal to the sum of the shear flow due to plane bending and shear flow due to torsion.

While the shear flow q_{s1} in the resulting open section can be determined by the use of Eq.(3-17). Contiguous points on either side of the imaginary opening at A will be free to move relative each other. This relative motion cannot take place in the actual closed section since the continuity of deformation of the section would then be broken at point A. The presence of the statically indeterminate shear flow at this point of the closed section ensures that contiguous points do not undergo any relative motion and, thus, the continuity of deformation is maintained.

Therefore, once the distribution of shear flow q_{s1} in the imaginary open section is determined, a shear flow q_0 of uniform intensity throughout the section can be superposed on it to obtain the actual shear flow q_s in the closed section. Thus, the formal expression for q_s is

$$q_s = q_0 + q_{s1} \tag{3-18}$$

Where q_{s1} is to be evaluated by the use of Eq.(3-17). The resolution of q_0 is accomplished by turning attention toward continuity of deformation (compatibility condition).

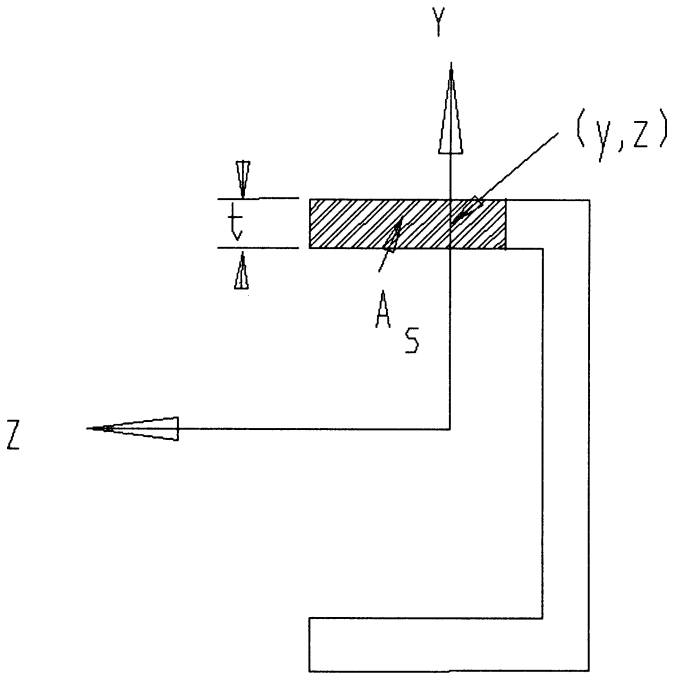

Fig. 3-4 Point(y,z) of the open channel section

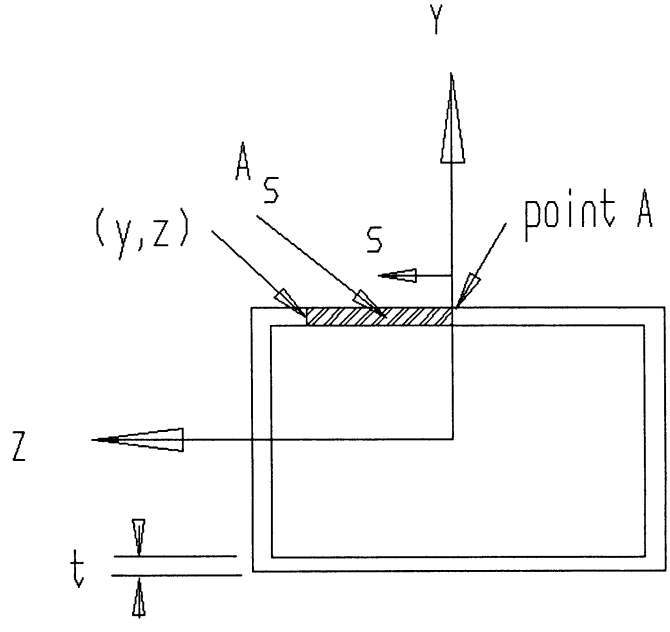

Fig. 3-5 Imaginary point A and point(y,z)
for the closed section

The shear flow q_0, being uniform over the entire cross section, is a constant. In other words, a point on the wall of the undeformed section cannot move to different points after deformation (the condition of compatible deformation). Thus, physically stating that the total relative displacement of the faces at the hypothetical slit is zero for the closed tube, the result for q_0 with t as a constant is

$$q_0 = - \frac{\oint q_{s1}\, ds}{\oint ds} \qquad (3\text{-}19)$$

The total shear flow may now be expressed in terms of F_y and F_z by introducing Eq. (3-17). The result is expressed in Eq.(3-20). The shear distribution can be explicitly determined by Eq.(3-22).

$$q = - \frac{Q_z - K_z}{I_z} F_y - \frac{Q_y - K_y}{I_y} F_z \qquad (3\text{-}20)$$

The terms K_z and K_y are defined as follows where t is treated as a constant;

$$K_z = \frac{\oint Q_z(s)\, ds}{\oint ds} \qquad (3\text{-}21)$$

$$K_y = \frac{\oint Q_y(s)\, ds}{\oint ds} \qquad (3\text{-}22)$$

$$T_s(s) = \frac{q(s)}{t} \qquad (3\text{-}23)$$

The symbol $\oint$ denotes the integral around the closed curve of the section center line and $Q_y(s)$, $Q_z(s)$ are the moments of the area A_s, shown in Fig. 3-5, about the z and y axes respectively. t is the thickness at the distance s measured in counter clockwise direction. $T_s(s)$ is the shear distribution at the distance s.

We have already discussed the individual effects of axial force, shear force, bending moment, and torsion, respectively. In the beam analysis, the cross sectional forces will produce normal stress σ and shear stress T. The analysis problem then consists in determining the variation of these two types of quantities and locating the positions where the combined stress are maximum.

The combination of normal stress and shear stress is a very complex subject, because the normal stress and shear stress are not all at their maximum values at the same transverse section along the length of the member. Therefore, determining the maximum values of the combined stresses for different types of cross sections is somewhat cumbersome. In many cases the combined stresses should be checked at several locations along the member.

Since each analysis element in a rectangular cross sectional case, has four walls and two ends, the stress level is sampled at eight locations at the end of each analysis element. Figure 3-6(a) shows the eight locations within the rectangular cross section where the stresses are sampled. Figure 3-6(b) shows the four locations within the circular cross section. The stress concentrations are accounted for at the reentrant corners of the channel cross section. The stress sampling locations in the channel cross section are shown in Fig.3-6(c).

The members of a framed structure are subjected to state of combined stress due to axial force, shear force, bending moment, and torsional moment. Thus the effect of combined stresses must be considered in implementing stress constraints. In the present work, all members are required satisfy a failure criteria based on Von Mises equivalent stress (also known as Distortion Energy Theory[7]). Generally, Von Mises yield criteria predicts failure quite accurately[8]. This failure criteria will be applied to the stress calculated at each node in the finite element model, and is expressed as

$$\sigma^2 + 3\ T^2 = \sigma_y^2 \qquad (3\text{-}24)$$

where σ_y is the yield stress for the material.

σ is the normal stress.

T is the shear stress.

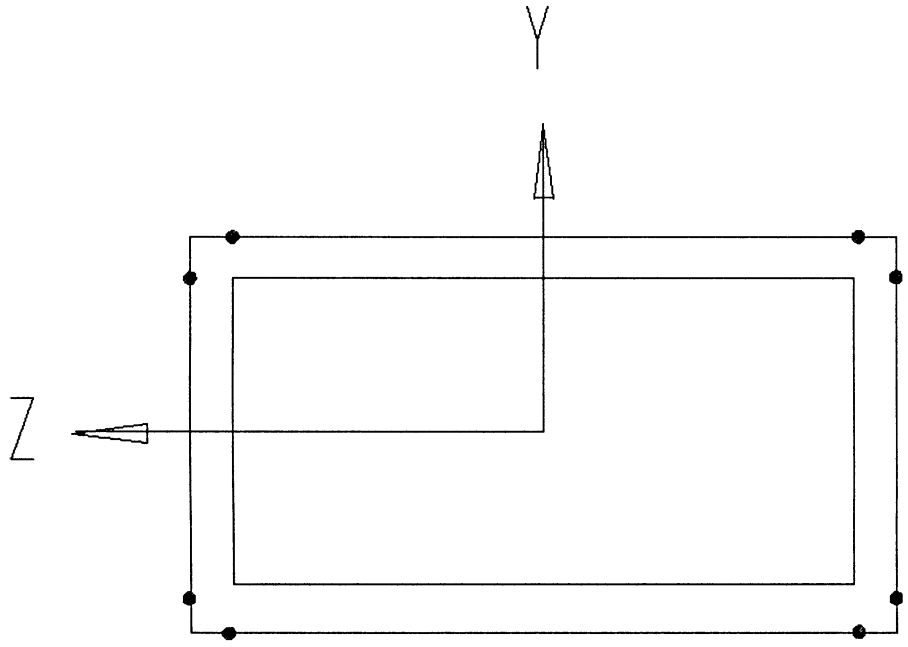

(a) Rectangular Cross Section

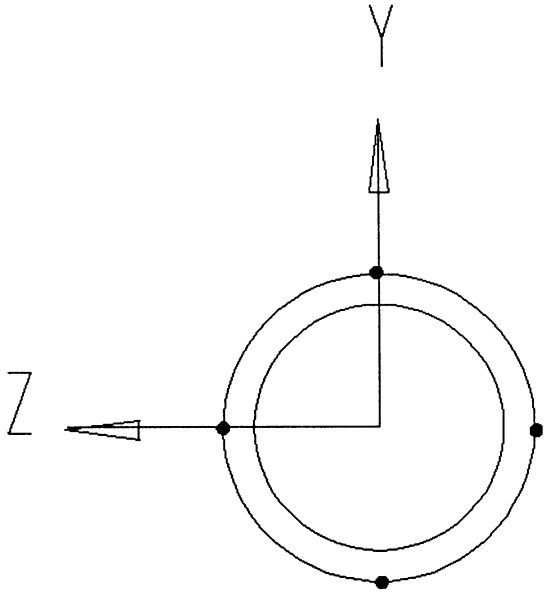

(b) Circular Cross Section

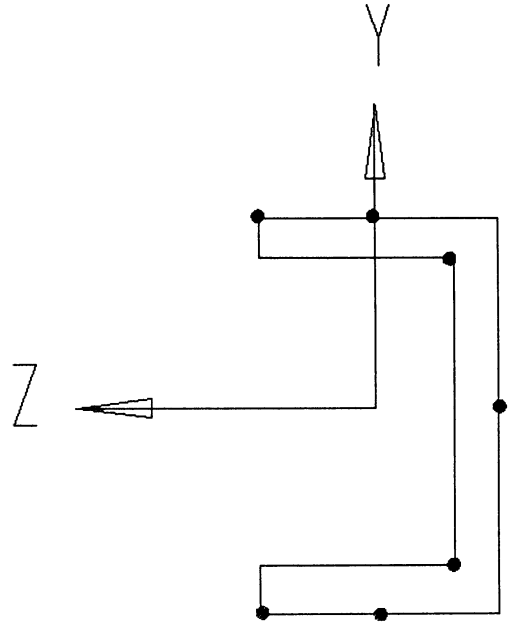

(c) Channel Cross Section

Fig.3-6 Stress Sampling Points

3.5 Optimization Methods for Structural Design

In the minimization of structural cost, the generalized reduced gradient approach will be applied to solve the nonlinear constrainted problem.

The structural optimization problem can be stated in mathematical form as:

$$\text{minimize } f(X);\ X=[X_1,X_2,X_3,.....X_N]^T \qquad (3\text{-}25)$$

$$\text{subject to } g_j(X) \geq 0 \quad j=1,2,3,.....J \qquad (3\text{-}26)$$

$$h_k(X) = 0 \quad k=1,2,3,.....K \qquad (3\text{-}27)$$

where

X = a column vector of design variable

N = total number of design variables

$f(X)$ = objective function

$g_j(X)$ = J inequality constraint functions

$h_k(X)$ = K equality constraint functions

With no loss of generality, this form can be transformed into the following form which is handled by the reduced gradient method.

$$\text{minimize } f(X);\ X=[X_1,X_2,X_3,.....X_N]^T \qquad (3\text{-}28)$$

$$\text{subject to } h_m(X)=0 \quad m=1,2,3,.....M \qquad (3\text{-}29)$$

$$A \leq X \leq B \qquad (3\text{-}30)$$

The Nx1 vectors A and B represent the upper and lower bounds on the design variables. The inequality constraints of Eq.(3-8) are converted to equality constraints by using the following transformation,

$$h_j(X) = g_j(X) - S_j = 0 \qquad (3\text{-}31)$$

$$0 \leq S_j \leq \infty \qquad j=1,2,3.....J$$

The variables S_j are nonnegative slack variables included in the original set of design variables. Hence, N now represents the total number of design variables plus the number of slack variables included to transform the inequality constraints to equality constraints. The parameter M represents the total number of constraints, equality and inequality. The constraints considered in Eq.(3-29) include only functional constraints. Variable bounds are contained in Eq.(3-30) and are handled separately.

Consider the following strategy. Divide the design vector X into two classes, (1) decision variables, and (2) state variables,

$$X = [z,y]^T \qquad (3\text{-}32)$$

$$z = [z_1,z_2,z_3,.....z_Q]^T; \text{ decision variables} \qquad (3\text{-}33)$$

$$y = [y_1,y_2,y_3,.....y_M]^T; \text{ state variables} \qquad (3\text{-}34)$$

$$Q = N - M \qquad (3\text{-}35)$$

The decision variables are independent, and the state variables are slaves to the decision variables used only to satisfy the constraints.

Let us examine the first variation of f(X) and h(X),

$$df = gg(z)^T\, dz + gg(y)^T\, dy \qquad (3\text{-}36)$$

$$dh = \frac{\partial h}{\partial z} dz + \frac{\partial h}{\partial y} dy = 0 \qquad (3\text{-}37)$$

where dz = Qx1 vector of differential displacements of z

dy = Mx1 vector of differential displacements of y

gg(z) = Qx1 vector of gradients of the objective function with respect to z

gg(y) = Qx1 vector of gradients of the objective function with respect to y

$\partial h/\partial z$ = MxQ matrix of gradients of the constraints with respect to z

$\partial h/\partial y$ = MxM matrix of gradients of the constraints with respect to y

Solving Eq.(3-37) for dy yields,

$$dy = - \left(\frac{\partial g}{\partial y}\right)^{-1} \frac{\partial g}{\partial z}\, dz \qquad (3\text{-}38)$$

Substituting Eq.(3-38) into Eq.(3-36) and rearranging will yield the following linear approximation to the reduced gradient

$$g_r(X)^T = gg(z)^T - gg(y)^T \left[\frac{\partial g}{\partial y}\right]^{-1} \frac{\partial g}{\partial z} \qquad (3\text{-}39)$$

The generalized reduced gradient is the rate of change of the objective function with respect to the decision variables with the state variables adjusted to maintain feasibility. The word "generalized" is included to underscore the presence of nonlinear constraints. When the constraints are linear the state variable adjustment is significantly simplified. Geometrically the reduced gradient can be described as a projection of the original N dimensional gradient onto the Q dimensional feasible region described by the decision variables. Hence the reduced gradient can be used in the same manner as the gradient for an unconstrainted problem to search for a minimum of f(X) in the reduced space. The state variables are adjusted during the course of the search to maintain feasibility.

The advantage of using the generalized reduced gradient method for a constrainted problem is the use of state variables to satisfy the constraints. In this dissertation the design sensitivity analysis is included in the generalized reduced gradient method.

3.5 References

[1]Cook, Robert D., "Concepts and Applications of Finite Element Analysis," 2nd ed., John Wiley & Sons Ltd., New York, 1981.

[2]Bathe, K. J., "Finite Element Procedures in Engineering Analysis," Prentice-Hall, Englewood Cliffs, N.J., 1981.

[3]Conte, S. D. and Carl Deboor, "Elemetary Numerical Analysis: An Algorithm Approach," 3rd ed., Mcgraw-hill, New York, 1980.

[4]Bathe, K. J., and Edward L. Wilson, "Numerical Methods in Finite Element Analysis," Prentice-hall, Englewood Cliffs, N.J., 1976.

[5]Timoshenko, S. P. and J. N. Goodier, "Theory of Elasticity," 2nd ed., Mcgraw-hill, New York, 1951

[6]Oden, J. T. and E. A. Ripperger, "Mechanics of Elastic Structures," Mcgraw-hill, New York, 1981.

[7]Ugural, A. C. and S. K. Fenster, "Advanced strength and Applied Elasticity," Elsevier, New York, 1975.

[8]Allen, David H. and Walter E. Haisler, "Introduction to Aerospace Structural Analysis," John Wiley & Sons, Ltd., New York, 1985

CHAPTER IV

SENSITIVITY AND APPROXIMATION

4.1 Introduction

One of the most serious problems that has inhibited the application of structural optimization techniques to practical problems is the high computational cost required for such an application. The high cost is typically associated with the evaluation of the constraint functions and their derivatives with respect to the design variables. For many structural optimization problems the evaluation of stress, displacement, or other behavioral constraints requires the execution of costly finite element analyses. The optimization process may require evaluating the constraint functions hundreds or thousands of times. The cost of repeating the finite element analyses so many times is usually prohibitive in both cost and time.

The problem is often exacerbated when we consider the calculation of sensitivity derivatives of the constraint functions. A straight forward and popular way of obtaining such derivatives is by employing a finite difference approximation. That is, to obtain a derivative with respect to a particular design variable, the value of that design variable is perturbed and the constraint function is

recalculated. The difference in the value of the constraint function divided by the design variable perturbation is the approximate derivative. When the number of design variables is large such a procedure increases the number of required finite element analyses.

One of the approaches that has been employed to alleviate the high cost of the very large number of finite element analyses that may be required for structural optimization is to develop efficient techniques for sensitivity derivative calculation. Efficient techniques for sensitivity derivative calculations are evaluated by comparison with the alternative of executing one additional analysis per design variable and employing finite differences. Optimum design sensitivity analysis seeks rates of change of predicted response quantities (e.g. displacements, stresses) with respect to changes in design variables. Once the optimum design sensitivity derivatives have been determined; these partial derivatives provide valuable information that can be used to guide the design process and estimate the revised optimum design without recourse to reoptimization.

The other approach is to employ a fast approximate structural reanalysis technique. The reanalysis techniques are evaluated by their ability to reduce the cost of a repeated structural analysis compared to the cost of a single analysis. The most popular reanalysis techniques are approximation techniques whereby the reduced cost is

obtained at the expense of reduced accuracy. However, in some cases it is possible to reduce the cost of reanalysis without compromising accuracy by avoiding repetition of parts of the analysis which are not affected by changes in the design variables.

In this chapter, the approaches for calculation of the derivatives of the constraint functions with respect to design variables(design sensitivity analysis) are discussed in Sec. 4-2 and Sec. 4-3. The constraint approximations are expressed in Sec. 4-4.

4.2 Gradient Computations

4.2.1 Variation of the Equilibrium Equation

The equation of equilibrium in Equation (3-9) may be differentiated with respect to the ith component of the design vector X_i to give:

$$[K]\{\frac{\partial r}{\partial X_i}\} + [\frac{\partial K}{\partial X_i}]\{r\} = \{\frac{\partial R}{\partial X_i}\} \qquad (4\text{-}1)$$

This equation can be arranged as

$$[K]\{\frac{\partial r}{\partial X_i}\} = \{\frac{\partial R}{\partial X_i}\} - [\frac{\partial K}{\partial X_i}]\{r\} = [R^+] \qquad (4\text{-}2)$$

where $[R^+]$ is called the force derivative for the design variable. For the complete set of displacement derivatives, Eq.(4-2) can be written as

$$[K]\left[\frac{\partial r}{\partial X_1}, \frac{\partial r}{\partial X_2}, \ldots\ldots\ldots, \frac{\partial r}{\partial X_n}\right] = [R_1^+, R_2^+, \ldots\ldots\ldots R_n^+]$$

$$\left[\left\{\frac{\partial R}{\partial X_1}\right\}, \ldots\ldots\ldots, \left\{\frac{\partial R}{\partial X_n}\right\}\right] - \left[\left[\frac{\partial K}{\partial X_1}\right]\{r\}, \ldots., \left[\frac{\partial K}{\partial X_n}\right]\{r\}\right] = [R^+]$$

(4-3)

If the partially inverted [K] matrix is stored during the Gaussian elimination process necessary to compute the displacements under the applied loading {R} in Eq.(3-9), then this matrix can be recalled and used to compute the displacement derivative using the psuedo-loads(dummy loads) $[R^+]$.

4.2.2 Analytical Method

For a problem with n design variables X_i(i=1,....n), finite difference derivative calculations of the displacements with respect to design variables requires one to repeat the analysis for (n+1) different stiffness matrices. However, the derivatives can be calculated analytically in more efficient ways, and the large number of

analyses associated with finite difference calculations can be avoided. In this section some approaches for the analytical calculation of derivatives are discussed.

Analytical calculations of derivatives of displacement and their functions have been described by Arora and Haug[1,2] and Haug and Arora[3]. In these references, three methods are described: The direct or design space method, the adjoint variable or state space method, and the virtual load method. The virtual load method is a special case of the state space method.

The equation of equilibrium in terms of the nodal displacement vector {r} is generated from a finite element model in Eq.(3-9). A typical constraint, such as a limit on a displacement or stress component may be written as

$$g = g(r,X) \geq 0 \tag{4-4}$$

The displacement r is a function of the design variables. It will be represented as

$$r = r(X) \tag{4-5}$$

From Eq.(4-4), the first derivative(first order change) of a constraint $g_j(\{X\},\{r\})$ is given as

$$\delta g_j = \{\frac{\partial g_j}{\partial X}\}^T \{\delta X\} + \{\frac{\partial g_j}{\partial r}\}^T \{\delta r\} \tag{4-6}$$

in which

$$\{\frac{\partial g_j}{\partial X}\}^T = \{\frac{\partial g_j}{\partial X_1}, \ldots\ldots\ldots, \frac{\partial g_j}{\partial X_n}\}$$

$$\{\frac{\partial g_j}{\partial r}\}^T = \{\frac{\partial g_j}{\partial r_1}, \ldots\ldots\ldots, \frac{\partial g_j}{\partial r_M}\} \qquad (4\text{-}7)$$

$$\{\delta X\}^T = \{\delta X_1, \ldots\ldots\ldots, \delta X_n\}$$

$$\{\delta r\}^T = \{\delta r_1, \ldots\ldots\ldots, \delta r_M\}$$

M = the number of components in $\{r\}$

n = the number of components in $\{X\}$

Note that $\{\frac{\partial g_j}{\partial X}\}$ is the partial derivative of g_j with respect to $\{X\}$, keeping $\{r\}$ constant. $\{\delta X\}$ is a small change in $\{X\}$ and $\{\delta r\}$ is the corresponding change in $\{r\}$. The derivatives $\{\frac{\partial g_j}{\partial X}\}$ and $\{\frac{\partial g_j}{\partial r}\}$ are calculated at the given point $\{X^*\}$ with the corresponding values $\{r^*\}$.

In Eq.(4-5), the dependent variables $\{r\}$ are expressed in terms of the independent design variables $\{X\}$. Thus, we can use the relation

$$\{\delta r\} = [\frac{\partial r}{\partial X}] \{\delta X\} \qquad (4\text{-}8)$$

in which

$$\left[\frac{\partial r}{\partial X}\right] = \begin{bmatrix} \frac{\partial r_1}{\partial X_1} & \cdots\cdots\cdots & \frac{\partial r_1}{\partial X_n} \\ \vdots & & \vdots \\ \frac{\partial r_M}{\partial X_1} & \cdots\cdots\cdots & \frac{\partial r_M}{\partial X_n} \end{bmatrix} \qquad (4\text{-}9)$$

In the procedure proposed by Arora and Haug[2], the terms $\{\partial g_j/\partial X\}^T \{\delta r\}$ are expressed as functions of $\{\delta X\}$, so that the vector $\{\delta r\}$ is eliminated and Eq.(4-6) can be written as

$$\delta g_j = \{\nabla g_j\}^T \{\delta X\} \qquad (4\text{-}10)$$

The vector $\{\nabla g_j\}$ is the gradient for the function g_j with respect to the design variables, at the current design point. It is the vector of total derivatives of g_j with respect to $\{X\}$, defined as

$$\{\nabla g_j\}^T = \{\frac{dg_j}{dX_1}, \cdots\cdots\cdots, \frac{dg_j}{dX_n}\} \qquad (4\text{-}11)$$

The objective of design sensitivity analysis is to find an expression for $\{\nabla g_j\}$. The design space approach to design sensitivity analysis was first suggested by Fox[4], and has been used by Schmit and Miura[5,6] and Arora and Haug[1]. In this approach the state variable is assumed to be given as

Eq.(4-5). Then Eq.(4-8) is substituted in Eq.(4-6) and the equation becomes

$$\delta g_j = \left(\{\frac{\partial g_j}{\partial X}\}^T + \{\frac{\partial g_j}{\partial r}\}^T [\frac{\partial r}{\partial X}] \right) \{\delta X\} \qquad (4\text{-}12)$$

Comparing Eqs. (4-12) and (4-10), we obtain the design derivative vector as:

$$\{\nabla g_j\}^T = \{\frac{\partial g_j}{\partial X}\}^T + \{\frac{\partial g_j}{\partial r}\}^T [\frac{\partial r}{\partial X}] \qquad (4\text{-}13)$$

The matrix $[\partial r/\partial X]$ required in Eq.(4-13) is computed by implicit differentiation of Eq.(3-9), as was first suggested by Fox[4].

$$[K] [\frac{\partial r}{\partial X}] = [R^+] \qquad (4\text{-}14)$$

$[R^+]$ is defined by Eq.(4-2). Since Eqs.(4-14) and (3-9) have the same coefficient matrix [K], the decomposed form of Eq.(3-11) is still available. For given values for [K], {r}, and $[\partial K/\partial X_i]$, the derivatives $[\partial r/\partial X_i]$ are computed by solving the set of simultaneous linear equations based on forward and backward substitutions. Thus, we obtain a very concise derivative formula for $\{\nabla g_j\}$.

In problems where the vector {R} is independent of the design variables $\{\partial R/\partial X_i\} = \{0\}$, Eq.(4-14) is reduced to

$$[K] \left\{\frac{\partial r}{\partial X_i}\right\} = - \left[\frac{\partial K}{\partial X_i}\right] \{r\} \qquad (4\text{-}15)$$

$$i=1,.....n$$

Assuming $g_j = r_j$, then $\{\partial g_j / \partial X\}=\{0\}$, $\{\partial g_j/\partial r\} =\{I_j\}$ and Eq.(4-13) becomes

$$\{\nabla r_j\}^T = \{I_j\}^T \left[\frac{\partial r}{\partial X}\right] \qquad (4\text{-}16)$$

Then, the desired derivative vector $\{\nabla r_j\}$ is computed by Eq.(4-16) and the matrix $[\partial r/\partial X]$ is computed by solving the X set of Eq.(4-14) for the n unknown vectors $\{\partial r/\partial X_i\}$, i=1,....n.

The second approach, called the adjoint variable method, has been extensively used in optimal control theory. The method defines an adjoint variable vector $\{C_j\}$ associated with the constraint variable function g_j, as defined the solution of the set of equations.

$$[K] \{C_j\} = \left\{\frac{\partial g_j}{\partial r}\right\} \qquad (4\text{-}17)$$

where $\{\partial g_j/\partial r\}$ is defined in Eq.(4-7). Then Eq.(4-13) is rewritten as

$$\{\nabla g_j\}^T = \{\frac{\partial g_j}{\partial X}\}^T + \{C_j\}^T [R^+]$$

$$= \{\frac{\partial g_j}{\partial X}\}^T + \{C_j\}^T [\{\frac{\partial R}{\partial X_i}\} - [\frac{\partial K}{\partial X_i}]\{r\}] \quad (4\text{-}18)$$

The adjoint variable $\{C_j\}$ needed in Eq.(4-18) is efficiently obtained from the adjoint equation Eq.(4-17) using the previously calculated factor of [K] in Eq.(3-11). The adjoint variable method requires the solution of Eq.(4-17) once for each constraint function g(X).

If the number of functions is smaller than the number of design variables, the adjoint variable method is more efficient. Conversely, if the number of design variables is smaller, the design space approach is more efficient. Both the design space and adjoint methods involve fewer computations than the finite difference approach which requires repeated factorization of the stiffness matrix, whereas the design space and adjoint methods require a single factorization with several right-hand sides.

The method chosen in this dissertation is design space method because it is reasonably efficient when there are a large number of design constraints. For beam-frame structures, there may be more than one constraint per element, and thus the number of constraints will be larger than the number of variables.

4.3 Sensitivity Derivatives of Static Displacement and Stress Constraints

The displacement constraint for the jth degree of freedom under the lth loading condition is:

$$g_j(r,X) = r_{allow} - r_j^l \geq 0 \qquad (4\text{-}19)$$

$$= 1 - r_j^l / r_{allow} \geq 0 \qquad (4\text{-}20)$$

$$j=1,2,....n_d$$

$$l=1,2,....n_c$$

where n_d = the number of displacement constraints

n_c = the number of loading conditions

r_j^l = the computed displacement

r_{allow} = an allowable displacement

The gradient of the constraint for the nodal displacement is computed using Eq.(4-13) and described in Sec.(4-2).

The stress constraint at the jth critical point or for the jth member of the structure under the lth loading condition is expressed as:

$$g_j(r,X) = \sigma_{allow} - \sigma_j^l \geq 0 \qquad (4\text{-}21)$$

$$= 1 - \sigma_j^l / \sigma_{allow} \geq 0 \qquad (4\text{-}22)$$

$$j=1,2,....n_s$$

$$l=1,2,....n_c$$

where n_s = the number of stress constraints

n_c = the number of loading conditions

σ_j^l = the computed stress

σ_{allow} = an allowable stress

The stresses in an element may be obtained from the displacement using

$$\{\sigma\} = [S]\{r\} \tag{4-23}$$

For the gradient of stress, we simply differentiate equation (4-23) with respect to each design variable.

$$\{\frac{\partial \sigma}{\partial X_i}\} = [S] \{\frac{\partial r}{\partial X_i}\} \tag{4-24}$$

Once the derivative of the displacement {r} is found, derivatives of the stresses {σ} can then be obtained by differentiation of the stress-displacement equation (4-23).

4.4 Constraint Approximation

In order to make the implicit constraint stated in Eq.(4-4) computationally tractable it is necessary to construct a series of explicit approximate constraints. These approximate problems must be algebraically explicit and they should capture the essential features of the

original implicit constraint. Various approximate representations can be generated. For example, Taylor series expansion can be used as a method for computing the new displacement vector {r}, corresponding to a modified set of design variables X_j by

$$\{r\}=\{r^*\} + \sum_{j=1}^{n} (X_j-X_j^*) \{\frac{\partial r^*}{\partial X_j}\} \qquad (4\text{-}25)$$

Equation (4-25) is a first order approximation of the Taylor Series. $\{\partial r^*/\partial X_j\}$ can be obtained by differentiation of Eq.(3-9) with respect to X_j,

$$[K^*] \{\frac{\partial r^*}{\partial X_j}\} = - [\frac{\partial K^*}{\partial X_j}] \{ r^*\} \qquad (4\text{-}26)$$

in which {R} is treated as independent of X_j. Since Eqs.(3-9) and (4-26) are similar, the same computational routine can be used to solve for $\{\partial r^*/\partial X_j\}$.

The computational cost of this operation is the same as that required for a single additional loading case, and is found to be much less than the cost of a complete analysis.

Higher order terms in the Taylor's expansion can be employed. This will lead to more accurate results but the computational time and storage requirements are more expensive. This is because of the requirement of generating and storing all the second-order derivatives.

4.5 References

[1]Arora, J. S. and Haug, E. J., "Efficient Optimal Design of Structures by Generalized Steepest Descent Programming," International Journal for Numerical Methods in Engineering, Vol. 10, 1976, pp. 747-766.

[2]Arora, J. S. and Haug, E. J., "Methods of Design Sensitivity Analysis in Structural Optimization", AIAA Journal, Vol. 17, Sept. 1979, PP.970-974.

[3]Haug, E. J. and Arora, J. S., "Design Sensitivity Analysis of Elastic Mechanical Systems," Computer Methods in Applied Mechanics and Engineering, Vol. 15, 1978, pp.35-62.

[4]Fox, R. L., "Constraint Surface Normals for Structural Synthesis Techniques," AIAA Journal, Vol. 3, Aug. 1965, pp.1517-1518.

[5]Schmit, L. A. and Miura, H., "A New Structural Analysis/Synthesis Capability-ACCESS 1,", AIAA Journal, Vol. 14, May 1976, pp.661-671

[6]Schmit, L. A. and Miura, H., "An Advanced Structural Analysis/Synthesis Capability-ACCESS 2,", International Journal for Numerical Methods in Engineering, Vol. 12, 1978, pp. 353-377.

CHAPTER V

GEOMETRIC MODELING AND TOPOLOGICAL DESIGN

5.1 Introduction

In the case of shape optimization, the design variables involved include not only member sizes, thickness and cross sectional areas, but also configuration parameters and nodal point locations. The choice of design variables will change the character of the problem by changing the degree of nonlinearity of the objective and constraint functions. For shape optimization, one choice of design variables might be the nodal coordinates of the members. The advantage of this choice is that one would be able to obtain a general shape geometry, consistent with the finite element model, in which the structure is allowed to assume whatever shape is necessary to obtain the optimum design. The major problem is the resulting large number of design variables. Another choice would be the configuration parameters, each of which relates the nodal points along a curve.

The most direct approach to shape optimization would be to include both member sizing and geometric variables in the design variable set. Pedersen[1] used this approach to solve plannar truss structure problems subject to a single loading condition and stress constraints. Another approach which has

been applied to discrete structures is multilevel design. Vanderplaats and Moses[2] used this technique, coupled with the method of feasible direction, to design trusses under stress constraints. In this dissertation shape geometry optimization based on parametric cubic curves is presented. The design variables are used either for the nodal coordinates or the shape parameters of parametric cubic curve.

In Sec.5-2 the parametric cubic geometric definition which controls the shape geometry is described. In Sec.5-3 the method for topological optimization is presented.

5.2 Geometric Modeling

It will be appropriate to divide the structure into several subregions when the number of master nodes on a boundary is equal to or greater than 4. Then we can connect these master nodes with straight lines, quadratic or cubic curves. In parametric cubic geometry, the parametric cubic curve (PC) can be represented by

$$\begin{aligned} P(u) &= S_1u^3 + S_2u^2 + S_3u + S_4 \\ &= [u^3\ u^2\ u\ 1]\ [S_1\ S_2\ S_3\ S_4]^T \\ &= [U]\ [S]^T \end{aligned} \qquad (5\text{-}1)$$

where P is defined as a general coordinate of n components. For a space curve, n is 3 and P thus represents

x, y, z. For convenience, the parametric variable, u, is defined to be in the region $0 \leq u \leq 1$, inclusive.

Equation (5-1) is called the algebraic format of a PC line. Thus, for a space curve, Eq.(5-1) become

$$\begin{aligned} X(u) &= S_{1x}u^3 + S_{2x}u^2 + S_{3x}u + S_{4x} \\ Y(u) &= S_{1y}u^3 + S_{2y}u^2 + S_{3y}u + S_{4y} \\ Z(u) &= S_{1z}u^3 + S_{2z}u^2 + S_{3z}u + S_{4z} \end{aligned} \qquad (5\text{-}2)$$

A unique set of 12 constant coefficients, called algebraic coefficients, determines a unique PC curve; it determines the size and shape of the curve and its position in space. Two curves of the same shape have different algebraic coefficients if they occupy different positions in space.

The algebraic coefficients are not always the most convenient way of controlling the shape of a curve in a typical modeling situation. Another form is given to define a PC curve in its geometric form. It uses the two end points and the corresponding tangent vectors to represent a PC curve.

The parametric derivative is

$$\frac{dP}{du} = P_{,u}(u) = 3S_1u^2 + 2S_2u + S_3 \qquad (5\text{-}3)$$

In which a comma denotes differentiation with respect to the subscript.

If we set u=0 and u=1 in Eq.(5-1) and Eq.(5-3), we

obtain

$$P(0) = S_4$$
$$P(1) = S_1 + S_2 + S_3 + S_4$$
$$P_{,u}(0) = S_3$$
$$P_{,u}(1) = 3S_1 + 2S_2 + S_3 \qquad (5\text{-}4)$$

Solving the linear system in Eq.(5-4) for the algebraic coefficient leads to

$$[S_1\ S_2\ S_3\ S_4]^T = [M]\ [P(0)\ P(1)\ P_{,u}(0)\ P_{,u}(1)]^T \qquad (5\text{-}5)$$

where

$$[M] = \begin{bmatrix} 2 & -2 & 1 & 1 \\ -3 & 3 & -2 & -1 \\ 0 & 0 & 1 & 0 \\ 1 & 0 & 0 & 0 \end{bmatrix}$$

substituting this into Eq.(5-1) yields

$$P(u) = [u^3\ u^2\ u\ 1] \begin{bmatrix} 2 & -2 & 1 & 1 \\ -3 & 3 & -2 & -1 \\ 0 & 0 & 1 & 0 \\ 1 & 0 & 0 & 0 \end{bmatrix} \begin{bmatrix} P(0) \\ P(1) \\ P_{,u}(0) \\ P_{,u}(1) \end{bmatrix}$$

$$= [F_1(u)\ F_2(u)\ F_3(u)\ F_4(u)]\ [P(0)\ P(1)\ P_{,u}(0)\ P_{,u}(1)] \qquad (5\text{-}6)$$

where $F_1(u) = 2u^3 - 3u^2 + 1$

$F_2(u) = -2u^3 + 3u^2$

$F_3(u) = u^3 - 2u^2 + u$

$F_4(u) = u^3 - u^2$

Eq.(5-6) is called the geometric form, and P(0), P(1), $P_{,u}(0)$ and $P_{,u}(1)$ are called geometric coefficients. The F_i's are the blending functions which serve the purpose of blending the quantities P(0), P(1), $P_{,u}(0)$ and $P_{,u}(1)$ together so as to form a continuous curve satisfying the end conditions.

5.3 Topological Design

The salient feature which differentiates the sizing variables and configuration variables from the topological variables is that the topological variables are usually treated as discrete variables and the sizing and configuration variables are usually treated as continuous variables. Therefore, gradient techniques may be used for sizing and configuration variables but may not, in general, be used for topological variables. Vanderplaats[3] has pointed out the topological design problem is perhaps the most difficult of the structural optimization tasks.

Despite its difficulty, the topological problem has remained of great interest because it is the basic problem that must be solved before either the configuration or sizing problem can be attacked. Basically, there are two approaches that can be used in handling topological problems: members may be deleted from an existing design or they may be added to a minimal design

Because of the extreme cost of the basic structural analysis, we are forced to discard exhaustive search as an approach in either deletion or addition. Therefore, we must develop and rely on heuristic methods[4] to identify which member should be added or deleted to improve the final design.

For member deletion, the user must specify a structure which contains all members that he thinks may be needed. This, of course, can lead to structures with many possible candidates for deletion. So it is necessary to devise a rational heuristic search technique to identify which members are to be deleted and to guide the optimization process in the most profitable direction.

The heuristic criteria will play an important part in guiding a search process efficiently toward a solution. In member deletion, a stress criteria is directly used for the heuristic function since this information is typically available from the last step in the optimization process. Based on the stress in a member, we can determine which member is the most promising candidate to be deleted in the subset of the structure.

After the structure has been optimized, we must assume that one or more performance constraints are active. Therefore, from the list of all the possible candidate members to be considered, we do not consider any member which is within a suitable tolerance of the stress constraint and only consider the remaining members which

have reached the minimum size. We select the remaining member with the lowest maximum stress level and remove it.

The next problem is to determine whether the design process has converged. If the optimum weight of the new structure is better than the optimum design of the previous best design, then the new structure is the optimum structure. If the new structure is not better than the previous structure, we have to replace the member just removed, take the member with the second lowest stress level and continue to search for the optimum structure.

This produces an algorithm which searches the design tree by a depth first search with pruning. Thus at any node in the tree a maximum of two branches will be considered. The maximum number of branches which will be considered will be 2n where n=number of possible bars to remove rather than 2^n bars which would be considered by exhaustive search.

Attempting to add elements to decrease the weight is considerably less straightforward. However, the topology of the structure can be optimized when members are allowed to be added. Hence, it is instructive to attempt to create an algorithm to handle this sort of problem.

To effectively determine from all possible members to add that member which will most likely reduce the overall weight, requires the development of a criteria which will identify at some node of the structure what member should be added to produce the minimum total weight. Also we have to develop a heuristic search technique to make the whole

search process easier.

The criteria in the adding algorithm is based on the stress level. The element considered for addition to the existing structure is found by starting from the load point with the maximum highest stress level and moving to the spatial point of a set of predefined nodal points with the maximum highest stress level. When the subset of the structure has been optimized, the active constraint at the load point is the most promising nodal point. If the active constraint set does not contain the load point, the next most promising nodal point is the point which has the maximum highest stress value.

The search process is similar to the deleting method except for the criteria. The maximum number of bars to add is predetermined in the optimization process. We choose to pursue the optimization in the minimum time. Thus if the possible process design is still greater than the previous design, the design is terminated.

While this approach could be used when a number of members are to be considered to be added, the extreme cost of the structural analysis could be a problem. This add algorithm cannot be expected to obtain the global(or even local) optimum. However, the heuristic method presented in this study is applicable for topology optimization. Also there is indication that this method can form the basis for an economically feasible tool for a learning algorithm in the area of the artificial intelligence.

5.4 REFERENCES

[1]Pederson, P., "On the Optimal Layout of Multipurpose Trusses," Computers and Structures, Vol.2, 1972, pp.695-712.

[2]Vanderplaats, G. N. and F. Moses, "Automated Design of Trusses for Optimum Geometry,", Proc. ASCE, St3, 4, pp.671-690, 1972.

[3]Vanderplaats, G. N., "Numerical Methods for Shape Optimization: An Assessment of the State of the Art", New Directions in Optimum Structural Design, Edited by E. Atrek, R. H. Gallagher, K. M. Ragsdell, and O. C. Zienkiewicz, John Wiley & Sons Ltd., N.Y., 1984

[4]Rich, E., "Artifical Intelligence," McGraw-Hill, Inc., New York, 1983.

CHAPTER VI

RESEARCH RESULTS

6.1 Introduction

In previous chapters of this dissertation, the idea and the approach of coupling finite element structural analysis and nonlinear mathematical programming to create optimum design capabilities were indicated. The parametric cubic function and topology addition and deletion method which were used to change the configuration and topology during the design process, were described.

In this chapter, this approach will be applied to actual applications in several examples in Sec. 6-3. Also development and implementation of the computer programs and computational considerations in structural optimization are described in Sec. 6-2.

6.2 Computer Algorithms and Computational Considerations

6.2.1 Computer Programs in the Development and Implementation of Structural Optimization

A schematic representation of the design process employed by the structural optimization algorithm is

illustrated in Fig.(6-1). The main program calls subroutine TRANSFER and the optimization routine. The subroutine TRANSFER reads member connectivity, joint boundary conditions and joint geometric coordinate data for the finite element model. The optimization routine performs the design process using the generalized reduced gradient method.

The analysis program by the finite element method is in subroutine INTRFACE and ANALYSIS. INTRFACE calls subroutines FORMRT, FORMSM, MULT, INDEX and LINF1F to calculate the bandwidth of the stiffness matrix and generate the stiffness matrix itself. The subroutine FORMRT forms the transformation matrix for each element and also forms the transpose of the transformation matrix. Subroutine FORMSM forms the element stiffness matrix. Subroutine MULT performs the multiplication of the transformation matrix, stiffness matrix and transpose of the transformation matrix. Subroutine ANALYSIS calls the BNDSOLV subroutine to solve the linear simultaneous equations to calculate displacement, force and stress. Subroutine BNDSOLV saves computer space and solves the equation based on the fact that a banded matrix is generated.

Subroutine INDEX computes the indices required to store the element stiffness matrix in the global stiffness matrix. The mth member of a finite element model showing member indices is given in Fig.(6-2). The 1, 2, 3, 4, 5, 6 references at the jth end describe the m member action and

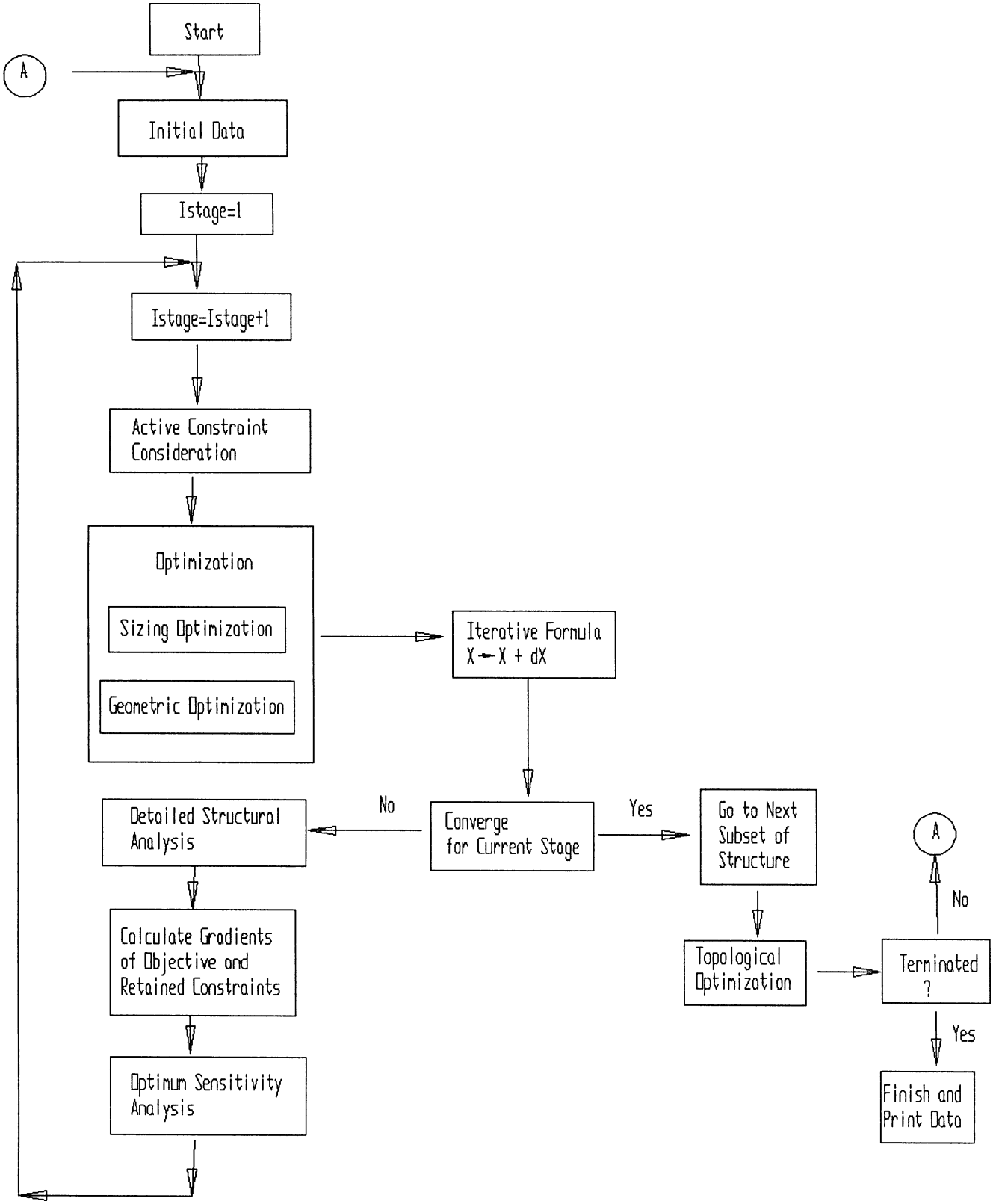

Fig.6-1 Design Procedure in Computer Algorithm

displacement vector at this end, while the 7, 8, 9, 10, 11, 12 references define the vector at the kth end. 'm' is the member number and 'j' and 'k' are the joint numbers of the near and far ends of the member, respectively. The origin of the member coordinate is at the near end. The method of computing the indices is shown in Fig.(6-3).

The design sensitivity analysis is calculated by subroutine PARTAL. It calculates numerical partial derivatives of the constraints with respect to the design variables using the Cholesky decomposition method.

Subroutine LINF1F is a linear equation solver. It decomposes the matrix into a product of an upper triangular matrix and a lower triangular matrix. It then solves the matrix equation by forward and backward substitutions.

6.2.2 Computational Considerations

To apply the algorithm described in the previous section to medium and large scale structures, all the calculations must be performed as efficiently as possible. In addition to computing design derivatives and applying constraint approximations, in this section several additional computational considerations are discussed.

The structural stiffness matrices are usually quite sparse and full advantage of sparsity must be taken in any

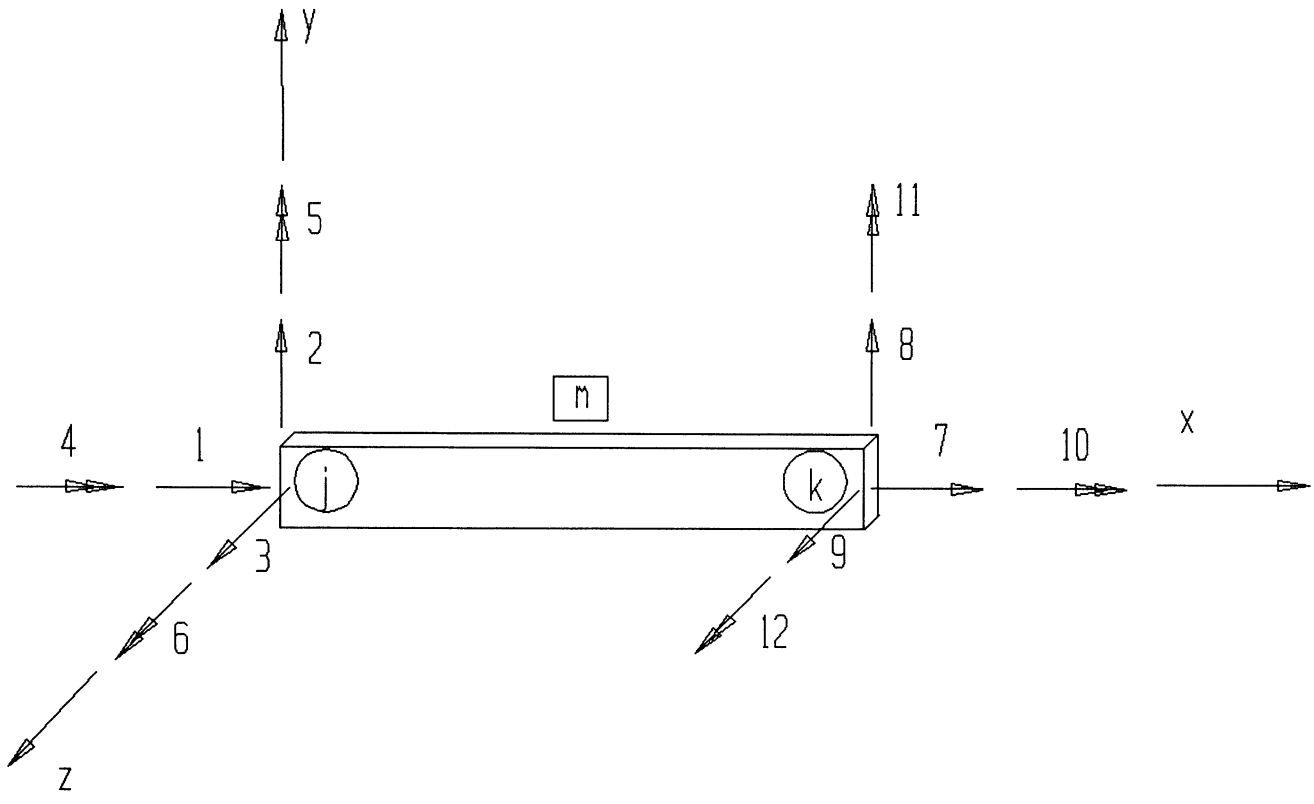

Fig. 6-2 Computation of indices for mth member

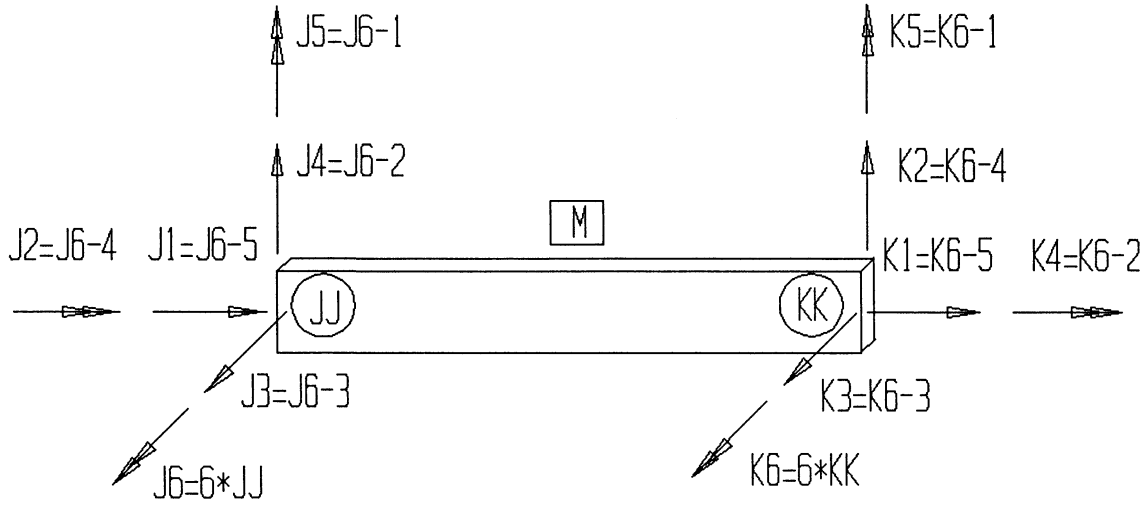

Fig. 6-3 Computation of indices for general member

structural analysis routine. The nodal point numbering of the structure can be arranged so that all nonzero elements of the stiffness matrix lie in a band along their main diagonals. Since stiffness matrices are symmetric, only half the bandwidth of the matrix needs to be computed and stored. It is far more efficient to work with banded matrices than with the full matrices[1]. For example, if a structure has 150 degrees of freedom, dimensions of the full stiffness matrix will be 150x150. If these matrices can be arranged in a banded form, with half-bandwidth of only 20 for example, then the arrays that must be stored only number 150x20. Computationally, it will be most efficient to work with 3000 nonzero elements for the banded matrices, as compared to 22,500 elements for the full matrices.

Eq.(3-9) can be adapted to employ the decomposition of the symmetric stiffness matrix. If the stiffness matrix is banded, with half bandwidth b_w, then the upper triangular Cholesky factor is also banded and has the same bandwidth b_w. Thus K and U can be computed and stored as banded matrices. In actual computations, U usually overwrites K. This procedure significantly reduces computer storage requirements and computation time.

The computational performance of most optimization algorithms is quite sensitive to the number of design variables and/or the number of constraints. Therefore, great care should be taken in formulating optimization problems to keep both of these numbers as low as possible. Design

variable linking is one means of improving computational performance by reducing the structural dimension. Because of practical design considerations such as symmetry in the structure, fabrication, and joint connection costs, it is desirable to require some families of elements of a structure to have the same design variable values. This is known as grouping of elements, or linking of design variables. Elements of the structure are divided into a number of groups and the same design variables are assigned to each group of elements.

One common technique for reducing the number of constraints is called constraint deletion. In the structural optimization process, there may be a large number of constraints, but most of the constraints are not active. The efficiency of the optimization routine is improved if only critical and potentially active constraints are considered. That is, at a given design point we delete constraints which are far from being active at that point. These constraints do not participate for a portion of the design process. Eventually, all the constraints have to be recalculated and the process of constraint deletion repeated.

In the constraint deletion process, we calculate the truncation boundary value with the defined truncation reduction factor. In the optimization process, all the active constraints will be considered if the constraint is over the truncation boundary value. By reducing the number of constraints considered at each stage in the design

process by temporary deletion of inactive and redundant constraints, we can increase the efficiency of the computational algorithm.

The last computational consideration is the "Worst" stress case design. This consideration becomes important if there are too many constraints which have to be considered in the design process, and/or the design optimization algorithm does not have the capability to handle this many constraints. The worst stress case in this research is defined as the case with the greatest combined stress magnitude among all of the sampling stress points at each end of the finite element. The total number of constraints treated in optimal structural design is quite large, so an effort should be made to logically consider the worst stress constraints to eliminate redundant constraints.

In the case of stress constraints, the worst violation among elements of a group, over all loading conditions, may be treated instead of enforcing a constraint on each element under each loading condition. Thus the ith stress constraint may be expressed as

$$g_i = \sum_{j=1}^{NMi} \sum_{n=1}^{NLC} \text{Max}\{ g_{ij}(X, r^n) \} \geq 0 \qquad (6\text{-}1)$$

where NMi = the number of element in the ith group

NLC = the number of loading conditions

r^n = displacement in the nth loading case

Similarly, a displacement constraint is composed on the the worst violation over all loading considerations as

$$g_i = \sum_{n=1}^{NLC} \text{Max}\{g_{in}(X, r^n\} \geq 0 \qquad (6\text{-}2)$$

With this worst case, the number of constraints that must be treated at each iteration is reduced considerably. This technique improves the efficiency of the algorithm.

6.3 Test Problems

Six examples were used for testing the optimization procedure.

1. Nine element space frame structure
2. Portal frame structure
3. Bartel structure
4. Thirty-Three frame structure
5. Seven frame structure
6. Car seat frame structure

6.3.1 Nine element space frame structure

A problem of minimum volume design of a spatial structure subjected to geometrical, displacement, and stress constraints is now considered. Geometric constraints are

placed on the cross section dimensions of the structure and stress constraints are based on the maximum combined normal and shear stresses.

In this section, the optimal design of framed structures using circular cross sections is considered. The structure is loaded by distributed forces that are applied at the top of the structure along each of the top members as shown in Fig.6-4(a) and Fig.6-4(b). The finite element model of this structure is represented in Fig.6-4(c).

The structure is composed of 9 members, 9 joints and 3 fixed supports. Design variables in this problem are the thickness(t) and diameter(D) of the cross section of the individual members. The design objective is to choose the element cross section dimensions so that the space frame is as light as possible, while satisfying constraints on stresses and displacements.

The objective function F is taken as the total volume of the structure. The total structural volume is calculated through multiplication of the element length and element area. The objective function for the space frame is expressed as Eq.(6-3), in which L_i is the element length and A_i is the element area. The summation in Eq.(6-3) is over all the members of the space frame.

$$F(X) = \sum_{i=1}^{9} L_i A_i \qquad (6\text{-}3)$$

$$L_i = \mathrm{SQRT}[(X_j - X_k)^{**2} + (Y_j - Y_k)^{**2} + (Z_j - Z_k)^{**2}] \qquad (6\text{-}4)$$

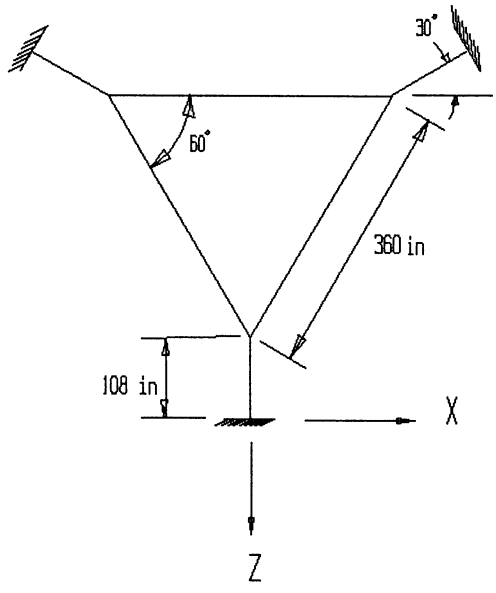

(a) Top View of Structure

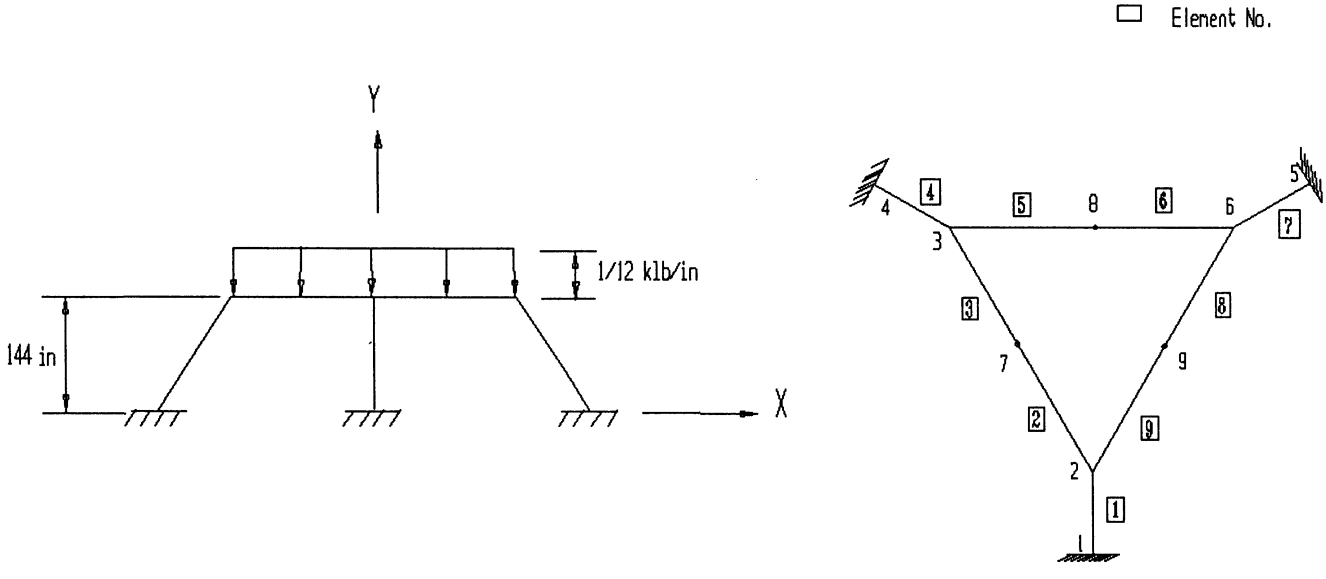

(b) Front View of Structure

(c) Finite element Model

Fig. 6-4 Space Frame Structure

$$A_i = 3.14159 * D_i * t_i \qquad (6\text{-}5)$$

Where X_j, Y_j, Z_j are the coordinate point of ith member at the near end.

X_k, Y_k, Z_k are the coordinate point of ith member at the far end.

D_i, t_i are its design variables.

The combined stresses limit is 24.9Kip/in^2 for all the member elements. Young's modulus and shear modulus are 30,000 kips/in^2 and 12,000 kips/in^2, respectively. The displacement limit at node 7, 8, and 9 in the y direction is 2.0 inches and the displacement limit at node 2, 3, and 6 in the y direction is 0.06 inch. The upper limit on diameter, lower limit on diameter, upper limit on thickness, and lower limit on thickness are 15.0in, 1.5in, 0.75in, and 0.075in, respectively. Initially, the volume of the structure is 30892.6 in^3. After six iterations, the volume was reduced to 13971.8 in^3 which is within 0.13 % of the optimum volume. With an additional four iterations, the design optimization process forces the design to move to a more feasible area. In this design, the displacement limits at 2, 3 and 6 are active. Finally, the volume of the optimum design for this structure is found to be 13783.9 in^3.

Considering the variable geometry that node 4 and node 5 are allowed to move in the X direction. The optimum volume is changed to 12372.5in^3. The node 4 and node 5 are moved to -272.1 in and 272.1 in, respectively. The optimum

results for sizing change only and sizing and confingurational change subject to displacement constraints and stress constraints are given in Table 6-1.

Table 6-1 Optimum results subjected to displacement and stress constraints (unit:inch)

Element & Design Variable	Optimum Value	
	Sizing Change Only	Sizing & Configurational Change
Element 1		
Diameter	10.0008	10.0578
Thickness	0.325068	0.315267
Element 2, 3		
Diameter	11.3681	15.0
Thickness	0.229158	0.100986
Element 4		
Diameter	10.063	10.148
Thickness	0.321124	0.307213
Element 5, 6		
Diameter	14.98	14.9806
Thickness	0.103235	0.10273
Element 7		
Diameter	10.7487	11.0615
Thickness	0.230893	0.2171
Element 8, 9		
Diameter	13.5008	13.5014
Thickness	0.263246	0.263107
Volume in^3	13783.928	12372.5041

6.3.2 Portal Frame Structure

In this section, the optimal design of framed structures using open channel cross sections is considered. It considers the problem of minimum volume design of the portal structure subjected to geometrical, displacement, and stress constraints is now considered. A concentrated load of 15 kips is applied in the positive X direction and negative Y direction on the shear center at node 4. The portal frame structure and finite element model are shown in Fig.6-5(a) and Fig.6-5(b), respectively.

A geometric constraints are placed on the cross section dimensions of the structure. The design data and cross section limit are shown in Table 6-2. Stress constraints are based on the maximum combined normal and shear stresses. The allowable yield stress is 24.9kips/in^3. Design variables in this problem are the cross section thickness(t), web height(H) , and flange width (B) of the individual members. The design objective is to choose the element cross section dimensions so that the portal frame structure is as light as possible, while satisfying constraints on stresses and displacements.

The objective function F is taken as the total volume of the structure. The total structure volume is calculated through multiplication of the element length and element area. The objective function for the portal frame is expressed as Eq.(6-6), in which L_i is the element length and

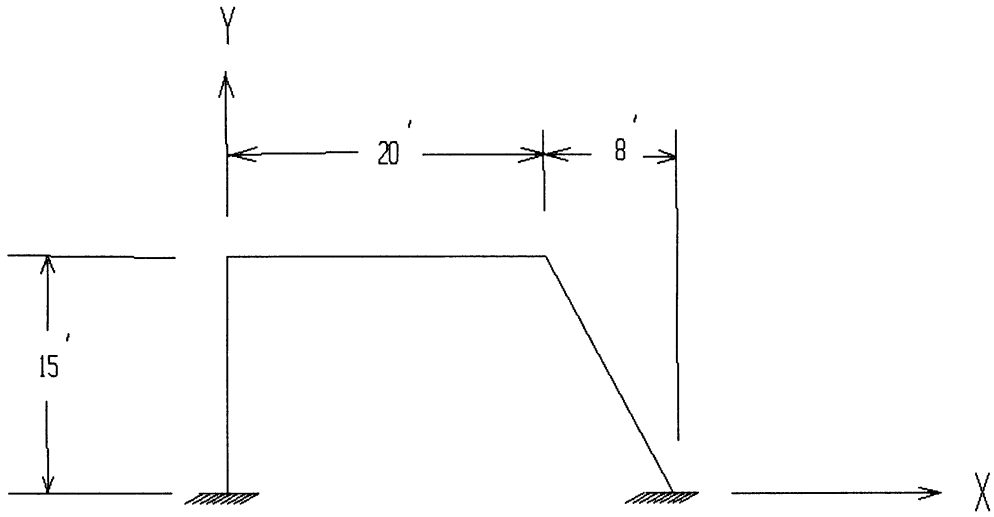

(a)Portal Frame

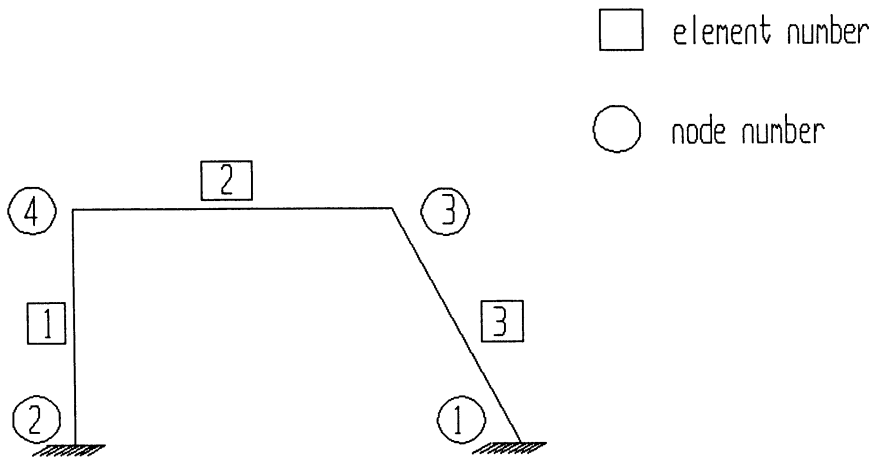

(b)Finite Element Model

Fig.6-5 Portal Frame Stucture

A_i is the element area. The summation in Eq.(6-6) is over all the members of the portal frame.

$$F(X) = \sum_{i=1}^{3} L_i A_i \qquad (6\text{-}6)$$

$$L_i = \text{SQRT}[(X_j-X_k)**2 + (Y_j-Y_k)**2 + (Z_j-Z_k)**2] \qquad (6\text{-}7)$$

$$A_i = (2*B_i + H_i)* t_i \qquad (6\text{-}8)$$

Where X_j, Y_j, Z_j are the coordinate point of ith member at the near end.

X_k, Y_k, Z_k are the coordinate point of ith member at the far end.

H_i, B_i, and t_i are its design variables.

The displacement limit at node 3 and node 4 in the x direction is 0.5 inches. Initially, the volume of the structure is 10156.8 in^3. After seven iterations, the volume is optimized to 6375.3 in^3. Next, the variable geometry is considered with the change of x coordinate of node 1. The final optimal volume is changed to 6369.094 in^3. The x coordinate of node 1 is moved to 338.27 inches. The optimal result for sizing change only and sizing and configurational change subject to displacement constraints and stress constraints are given in Table 6-3.

The stress concentration at the reentrant corners in the open channel was considered in the stress calculation.

The inside sampling point within the cross section was taken for stress calculation. The radius of the fillet is assumed to be equal to the thickness of the cross section of the element. Actually, the maximum torsional shear stress at the fillet is 74 percent greater than at the edge of the element.

Table 6-2 Design data for portal frame

Parameter	Value
Modulus of elasticity	E=30000 Kips/in^2
Shear modulus	G=12000 Kips/in^2
Upper limit on height	15.00 inches
Lower limit on height	5.00 inches
Upper limit on width	12.00 inches
Lower limit on width	4.00 inches
Upper limit on thickness	0.75 inches
Lower limit on thickness	0.075 inches

The cross sectional force will produce normal stresses and shear stresses. Each of these will be composed of the sum of the stresses due to axial force, bending, and torsion. Within the elastic limits of the assumptions, we can superimpose these stresses. In this example, it is assumed that the torque is constant throughout the length of the member and also the warping displacements are

unrestrained. So, the warping stress was not considered in this example. In some practical cases, the warping stresses must be considered when the warping of the cross section is restrained. This is one of the limitations in this open channel design.

Table 6-3 optimum results subjected to displacement and stress constraints (unit:inch)

	optimum result	
Element & Design Variable	sizing change	sizing & configurational change
Element 1		
Width	4.00	4.0
Height	15.00	15.0
Thickness	0.5273	0.5275
Element 2		
Width	4.0	4.0
Height	14.0472	13.8049
Thickness	0.412068	0.415433
Element 3		
Width	4.0	4.0
Height	15.0	15.0
Thickness	0.428793	0.426326
Volume in^3	6375.327	6369.09

6.3.3 Bartel Structure

The next structure was considered by Bartel[2] and is chosen here for comparison purposes. This structure consists of two cantilevered beams lying in the x-z plane. The beams are mutually perpendicular and jointed at their ends by rigid joints. Fig.(6-6) shows this structure.

The structure consisting of rectangular, hollow beams is treated. The structure is loaded by force that is applied at the joint locations. The force, bending moments and twisting moments are transmitted from member to member. Bending, shear, extension and twisting effects in each member are considered.

The optimal design of the structure subjected to geometrical, displacement, and stress constraints is considered. Geometrical constraints are placed on the cross section dimensions of the structure. A displceament constraint is imposed on the second node in the y direction. Stress constraints are based on maximum distortion energy failure criteria. Fig.(6-7) shows the design variables in the member cross section. The design objective is to minimize volume, and satisfy the displacement constraint, stress constraints and design variable bounds.

The volume of the frame is shown in Eq.(6-9). In Eq.(6-6), L_i is the length of the ith member, A_i is the area of ith member. A_i and L_i are expressed in Eq.(6-10) and Eq.(6-11), respectively, and t_i, d_i, and h_i are its design

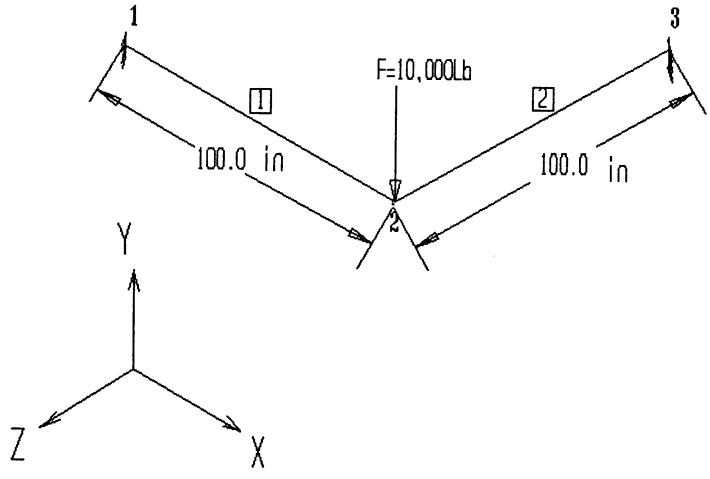

Fig. 6-6 Bartel Structure

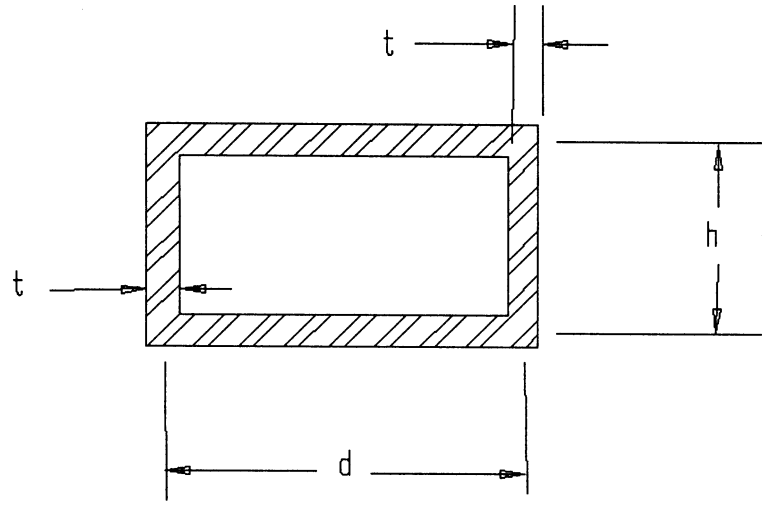

Fig. 6-7 Cross Section of Bartel Structure

variables. The summation of Eq.(6-9) is over both members of the frame.

$$V = \sum_{i=1}^{n} V_i = \sum_{i=1}^{n} A_i L_i \qquad (6\text{-}9)$$

$$L_i = \mathrm{SQRT}[X_j - X_k)^{**2} + (Y_j - Y_k)^{**2} + (Z_j - Z_k)^{**2}] \qquad (6\text{-}10)$$

$$A_i = 2t_i d_i + 2t_i h_i \qquad (6\text{-}11)$$

Where X_j, Y_j, Z_j are the coordinate point of ith member at the near end.

X_k, Y_k, Z_k are the coordinate point of ith member at the far end.

d_i, h_i, t_i are its design variables.

n is the number of the element.

In formulating stress constraints, one needs to perform a stress analysis of the frame. Stresses in members can be computed from the nodal displacements of the frame. The following set of generalized displacements(state variables) is defined for the two member frame shown in Fig.(6-6).

1. z_1 = the vertical displacement of joint 2.
2. z_2 = the angle of rotation of joint 2 about the Z axis.
3. z_3 = the angle of rotation of joint 2 about the X axis.

z_2 is the slope of the X axis at joint 2 due to bending. It is also the angle of twist for the Z axis. Similarly, z_3 plays a dual role as the slope of the Z axis and angle of twist of the X axis.

A constraint is placed on the maximum stress that occurs in the frame. This stress is calculated from maximum distortion energy failure criteria, using the expression

$$\sigma_f = \text{SQRT}(\sigma^2 + 3\ T^2) \qquad (6\text{-}12)$$

where σ is normal stress that results from the axial force and plane bending moment of the members and T is shear stress that results from shear force and twisting moment of the members. σ_f is the combined stress. SQRT is the square root of the function value. A stress constraint at each of eight sampling points at each end is now written as

$$\text{SQRT}(\sigma^2 + 3\ T^2) - \sigma_{max} = 0 \qquad (6\text{-}13)$$

where σ_{max} is the maximum yield stress. The sampling points on the rectangular cross section are described in Sec.(3-4).

The design data for the Bartel structure is shown in Table(6.4). The algorithm of Sec.(6-2) is applied directly to the preceding design formulation.

The initial values of the design variables for the Bartel structure subjected to stress constraints are shown in Table 6-5. Initially, the volume of the structure is 6480 in^3 with no stress violation. This design has 32 stress constraints, but only 16 constraints are active at the optimum. The active constraints exist at both of the fixed ends. In Table 6-5 the results from this solution are compared to that given by Bartel. One can see by the number

of iterations required, this method possess a suitable convergence property.

Next a study is made for this structure when the design is subjected to stress constraints and a displacement constraint. The displacement limitation at node 2 in the y direction is 0.65 in. The initial value and optimum value for this study are shown in Table 6-6. The displacement constraint is active during the entire optimization process. The optimum volume of the structure is 770.361 in^3.

Table 6-4 Design Data for Bartel Structure

Parameter	Value
Modulus of Elasticity	$E=3x10^7$ psi
Material	Steel
Poisson's Ratio	0.3
Upper limit on height	10.00 inch
Lower limit on height	2.5 inch
Upper limit on width	10.00 inch
Lower limit on width	2.5 inch
Upper limit on thickness	1.0 inch
Lower limit on thickness	0.1 inch
Maximum yield stress	40,000 psi

Table 6-5 Initial Data and Optimum Data of the Bartel Structure Subjected to Stress Constraints (unit: inch)

Design Variable	Initial Value	Optimum Value	
		Bartel	This Work
h_1	9.0	10.00	8.2404
d_1	9.0	9.547	10.0
t_1	0.9	0.1	0.1
h_2	9.0	10.00	8.2404
d_2	9.0	9.547	10.0
t_2	0.9	0.1	0.1
Volume (in^3)	6480	773.9	729.616
# of iterations		15	4

The variable geometry problem simultaneously considered the size of the dimensions of the elements and joint coordinates. In this example, node points 1 and 2 are fixed and the X and Z coordinates of the node 3 are allowed to vary. Table 6-7 shows the summary of the results for the variable geometry case. It shows the optimum result was reduced from 729.616 in^3 to 701.316 in^3.

The iteration history for the fixed geometry and variable geometry cases is shown in Fig.(6-8). It shows the convergence rate is quite good. As can be seen in the fixed

geometry case, the actual volume is reduced to a value within 5% of the optimum value after one iteration. From design iterations 2 to 4, the optimization routine tries to force the design into a more feasible region.

Table 6-6 Initial Data and Optimum Data of the Bartel Structure Subjected to Stress and Displacement Constraints.

	Initial Value	Optimum Value
h_1	9.0 inch	9.2286 inch
d_1	9.0 inch	10.00 inch
t_1	0.9 inch	0.1 inch
h_2	9.0 inch	9.2899 inch
d_2	9.0 inch	9.9996 inch
t_2	0.9 inch	0.1 inch
Volume	6480 in^3	770.361 in^3

The stress concentration in the fillet inside the rectangular cross section was not considered in this example. According to the design tables for stress concentration factors by Peterson[3], the maximum torsional shear stress at the fillet is 25 percent greater than that on the edge of the element if the radius of the fillet ie equal to the thickness of the element. However, the normal stress in the fillet is smaller than the outside edge of the

element. From the point of view of the maximum combined stress, we consider the sampling point at the outside edge of the element instead of the inside fillet point.

This simple example shows that the structural optimization algorithm used is very efficient in this particular application. The gradient method appears to be superior to the extended quadratic interior penalty function optimization method[4]. It is also noted here that the maximum yield stress 40,000 psi used in example is only for the purpose of comparison. In actual design practice, one must include a safety factor.

Table 6-7 Initial Data and Optimum Data of the Bartel Structure for Variable Geometry

	Initial Value	Optimum Value
h_1	9.0 inch	6.0404 inch
d_1	9.0 inch	9.9997 inch
t_1	0.9 inch	0.10 inch
h_2	9.0 inch	9.9999 inch
d_2	9.0 inch	9.9995 inch
t_2	0.9 inch	0.1 inch
Volume	6480 in^3	701.306 in^3
X coordinate of Joint 3	100.0	105.0
Z coordinate of Joint 3	-100.0	-95.0

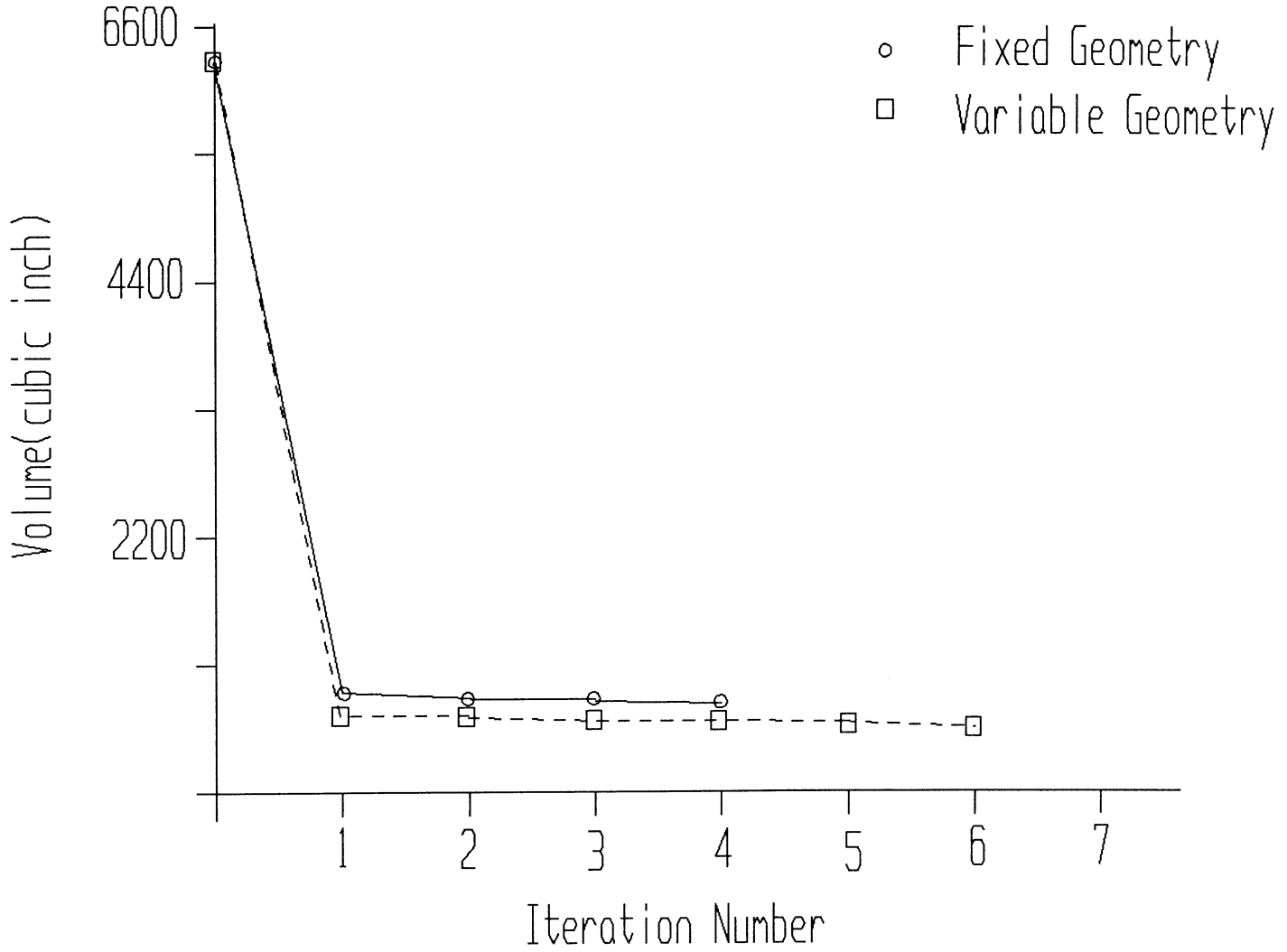

Fig.6-8 Design History of Bartel Structure

6.3.4 Thirty-Three Frame Structure

The automobile structure used today is an assemblage of sheet metal stampings made rigid by properly placed beam, columns, and corrugations. In the case of most U.S. made smaller cars, so-called compacts and subcompacts, the structure is constructed as a unit-body module. In these vehicles, the body, frame, and front sheet metal(except the outer front fenders) are constructed as a single structural unit welded together. Beam members are used in the unit-body structure to provide the required structural stiffness. In order to reduce weight and fuel consumption, the unit-body structure is very attractive.

A typical prototype thirty-three unit-body structure model shown in Fig.(6-9) is treated as an example of sizing and configurational change for optimal structural design. The structure is modeled as a 33-member frame with 22 joints and 120 degrees of freedom. The joint numbering and member numbering of the finite element model are shown in Fig.(6-10). The geometry coordinates of the finite element nodal points for the frame structure are given in Table 6-8. The member locations for the structure are given in Table 6-9. The top view and side view showing the side of the whole body are given in Fig.(6-11) and Fig.(6-12).

The problem is to minimize the total weight of the structure and at the same time to ensure the member stress

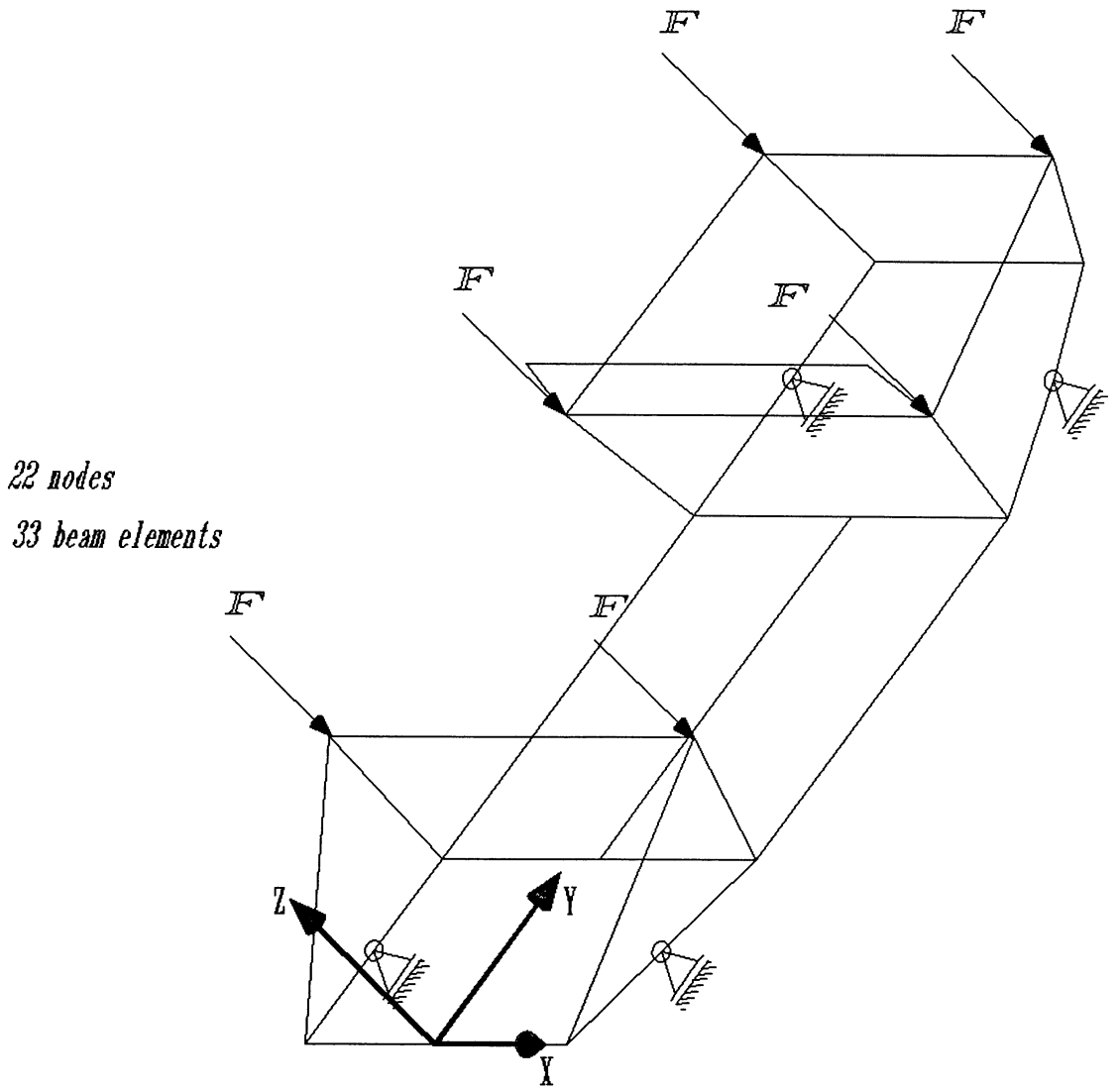

Fig.6-9 Thirty-Three Frame Structure

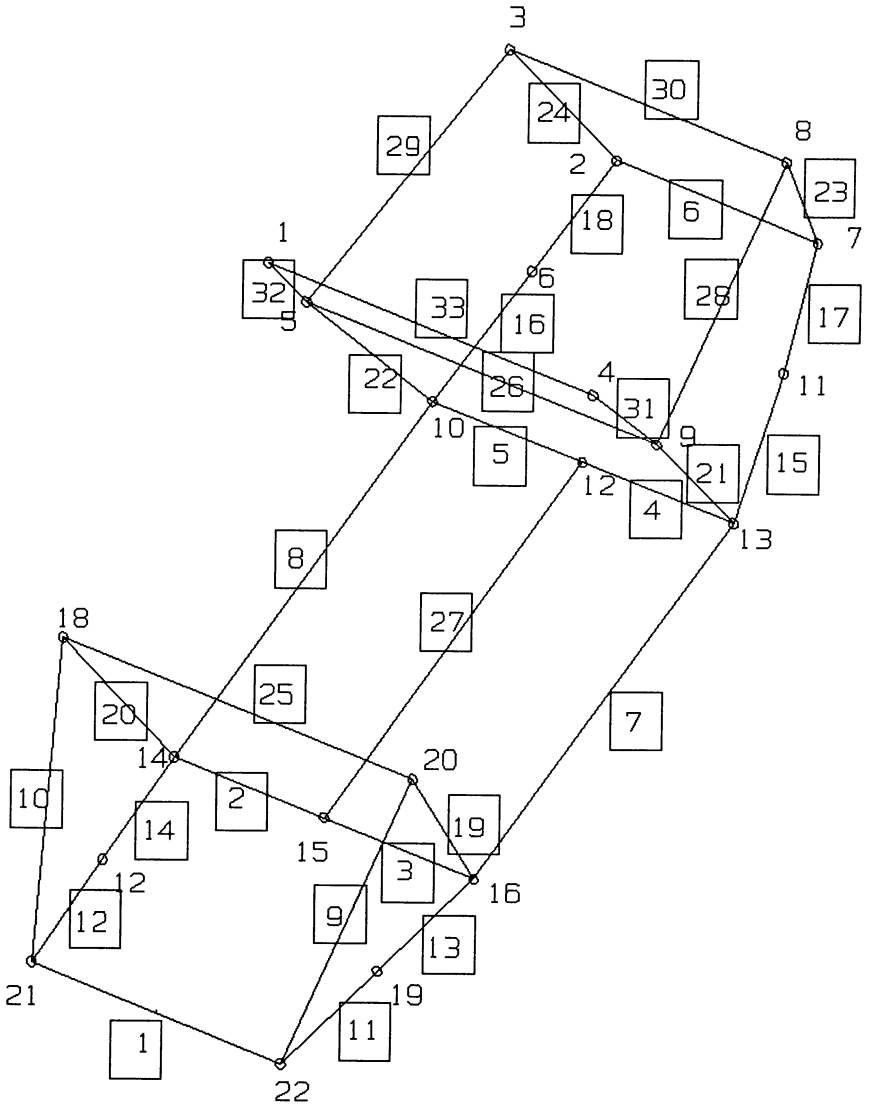

Fig.6-10 Finite Element Model of Thirty-Three Frame Structure Showing Joint and Member Numbering

TABLE 6-8 The Geometry Coordinates of Nodal Points for Thirty-Three Frame Structure
(Unit : cm)

JOINT	Coordinate in Direction X	Y	Z
1	-130.00	270.00	80.00
2	-80.00	380.00	10.00
3	-110.00	390.00	60.00
4	130.00	270.00	80.00
5	-140.00	270.00	50.00
6	-100.00	330.00	0.00
7	80.00	380.00	10.00
8	110.00	390.00	60.00
9	140.00	270.00	50.00
10	-120.00	270.00	-10.00
11	100.00	330.00	0.00
12	0.00	270.00	-10.00
13	120.00	270.00	-10.00
14	-120.00	100.00	-10.00
15	0.00	100.00	-10.00
16	120.00	100.00	-10.00
17	-110.00	50.00	-5.00
18	-140.00	110.00	50.00
19	110.00	50.00	-5.00
20	140.00	110.00	50.00
21	-100.00	0.00	0.00
22	100.00	0.00	0.00

TABLE 6-9 Element Group and Connectivity Data of Thirty-Three Frame Structure

MEMBER NO.	GROUP NO.	NEAR END	FAR END	MEMBER NO.	GROUP NO.	NEAR END	FAR END
1	1	22	21	2	1	15	14
3	1	16	15	4	1	13	12
5	1	12	10	6	1	7	2
7	2	16	13	8	2	15	12
9	2	22	20	10	2	21	18
11	3	22	19	12	3	21	17
13	3	19	16	14	3	17	14
15	4	13	11	16	4	10	6
17	4	11	17	18	4	6	2
19	5	16	20	20	5	14	18
21	6	13	9	22	6	10	5
23	6	7	8	24	6	2	3
25	7	20	18	26	7	9	5
27	7	14	10	28	7	9	8
29	7	5	3	30	7	8	3
31	8	9	4	32	8	5	1
33	8	4	1				

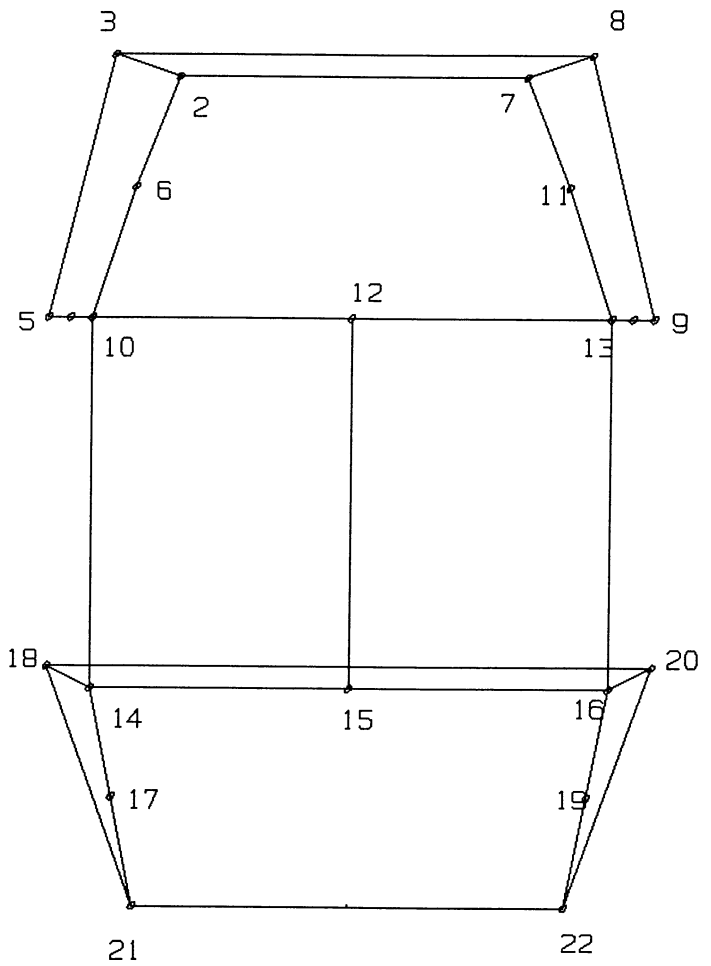

Fig. 6-11 Top View of Thirty-Three Frame Structure

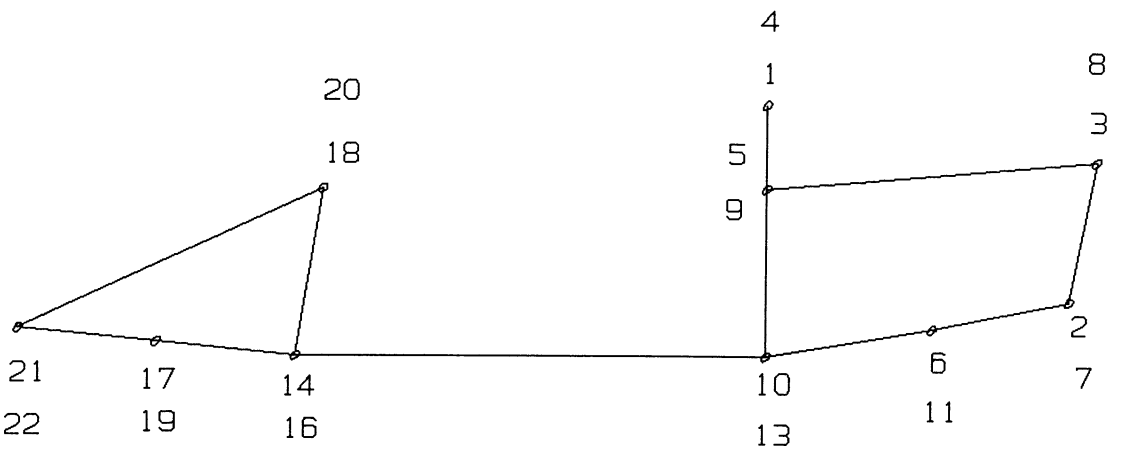

Fig.6-12 Side View of Thirty-Three Frame Structure

and nodal displacements are satisfied under the loading conditions.

The design parameters to be calculated are the cross sectional dimensions of the members and the coordinates of the joints. An upper and lower bound constraint is also imposed on cross section dimensions and coordinates of the joints.

The members of the thirty-three frame structure are taken to be tubular rectangular sections. The stress constraints are based on the maximum distortion energy failure criteria. In stress analysis, the twisting, bending, shear, and normal(extension and compression) of the members are to be calculated. The loading data for the thirty-three frame structure, listed in Table 6-10, were used to compute the stress.

Design data for the structure is given in Table 6-11. To maintain symmetry and to facilitate fabrication of the structure, 33 members of the structure are divided into a total of eight groups and each group is assigned three design variables.

The grouping of members, with members of a group required to have the same cross sectional area, is used to maintain symmetry in the structure. The grouping data is shown in Table 6-12.

Table 6-10 Loading Data for Thirty-Three Frame Structure

Loading Case	Node	load component in direction		
		X	Y	Z
I	2	1250 Nt	0	-1250 Nt
	21	1250 Nt	0	-1250 Nt
II	5	0	0	-1500 Nt
	3	0	0	-1500 Nt
	8	0	0	-1500 Nt
	9	0	0	-1500 Nt
	18	0	0	-1500 Nt
	20	0	0	-1500 Nt

Table 6-11 Design data for Thirty-Three Frame Structure

Parameter	Value
Material	Steel
Modulus of Elasticity	2.07×10^{7} Nt/cm^3
Material density	2.77×10^{-2} Kg/cm^3
Maximum yield stress	1.725×10^{4} Nt/cm^2
Upper limit on thickness	1.25 cm
Lower limit on thickness	0.125 cm
Upper limit on width	13.5 cm
Lower limit on width	2.5 cm
Upper limit on height	13.5 cm
Lower limit on height	2.5 cm

Table 6-12 Grouping Number for Thirty-Three Frame Structure

Group Number	Member Number
1	1 - 6
2	7 - 10
3	11 - 14
4	15 - 18
5	19 - 20
6	21 - 24
7	25 - 30
8	31 - 33

The initial values of the design variables for loading case one are listed in Table 6-13(A). Initially, the volume of the structure with loading case one is 1507.26 cm^3 with no stress constraint violation. After seven design iterations, it is reduced to 210.33 cm^3, a design value within 9.0% of the optimum value found which could be reduced further by continuing the optimization process. The summary of the results under load case one is shown in Table (6-14).

The initial values of the design variables for loading case two are listed in Table 6-13(B). Initially, the volume of the structure for load case two is 1171.53 cm^3 with no stress constraint violation. After ten design iterations, an optimum value was achieved in the the optimization process.

The summary of the results under load case two is shown in Table (6-15).

Table 6-13(A) Initial Data for Thirty-Three Frame Structure for Loading Case One. (unit: cm)

Group Number	Element Number	Initial Data		
		Width	Height	Thickness
1	1-6	6.5	5.5	0.6
2	7-10	5.5	5.5	0.6
3	11-14	4.5	3.5	0.6
4	15-18	4.5	6.5	0.6
5	19-20	4.5	5.5	0.6
6	21-24	7.3	5.3	0.6
7	25-30	4.95	6.26	0.6
8	31-33	5.8	4.8	0.6

Initial Weight: 1507.26 Kg

Considering the variable geometry, The X coordinate of nodes 7, 11 and the X coordinate of nodes 2 and 6 are allowed to move. By considering the combination of the cross sectional dimensions and joint coordinates in the optimization, a considerable weight reduction is achieved as a result of changes in the geometry. The optimum design for the thirty-three frame structure due to coordinate changes for loading one and two is given in Table 6-16(A) and Table 6-16(B), respectively. Comparing the results for both the

case of fixed geometry and variable geometry, an improvement 4.7% over the normal condition for loading case one and 2.0% over loading case two was achieved. There is essentially no penalty in the weight of the structure.

Table 6-13(B) Initial Data for Thirty-Three Frame Structure for Loading Case Two (unit: cm)

Group Number	Element Number	Initial Data		
		Width	Height	Thickness
1	1-6	6.5	6.5	0.4
2	7-10	6.5	6.5	0.4
3	11-14	6.5	6.5	0.4
4	15-18	6.5	6.5	0.4
5	19-20	6.5	6.5	0.4
6	21-24	6.5	6.5	0.4
7	25-30	6.5	6.5	0.4
8	31-33	6.5	6.5	0.4

Initial Weight: 1171.53 Kg

The convergence characteristics of the optimization process for fixed geometry is indicated by the design history shown in Fig. (6-13). One can observe that the convergence rate is quite good. For both cases after a few iterations, the weight is very close to the final value. However, the optimization routine is trying to force the design into the feasible region in the subsequent steps.

Table 6-14 Optimum Result for Thirty-Three Frame Structure For Loading Case one (Unit: cm)

Group Number	Element Number	Optimum Data		
		Width	Height	Thickness
1	1-6	2.8867	4.5356	0.125
2	7-10	2.50	2.50	0.125
3	11-14	5.64197	2.50	0.125
4	15-18	4.2421	5.96304	0.125
5	19-20	3.61984	2.5	0.125
6	21-24	5.7448	3.46017	0.125
7	25-30	2.5	2.5	0.125
8	31-33	3.48589	2.58375	0.125

Optimum Weight: 189.09794 Kg

Loading Case one

It is also noted here that all design variables associated with the thickness of members for this example are at their lower bounds at the optimum. This indicates that the lower bound on the thickness, selected on the basis of local buckling considerations, is critical in that design. Therefore, in many practical design problems it may be possible to fix the member thickness based on just local buckling considerations. This will reduce the number of

design variables for the problem, which will result in further computational efficiencies.

The design variable linking is imposed to account for maintaining a symmetrical structure. In some cases, it is possible to change the grouping structure for practical application.

Table 6-15 Optimum Result for Thirty-Three Frame Structure for Loading Case Two.
(Unit: cm)

Group Number	Element Number	Optimum Data		
		Width	Height	Thickness
1	1-6	2.5001	2.5	0.125
2	7-10	2.5007	5.0679	0.125
3	11-14	2.7109	3.3149	0.125
4	15-18	8.6686	3.1785	0.125
5	19-20	3.9574	4.2215	0.125
6	21-24	12.3777	4.4396	0.125
7	25-30	8.0733	5.39171	0.125
8	31-33	2.50	2.50	0.125

Optimum Weight: 271.202 Kg

Loading Case two

Table 6-16(A) Optimum Result for Thirty-Three Frame Structure for Variable Geometry under Loading Case one (Unit: cm)

Group Number	Element Number	Optimum Data		
		Width	Height	Thickness
1	1-6	3.0492	4.3273	0.125
2	7-10	2.50	2.50	0.125
3	11-14	5.666	2.50	0.125
4	15-18	3.8979	6.5639	0.125
5	19-20	2.50	2.50	0.125
6	21-24	4.1799	3.93078	0.125
7	25-30	2.50	2.50	0.125
8	31-33	2.50	2.50	0.125

Beginning Coordinate in the x direction at node 7 and 2	80.0	-80.0
Beginning Coordinate in the x direction at note 11 and 6	100.0	-100.0
Final Coordinate in the x direction at note 7 and 2	84.99	-84.99
Final Coordinate in the x direction at note 11 and 6	101.04	-101.04

Optimum Weight: 184.7042 Kg

Loading Case one

Table 6-16(B) Optimum Result for Thirty-Three Frame Structure for Variable Geometry under Loading Case Two (Unit: cm)

Group Number	Element Number	Optimum Data		
		Width	Height	Thickness
1	1-6	2.5006	2.500	0.125
2	7-10	2.50	4.9436	0.125
3	11-14	2.8061	3.4521	0.125
4	15-18	9.51994	2.50138	0.125
5	19-20	3.91954	4.1244	0.125
6	21-24	12.4384	4.3767	0.125
7	25-30	7.6153	5.8028	0.125
8	31-33	2.50	2.50	0.125

Beginning Coordinate in the x direction 80.0 -80.0
at node 7 and 2

Beginning Coordinate in the x direction 100.0 -100.0
at note 11 and 6

Final Coordinate in the x direction 82.0496 -82.0496
at note 7 and 2

Final Coordinate in the x direction 100.176 -100.176
at note 11 and 6

Optimum Weight: 270.99 Kg

Loading Case two

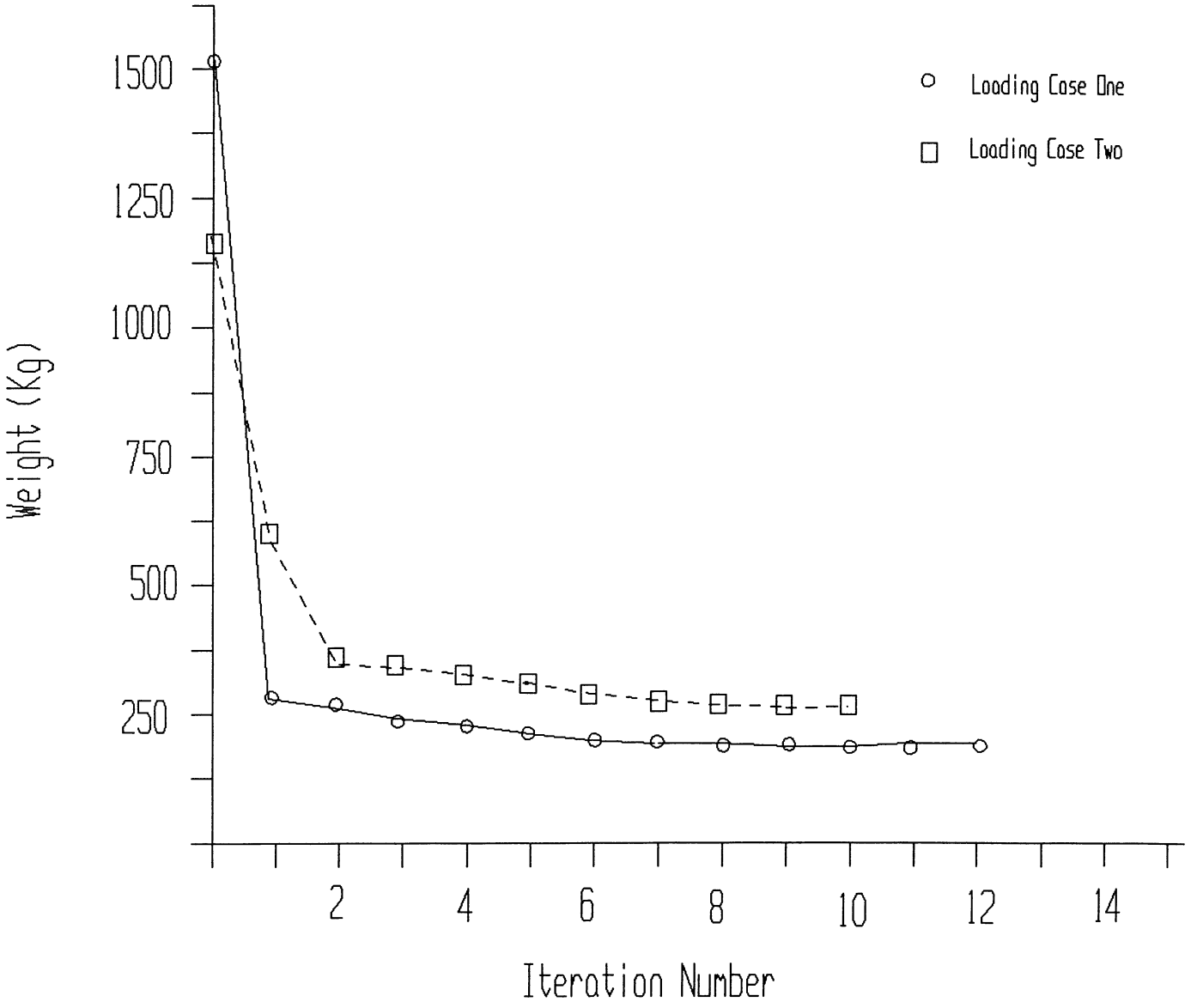

Fig.6-13 Design History of Thirty-Three Frame Structure

6.3.5 Seven Frame Structure

The seven frame structure shown in Fig.(6-14) is now considered. The finite element model, which is shown in Fig.6-14(a), contains five nodal points and seven finite elements. The frame members are all square tubes 7.62 cm on a side. A concentrated load of 3340Nt is applied in the negative x axis and negative y axis at node one. Another concentrated load of 4450Nt is applied in the negative x axis direction and negative y axis direction at node four. The material is steel. The cross section dimensions and loading conditions are shown in Fig.6-14(b) and Fig.6-14(c), respectively. Young's modulus, Poisson's ratio, and material density are $2.07 \times 10^{7} Nt/cm^{3}$, 0.3, $2.77 \times 10^{-2} Kg/cm^{3}$, respectively. The allowable yield stress is 17,250 Nt/cm^{2}.

The design problem is to find the optimum topology of the frame structure, which will minimize the total weight, such that the combined normal and shear stresses are less than the maximum allowable yield stress value and the deflection in the y direction at node 1 is less than 0.6 inch. The wall thickness of each tube cross section is taken as a design variable. In addition, the x coordinate of node 2 is also allowed to move and is treated as a design variable in the design space.

The initial topology of the structure has 7 members, and its optimum mass is 25.3Kg. The thicknesses from member one through seven are 0.06303cm, 0.05945cm, 0.04687cm,

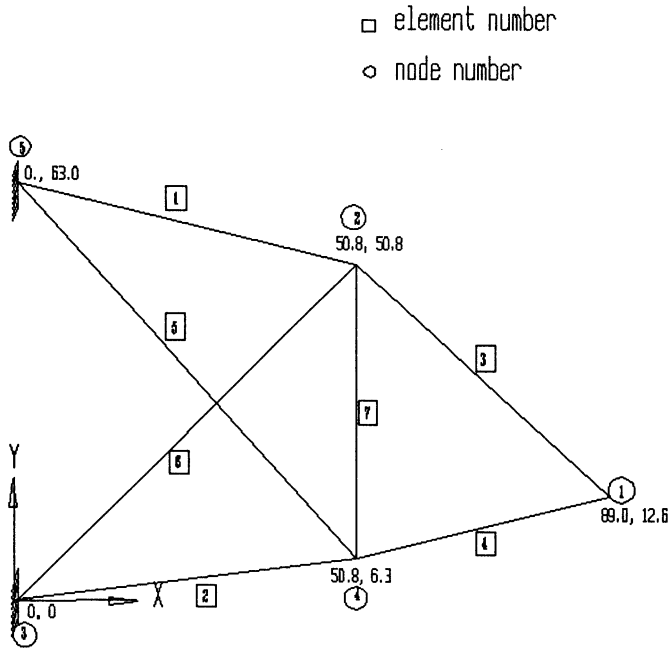

(a)Beam Layout

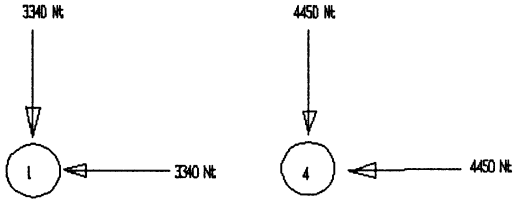

(b)Loading Condition

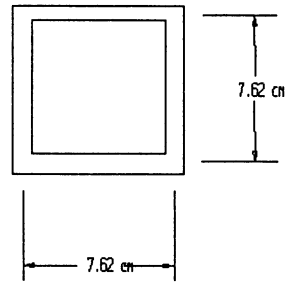

(c)Cross Section

Fig.6-14 Seven Frame Structure

0.09369cm, 0.04cm, 0.1574cm, and 0.07763cm, respectively, and the x coordinate of node 2 is 48.3692 cm. Based on the stress criteria from the last step in the optimization process, member 6 is the most promising member to be deleted in the structure.

After member 6 is deleted from the structure, and the design process procedes to the next subset of the structure. The optimization process is continued and the optimum mass value for the subset of the structure is 21.2567Kg. The design variables for this subset of the structure become 0.04cm, 0.2766cm, 0.04cm, 0.05102cm, 0.04cm, 0.04cm, respectively, and the x coordinate is moved to 46.6999cm.

As can be seen from the previous subset result, the new topology is better than the previous basic structure. The heuristic search process is continued and member 7 is determined to be the next most promising member to delete. Therefore, the algorithm moves to the next state which has only five members in the structure. After it executes the optimization task, the optimum value is found to be 18.2082Kg. The design variables in this subset of the structure are 0.04cm, 0.08166cm, 0.04cm, 0.2413cm, 0.50652cm, respectively, and x coordinate of node 2 is changed to 47.6699 cm.

The previous result have been improved again, so the heuristic search process procedure to the next subset of the structure and member 5 is to be deleted. Finally, the search process goes to the final state which only has four

members in the structure. The final optimum value for the four member structure is 32.1Kg. It is found that the new design is not better the previous design, so the design process is terminated. The entire search processes in sequence as obtained by the optimization is shown in Fig. 6-15.

Next study demonstates this frame structure designed with cross sectional dimensional change and the change of X and Y coordinate of node 2 and node 4. It allowed the X and Y coordinate of node 2 and node 4 to move as much as possible in the optimization. Starting from the initial topology with 7 members, the structure is optimized under the sizing and configurational change. The result showed coordinate change of node 2 and node 4 to make element 1 and 3, and element 2 and 4 to become a straight line. The optimal coordinate change for X coordinate of node 2, Y coordinate of node 2, X coordinate of node 4, and Y coordinate of node 4 is 41.76cm, 39.34cm, 46.96cm, and 6.6cm, respectively. The optimal thickness for this initial topology is 0.07106cm, 0.372568cm, 0.05419cm, 0.08597cm, 0.04cm, 0.3458cm and 0.11106cm. From the previous optimization result, member 6 is the most promising member to be deleted. After member 6 is deleted from structure, the structure is optimized with 6 members. The final optimal mass for second topology is improved, member 7 is deleted from the topology. Then, the structure continue to be optimized with 5 members. The final mass for this topology

is 19.03kg. The optimal mass is improved again, member 5 is deleted from the topology. But the final mass is not improved, therefore the design process is terminated. The optimization path with sizing change and coordinate change is shown in Fig.6-16.

We develop and rely on heuristic methods to identify which member should be deleted to improve the final design. The method is presented to indicate how one can perform this particular analysis task. Because of the extreme cost of the basic structural analysis, we are forced to discard exhaustive search as an approach in deletion. However, the heuristic will introduce some possibility of choosing the wrong members to delete. When using a deletion method based on stress criteria, some false steps can be involved to check if this happens.

Optimization Path	Configuration	Mass
Initial	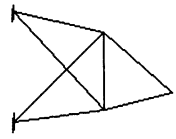	25.307Kg
1st	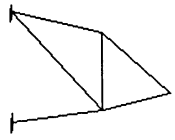	21.2569Kg
2nd	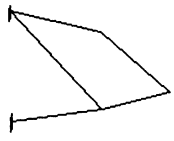	18.2082Kg
3rd	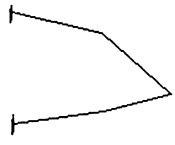	32.1249Kg
Final	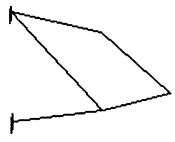	18.2082Kg

Fig. 6-15 Topological Optimization Path

optimization path initial	first	second	third	fourth
topology	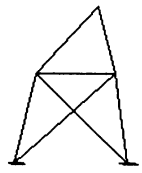	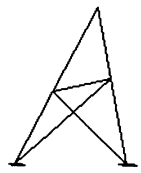	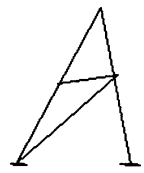	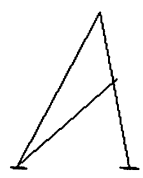	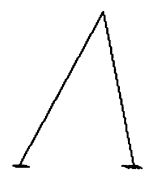
optimal mass (Kg)	45.70	31.53	19.03	35.44
x(1)	0.07106	0.05878	0.04	0.12462
x(2)	0.37257	0.41973	0.09258	0.32047
x(3)	0.054186	0.048146	0.04	0.109521
x(4)	0.08597	0.148168	0.229296	0.349763
x(5)	0.04	0.04	0.058939	
x(6)	0.345860	0.0839743		
x(7)	0.11106			
x at node 2	41.7651	41.766	41.766	41.766
y at node 2	39.3456	39.3468	39.347	39.347
x at node 4	46.9688	46.9693	46.9698	46.97
y at node 4	6.65078	6.65035	6.65073	6.65001

Fig.6-16 Topological optimization path

6.3.6 Car Seat Frame Structure

The final test problem is a vehicle seat frame structure; which was designed for optimal volume and geometry subject to multiple load conditions with displacement and stress constraints. The seat frame structure is shown in Fig.(6-17). The finite element model considered herein is to simplify the structure. It was idealized with 71 beam elements, 60 nodes and 351 degrees of freedom. The element numbering and joint numbering of the finite element model is shown in Fig.6-18(a) and Fig.6-18(b).

The geometry coordinates of the nodal points for the car seat frame are given in Table 6-17. The member locations for the structure are given in Table 6-18. The top view and its section view are shown in Fig.6-19(a) and Fig.6-19(b). The front view and side view of the seat frame structure are given in Fig.(6-20) and Fig.(6-21).

The use of hollow circular sections and rectangular sections as structural components has increased considerably in recent years. These sections are unsurpassed in their efficiency, especially when weight and appearance become important design considerations or when weight saving may be a substantial economical consideration.

Due to weight saving and symmetry maintenance, the structure is divided into 8 groups where elements of each

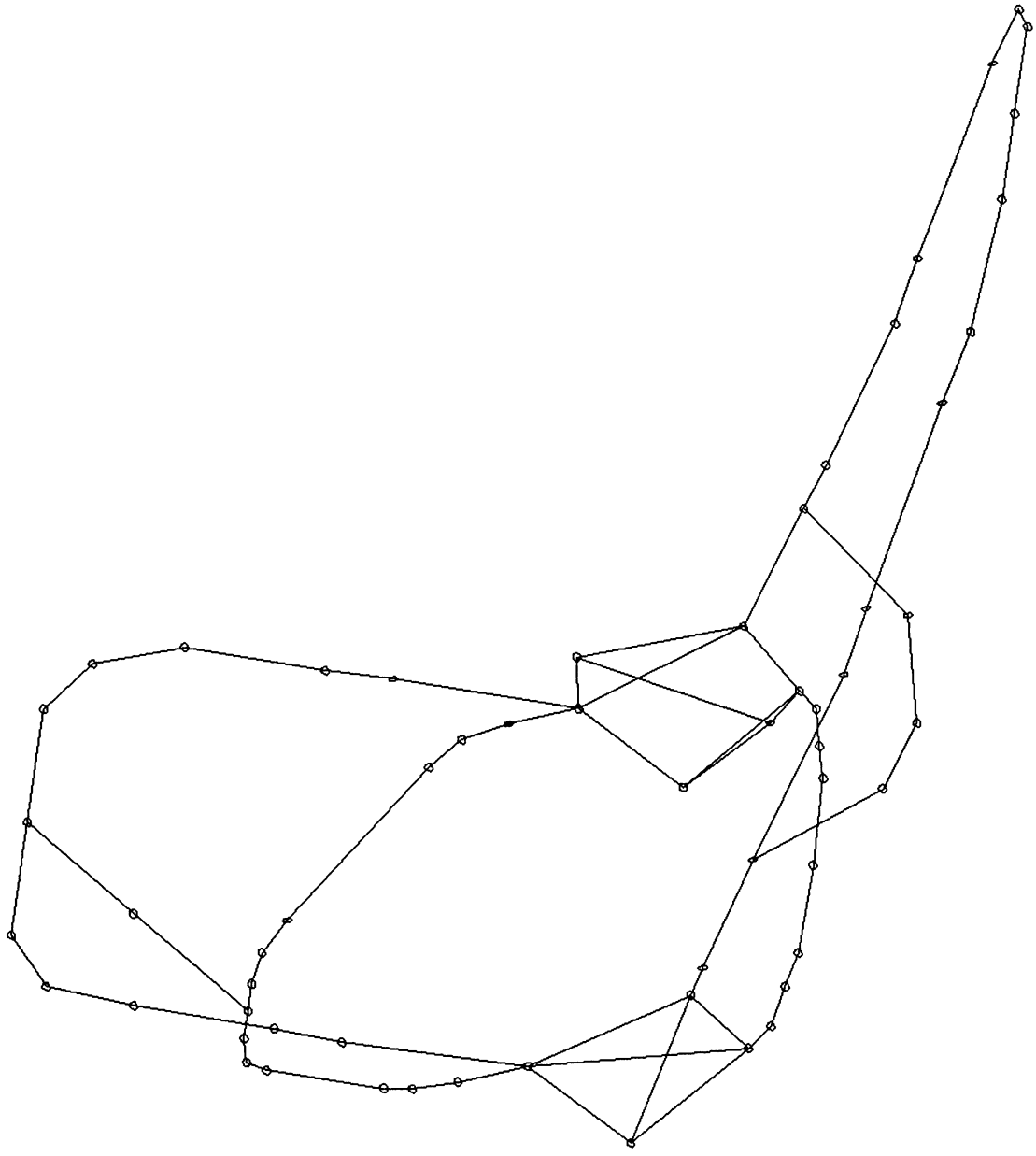

Fig. 6-17 Vehicle Seat Frone Structure Model

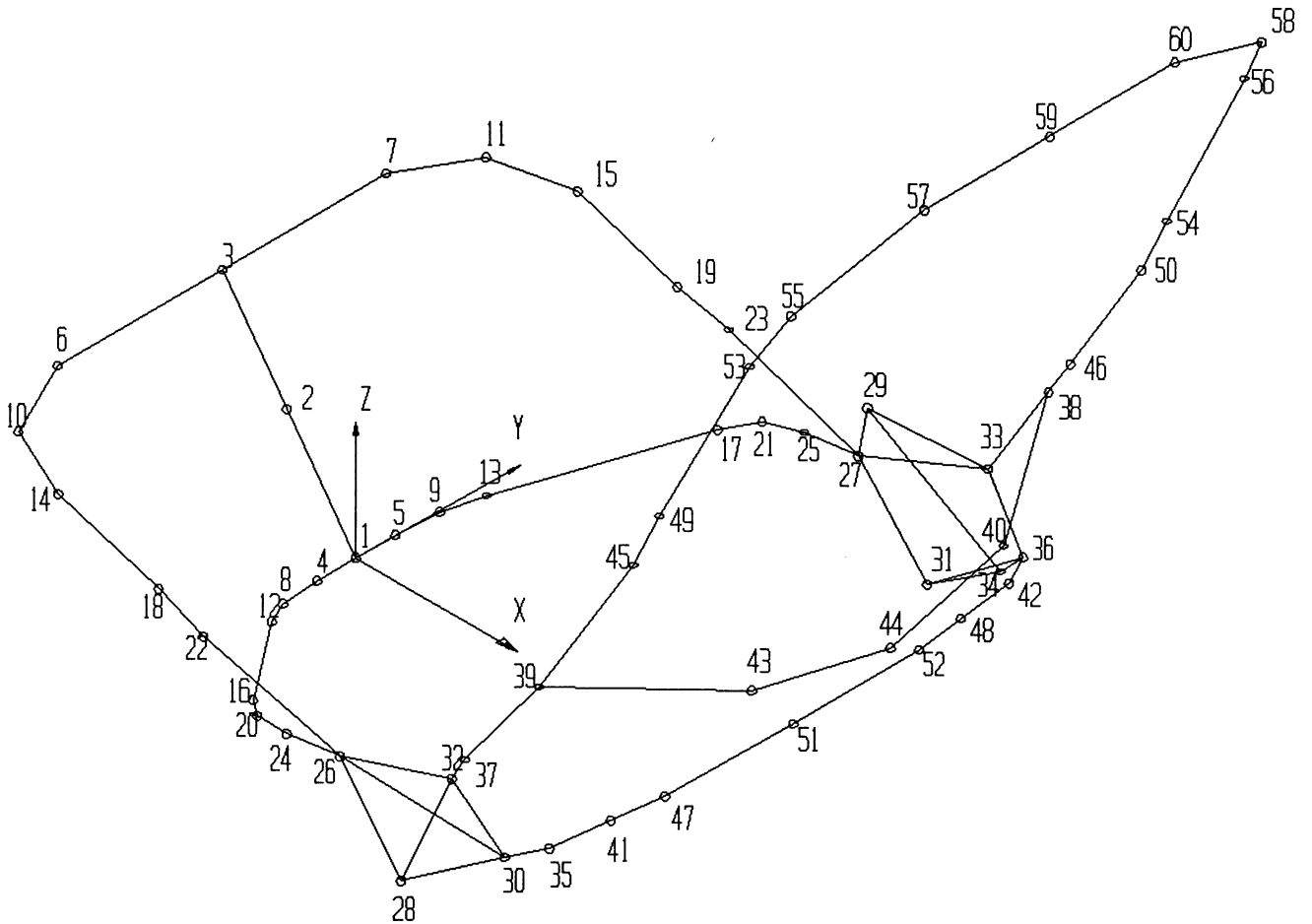

Fig.6-18(a) Finite Element Model of Car Seat Frame Showing Joint Numbering

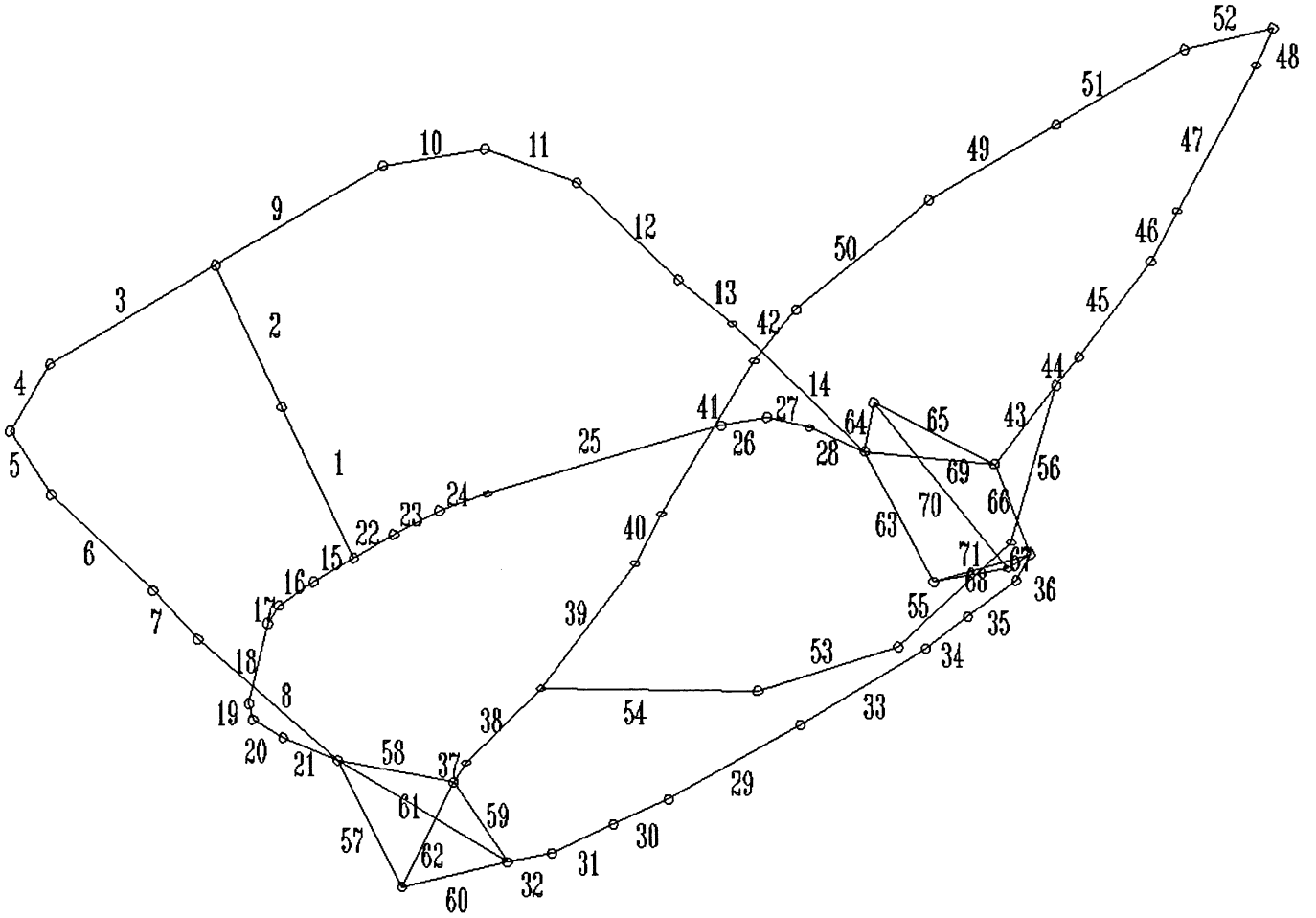

Fig.6-18(b) Finite Element Model of Car Seat Frame Showing Element Numbering

TABLE 6-17 The Geometry Coordinates of Nodal Points for the Car Seat Frame Structure
(Unit : Inch)

JOINT	X	Y	Z	JOINT	X	Y	Z
1	0.00	0.00	0.00	31	9.57	8.15	0.02
2	-2.17	0.00	2.90	32	11.70	-8.70	4.30
3	-4.17	0.00	5.63	33	11.70	7.90	4.30
4	0.00	-1.22	0.00	34	11.85	8.15	1.51
5	0.00	1.22	0.00	35	13.14	-7.12	2.36
6	-4.17	-5.08	5.63	36	12.68	8.03	2.36
7	-4.17	5.08	5.63	37	12.10	-8.70	5.00
8	0.16	-2.44	0.08	38	13.60	7.90	7.30
9	0.16	2.44	0.08	39	13.60	-7.90	7.30
10	-3.23	-7.24	5.43	40	16.20	3.90	6.50
11	-3.23	7.24	5.43	41	13.34	-5.43	2.36
12	0.73	-3.35	0.35	42	13.14	7.12	2.36
13	0.73	3.35	0.35	43	16.20	-3.90	6.50
14	-1.20	-8.03	5.16	44	16.60	0.00	5.90
15	-1.20	8.03	5.16	45	16.50	-7.90	12.00
16	4.00	-7.20	1.81	46	14.30	7.90	8.40
17	4.00	7.20	1.81	47	13.54	-3.94	2.36
18	1.90	-8.03	4.17	48	13.34	5.43	2.36
19	1.90	8.03	4.17	49	17.30	-7.90	13.70
20	4.76	-7.83	2.09	50	16.50	7.90	12.00
21	4.76	7.83	2.09	51	13.60	0.00	2.36
22	3.40	-8.15	3.70	52	13.54	3.94	2.36
23	3.40	8.15	3.70	53	19.90	-7.70	18.90
24	5.87	-8.03	2.26	54	17.30	7.90	13.70
25	5.87	8.03	2.26	55	20.80	-7.32	20.50
26	7.54	-8.03	2.48	56	19.90	7.70	18.90
27	7.54	8.03	2.48	57	21.50	-3.91	22.00
28	9.57	-8.15	0.24	58	20.80	7.32	20.50
29	7.70	8.15	3.78	59	21.50	0.00	22.00
30	12.68	-8.03	2.36	60	21.50	3.91	22.00

TABLE 6-18 Element Group and Connectivity Data for the Car Seat Frame Structure

MEMBER NO.	GROUP NO.	NEAR END	FAR END	MEMBER NO.	GROUP NO.	NEAR END	FAR END
1	1	1	2	2	1	2	3
3	2	3	6	4	2	6	10
5	2	10	14	6	2	14	18
7	2	18	22	8	2	22	26
9	2	3	7	10	2	7	11
11	2	11	15	12	2	15	19
13	2	19	23	14	2	23	27
15	3	1	4	16	3	4	8
17	3	8	12	18	3	12	16
19	3	16	20	20	3	20	24
21	3	24	26	22	3	1	5
23	3	5	9	24	3	9	13
25	3	13	17	26	3	17	21
27	3	21	25	28	3	25	27
29	4	51	47	30	4	47	41
31	4	41	35	32	4	35	30
33	4	51	52	34	4	52	48
35	4	48	42	36	4	42	36
37	5	32	37	38	5	37	39
39	5	39	45	40	5	45	49
41	5	49	53	42	5	53	55
43	5	33	38	44	5	38	46
45	5	46	50	46	5	50	54
47	5	54	56	48	5	56	58
49	6	59	57	50	6	57	55
51	6	59	60	52	6	60	58
53	7	44	43	54	7	43	39
55	7	44	40	56	7	40	38
57	8	28	26	58	8	26	32
59	8	32	30	60	8	30	28
61	8	26	30	62	8	32	28
63	8	31	27	64	8	27	29
65	8	29	33	66	8	33	36
67	8	36	34	68	8	34	31
69	8	27	33	70	8	29	34
71	8	36	31				

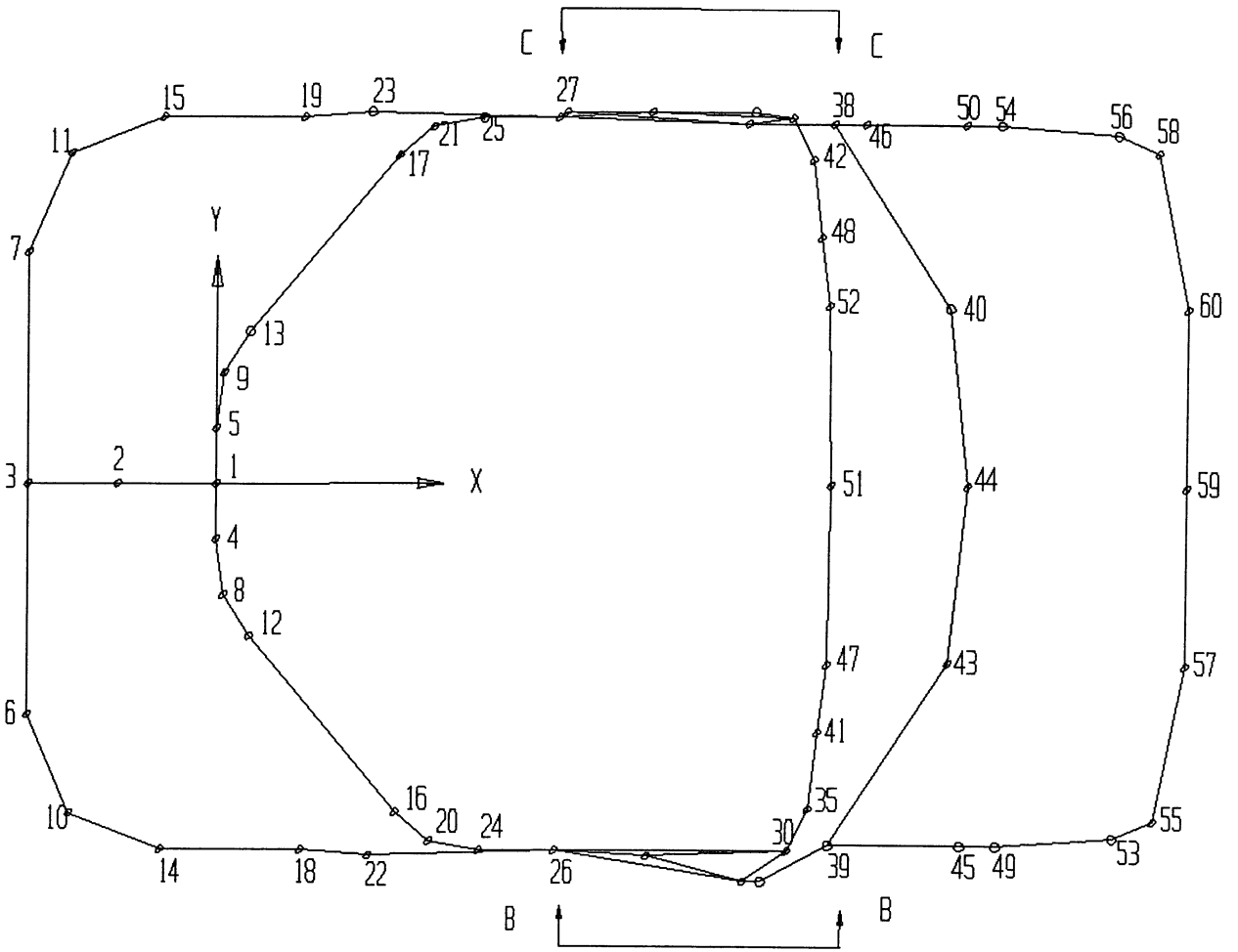

Fig.6-19(a) Top View of Car Seat Frame Structure

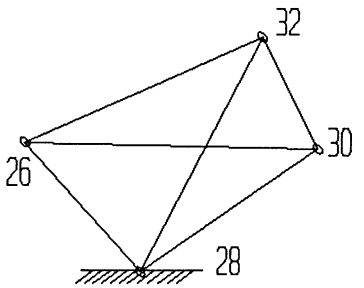

B-B Section

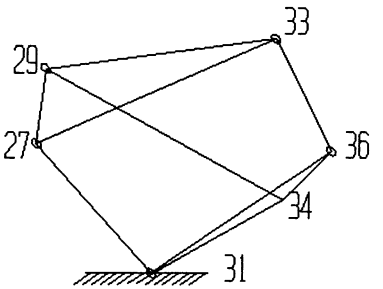

C-C Section

Fig.6-19(b) Section View of Sec. C-C and Sec. B-B

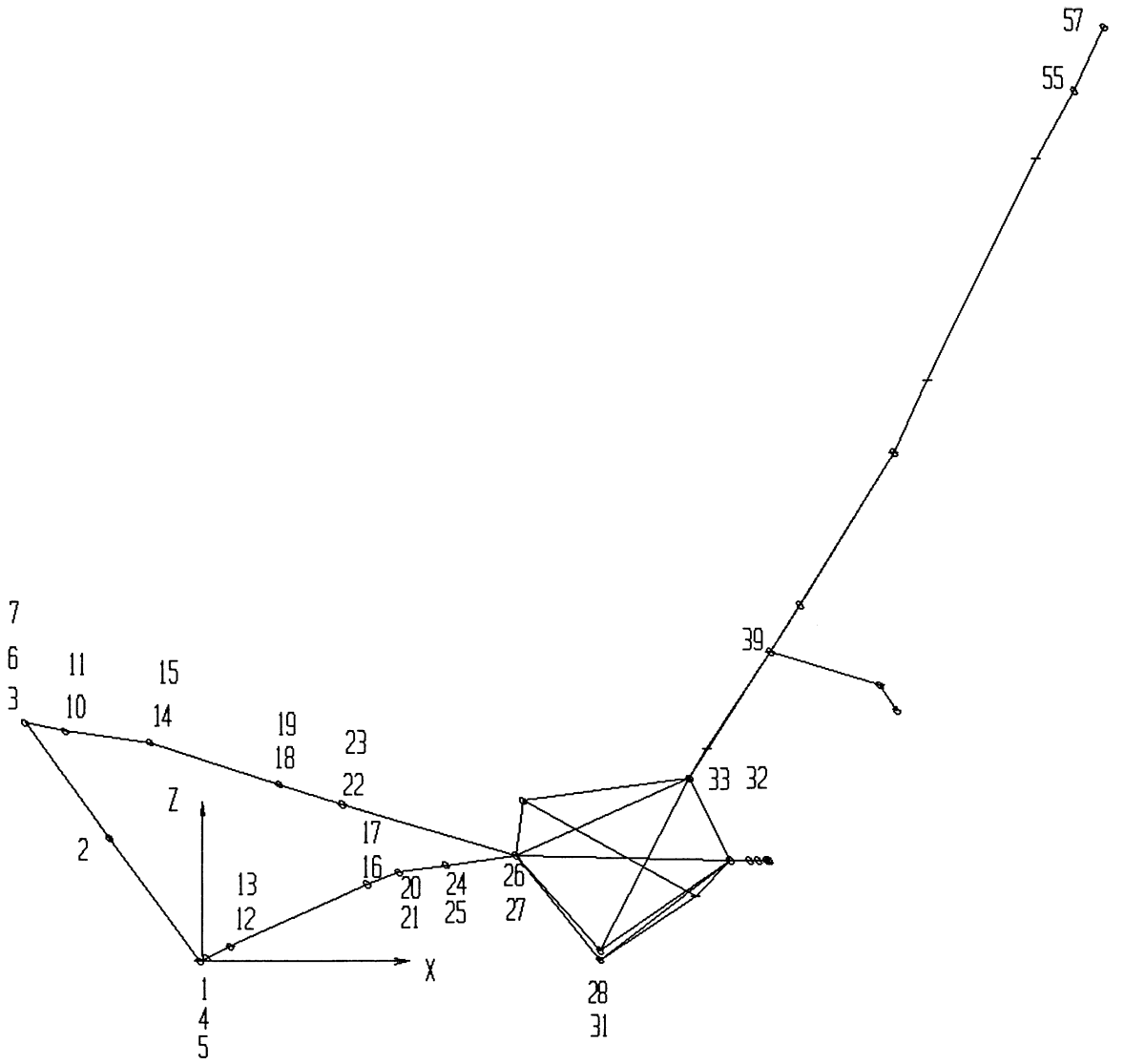

Fig. 6-20 Front View of Car Seat Frame

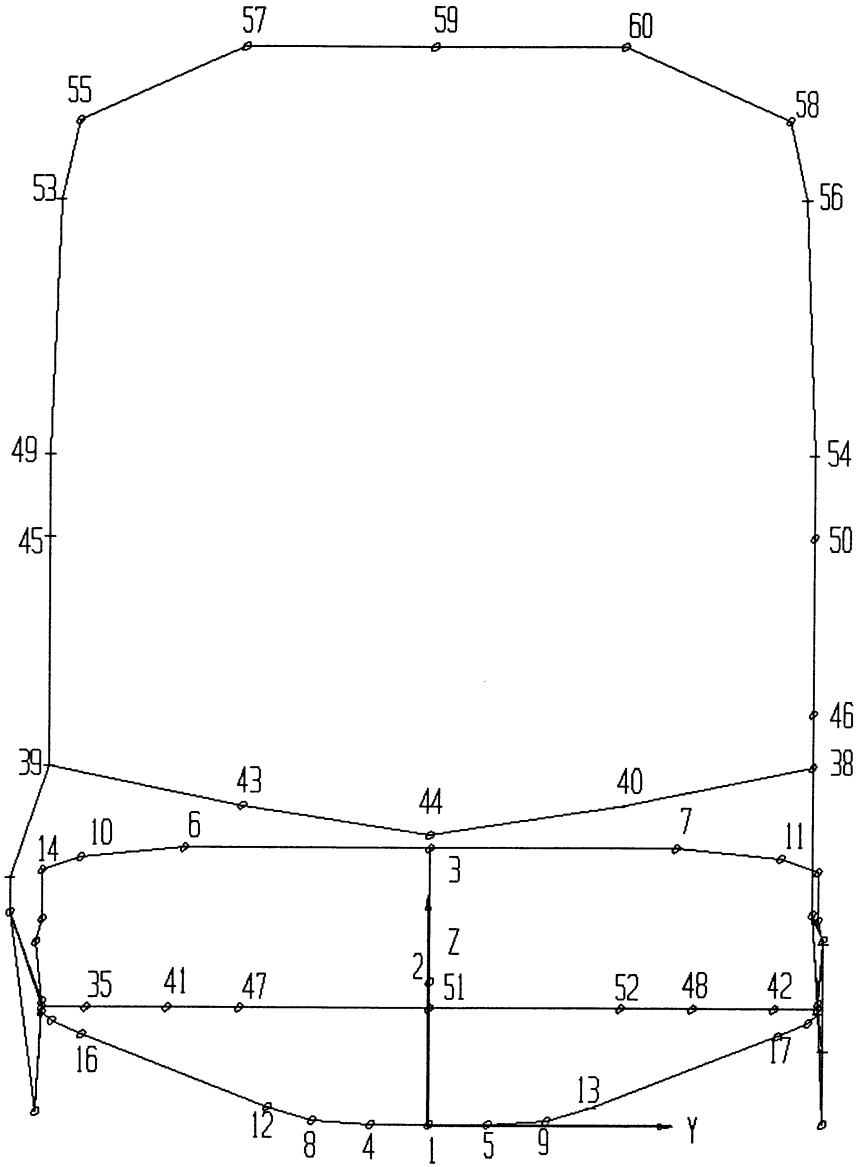

Fig.6-21 Right View of Car Seat Frame

group are required to have the same cross sectional area. The design parameters to be calculated include the mean diameter and thickness of circular cross sections and inner height, inner width, and wall thickness of the rectangular cross sections. The design variable assignment is shown in Table 6-19. The element grouping number and group cross section type are shown in Table 6-20. The element groups 1, 6, and 8 have hollow rectangular cross section, and the others have hollow circular cross sections. Design variable linking is used to impose the conditions of symmetry on the structure. A typical cross section is shown in Fig.(6-22).

The design data for the structure is given in Table 6-21. The working stress for each member is assumed to be approximately 60%(24.9ksi) of the yield stress(42ksi) of the

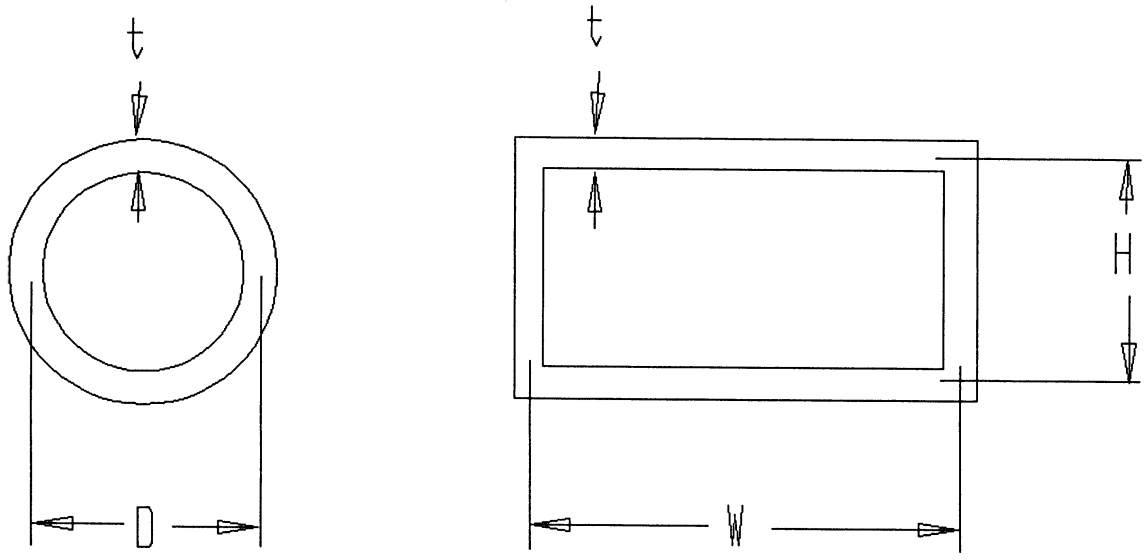

Fig. 6-22 Typical Cross Section and Design Variables

material used. The working stress corresponds to a safety factor of roughly 1.68. The loading cases for the structure are given in Table 6-22.

TABLE 6-19 Design Variables Assignment

Group Number	Mean Diameter	Inner Width	Inner Height	Thickness
1		X(1)	X(2)	X(3)
2	X(4)			X(5)
3	X(6)			X(7)
4	X(8)			X(9)
5	X(10)			X(11)
6		X(12)	X(13)	X(14)
7	X(15)			X(16)
8		X(17)	X(18)	X(19)

The objective function is taken as the total volume of the frame which is expressed as

$$F = \sum_{i=1}^{NG} \sum_{j=1}^{NM} A_{ij} L_{ij} \qquad (6\text{-}14)$$

Where NG = total number of groups

NM = total number of members in the ith group

L_{ij} = length of jth member in the ith group

A_{ij} = area of jth member in the ith group

Table 6-20 Element Groups of the Car Seat Frame Structure

Group Number	Cross Section Type	Element Number
1	Rectangular	1-2
2	Circular	3-14
3	Circular	15-28
4	Circular	29-36
5	Circular	37-48
6	Rectangular	49-52
7	Circular	53-56
8	Rectangular	57-71

The cross sectional area of the circular hollow section is

$$A = 3.14159 \times D \times t \qquad (6\text{-}15)$$

and the cross sectional area of the rectangular section is

$$A = 2 \times (H+W) \times t \qquad (6\text{-}16)$$

Where H = inner height

W = inner width

D = mean diameter

t = thickness

Table 6-21 Design Data of the Car Seat Frame Structure

Material	Steel
Modulus of Elasticity	3×10^7 ksi
Poisson's Ratio	0.30
Allowable Working Stress	24.9 ksi
Circular cross section	
Upper limit on diameter	2.00 in
Lower limit on diameter	0.174 in
Upper limit on thickness	0.25 in
Lower limit on thickness	0.047 in
Rectangular cross section	
Lower limit on width	0.125 in
Lower limit on height	0.125 in
Upper limit on thickness	0.25 in
Lower limit on thickness	0.047 in

Table 6-22 Loading Case Data for Car Seat Frame Structure (Unit: pound)

Loading Case	Node	Load Component in Direction		
		X	Y	Z
I	59	326.98	0	-138.7
II	3	138.9	0	-292.3
	6	154.45	0	-348.5
	10	154.45	0	-348.5
	14	154.45	0	-348.5
	18	76.68	0	-224.8
	22	62.95	0	-146.1
	7	154.45	0	-348.5
	11	154.45	0	-348.5
	15	154.45	0	-348.5
	19	76.68	0	-224.8
	23	62.95	0	-146.1
III	58	270.08	0	-135.0
IV	3	138.9	0	-292.3
	6	154.45	0	-348.5
	10	154.45	0	-348.5
	14	154.45	0	-348.5
	18	76.68	0	-224.8
	22	62.95	0	-146.1
	7	154.45	0	-348.5
	11	154.45	0	-348.5
	15	154.45	0	-348.5
	19	76.68	0	-224.8
	23	62.95	0	-146.1
	59	326.98	0	-138.7

In this car seat frame structure, the stress constraints are imposed at all the members. The twisting, bending, shear, and normal stress of rectangular and circular cross sections of the members are to be calculated in the stress analysis. The normal stresses due to plane bending and axial force, and shear stresses due to torsion and plane bending are computed independently and then combined to determine the total stresses. The maximum distortion energy failure criteria is applied in the design optimization process. The sampling points on the rectangular cross section and circular cross section are shown in Fig.(3-6).

Symmetric and nonsymmetric boundary conditions were considered in this example with different loading conditions. When the translations in the X, Y, and Z direction are fixed in both sides at node 28 and node 31, the structure is considered to have symmetric boundary conditions. If the translations and rotations in the X, Y, and Z direction are fixed at only one side at node 28, and translations and rotations are released at the other side at node 31, the structure is considered for nonsymmetric boundary conditions. The translations in the X, Y, and Z direction are fixed at node one for both sets of boundary conditions.

First of all, the study documents the car seat frame structure designed for different loading conditions with symmetric and nonsymmetric boundary conditions. Now, we

consider the symmetric boundary condition first. Initially, the volume of the structure is 311.546 in^3 with no stress violation. Table 6-23 also gives results for the three different loading cases for symmetric boundary conditions. The optimum volume with loading case one, three, and four is 58.7184 in^3, 35.1675 in^3, and 71.455 in^3 respectively. Next we consider the nonsymmetric condition. Table 6-24 gives results for the three different loading cases with a nonsymmetric boundary condition. The optimum volume with loading case one, three and four is 70.2865 in^3, 48.6 in^3, and 84.47 in^3 respectively. Comparing Table 6-23 and Table 6-24, the fact is shown that the nonsymmetric boundary condition is comparatively expensive in the design optimization process compared to the symmetric boundary condition.

Another study demonstrate the car seat frame structure designed to withstand multiple loading conditions. Under the loading cases one, two, and three, the initial volume is 297.46 in^3. After four design iterations, the constraints were completely satisfied. The final numerical result under multiple loading for the fixed geometry case is 108.66 in^3. It is shown the volume has increased over the single loading case. The iteration design history is shown in Fig.(6-23). As can be seen from the iteration history, the convergence is very fast and the algorithm possesses suitable convergence properties.

Next, we consider the car seat frame structure designed under variable geometry. It considers the structural design as more art than science. Based on the parametric cubic representation, the curve on nodes 7, 11, 15, 19 and 6, 10, 14, 18 are represented by Eq.(5-2). Now the design variables are the coordinate parameters and sizing variables. The initial and optimum data for this case study are shown in Table 6-26. It is shown the optimum volume under the geometric optimization is reduced about 16.9%. The final optimum value under multiple loading cases for variable geometry is 90.199 in^3.

The final study is for the car seat frame designed under topological change. The design is carried out by adding elements to decrease the volume under loading case four. There are 12 load points in the structure. The loading conditions are shown in Table 6-22. An initial design which has 60 nodes and 71 elements, has been optimized under 12 loadings. The result of the initial topology design is shown in Table 6-27. The initial optimal volume is 71.455in^3.

In order to maintain symmetry, element addition and element replacement are considered on both sides of the subset of the structure. The cross section of elements added is assumed to be circular. Also they maintain the same cross sectional area as the second group of elements. In case adding and/or replacing elements is needed, we have to consider adding(replacing) two elements each time. From the initial optimized results, the load point at node 6 has the

Table 6-23 Initial Data and Optimum Data Under Three Different Loading Cases at the Symmetric Boundary Condition

Design Variable	Starting Value	Optimum Value		
		Loading Case One	Loading Case Three	Loading Case Four
X(1)	3.7	3.6	1.1736	3.69864
X(2)	1.4	1.3	1.25	1.39865
X(3)	0.2	0.047	0.047	0.10673
X(4)	2.5	1.5503	1.18514	1.9574
X(5)	0.25	0.047	0.047	0.05998
X(6)	2.5	1.8166	1.03074	1.99636
X(7)	0.1	0.047	0.047	0.047
X(8)	1.8	1.61834	0.2975	1.79754
X(9)	0.14	0.047	0.047	0.047
X(10)	2.5	1.9824	1.6955	1.9969
X(11)	0.22	0.04785	0.047	0.047
X(12)	1.5	0.7944	0.3239	0.99857
X(13)	4.0	3.79439	2.2379	3.94854
X(14)	0.25	0.047	0.047	0.047
X(15)	2.4	1.87293	0.3709	1.9975
X(16)	0.09	0.047	0.047	0.047
X(17)	1.4	1.5	1.40	1.4022
X(18)	1.4	1.2101	0.4937	1.3969
X(19)	0.25	0.0487	0.047	0.05157
Volume	311.546	58.7184	35.1675	71.455

Table 6-24 Initial Data and Optimum Data Under Three Different Loading Cases at the Nonsymmetric Boundary Condition

Design Variable	Starting Value	Optimum Value		
		Loading Case One	Loading Case Three	Loading Case Four
X(1)	3.7	3.5825	0.6404	3.71136
X(2)	1.4	1.2825	0.61277	1.4114
X(3)	0.2	0.047	0.047	0.047
X(4)	2.5	1.3955	1.1581	2.0
X(5)	0.25	0.047	0.047	0.08147
X(6)	2.5	1.79145	0.8491	2.0
X(7)	0.1	0.047	0.047	0.047
X(8)	1.8	1.57705	1.11975	1.80735
X(9)	0.14	0.047	0.047	0.047
X(10)	2.5	2.0	1.96885	2.0
X(11)	0.22	0.06162	0.047	0.0586
X(12)	1.5	0.74985	0.99977	1.01211
X(13)	4.0	3.7498	0.94235	3.96214
X(14)	0.25	0.047	0.047	0.047
X(15)	2.4	1.8554	0.8985	2.0
X(16)	0.09	0.047	0.047	0.047
X(17)	1.4	1.5	1.5	1.49994
X(18)	1.4	1.37591	1.5	1.49994
X(19)	0.25	0.07812	0.06355	0.0776
Volume	311.546	70.2865	48.6	84.478

Table 6-25 Initial Data and Optimum Data under Multiple Loading Cases for Fixed Geometry

Design Variable	Starting Value	Optimum Value
X(1)	3.7	3.6983
X(2)	1.4	1.3983
X(3)	0.2	0.15643
X(4)	2.5	1.9856
X(5)	0.25	0.056048
X(6)	2.5	1.9932
X(7)	0.14	0.047
X(8)	1.8	1.79562
X(9)	0.14	0.0836933
X(10)	2.5	1.98424
X(11)	0.2	0.0767
X(12)	1.5	1.4953
X(13)	4.0	3.9953
X(14)	0.2	0.14671
X(15)	2.4	1.99696
X(16)	0.14	0.047
X(17)	1.4	1.38438
X(18)	1.4	1.38438
X(19)	0.2	0.075094
Volume	297.455	108.6639

Table 6-26 Initial Data and Optimum Data under Multiple Loading Cases for Variable Geometry

Design Variable	Starting Value	Optimum Value
X(1)	3.7	3.69803
X(2)	1.4	1.39803
X(3)	0.2	0.14941
X(4)	2.5	1.9836
X(5)	0.25	0.047
X(6)	2.5	1.99223
X(7)	0.14	0.047
X(8)	1.8	1.79497
X(9)	0.14	0.074629
X(10)	2.5	1.982
X(11)	0.2	0.05366
X(12)	1.5	1.4946
X(13)	4.0	3.99461
X(14)	0.2	0.13007
X(15)	2.4	1.99651
X(16)	0.14	0.047
X(17)	1.4	1.38223
X(18)	1.4	1.38223
X(19)	0.2	0.051449
New coordinate in X direction On node 6, 7		-4.07932
New coordinate in X direction On node 10, 11		-3.11909
New coordinate in X direction On node 14, 15		-1.0899
New coordinate in X direction On node 18, 19		1.58005
Volume	297.455	90.19943

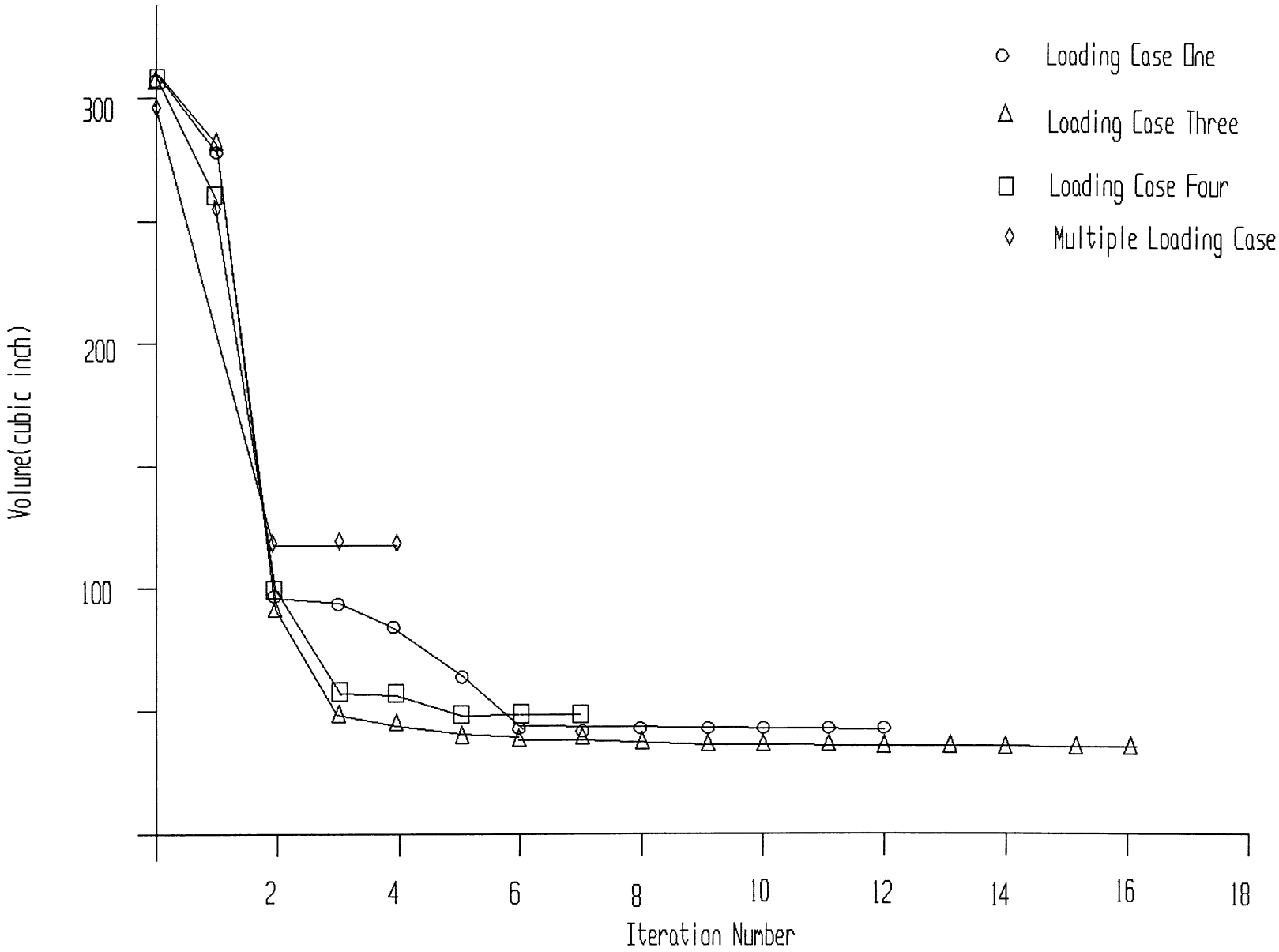

Fig.6-23 Iteration Design History of the Car Seat Frame Structure

maximum stress value. Therefore, we add two connectivities at node 6 and node 4, and node 7 and node 5.

In the first step, the subset of the structure which has 73 elements is to be optimized. The result of the first step is shown in Table 6-27. The optimum volume is 56.69in^3. This design is better than the initial design, so we continue to add the another two elements. In the second step, the subset of the structure which has 75 elements is to be optimized. The optimum volume in the second step is 65.128in^3. The result is not better than the previous design. Therefore, we replace another two elements instead of adding an element. In the third step, the subset of the structure which has 73 elements is to be optimized. The optimum volume of the third step is 57.97in^3. The results do not improve again, so the design is terminated. The sequence of beams added and the optimized volume at each step is given in Fig. 6-24. It is shown that the optimum volume under the topological optimization is more improved than the sizing optimization.

So far we have considered sizing and topological optimization in which no configuration step was included. However, the configuration optimization has a large influence on the structural design. Therefore, the following study on the car seat frame structure considers sizing, configurational, and topological change. Also we consider the structure with a nonsymmetrical boundary condition, i.e. the translations and rotations in the X, Y, and Z direction

at node 28 are fixed and translations and rotations at node 31 are released.

In the configuration of the car seat frame structure, node 1 and node 28 are the ground points and nodes 3, 26, 27 are the connecting points. The coordinates of joints 26 and 27 in the X and Z direction as well as the coordinate of joints 1, 3, 28 in the Y direction are allowed to change in the configuration optimization.

When the boundary condition are considered to be nonsymmetrical, the optimum volume for sizing change only is $84.478in^3$. The optimum volume for sizing and configurational change is $81.094in^3$. The result for the nonsymmetrical condition is shown in Table 6-28. It also indicates that configurational optimization generates more improvement than sizing optimization by about 4.0%.

In the topological design with the nonsymmetrical boundary condition, the initial volume which has 71 elements is $81.094in^3$. Then we want to add a element or elements to decrease the volume. For the element addition, the cross section dimension is circular. Also it has the same cross sectional dimensions as the second group of elements. Because it begins with a nonsymmetrical boundary condition, the added element can be considered one element at a time.

After the structure has been optimized under sizing and configurational change, node 5 at element 22 and node 3 at element 9 have the maximum stress value. The 72nd member is added to the subset of the structure and the design process

proceeds. For the first step, the optimum volume is 85.16 in^3. It is not better than the previous structure. Instead of adding an element, we replace another element (from node 5 to node 11) to add to the subset of the structure. The result of the subset of the structure is 78.75in^3. It is shown the design is improved. Then, we add one more element(from node 3 to node 18) to the structure.

In the third step, the subset of the structure which has 73 elements is to be optimized. However, the result is not better than the previous structure. Therefore, the design is terminated. The overall topological design process is shown in Table 6-29. It is shown that topological optimization for element addition under the sizing, configurational, and topological change can be improved.

Adding elements to decrease the volume with a heuristic search process have been attempted. It is shown that the search process is applicable for topology optimization. However, this heuristic search process cannot guarantee to obtain the global optimum. The topology of a structure can be optimized by this heuristic search method. A global search process could be developed by the application of artificial intelligence.

Table 6-27 Result of Topological Optimization Process Under the Symmetry Boundary Condition

Design Variable	Initial	First Step	Second Step	Third Step
X(1)	3.69864	4.0	3.5245	4.0
X(2)	1.39865	1.5	1.22465	1.5
X(3)	0.10673	0.047	0.047	0.047
X(4)	1.9574	1.67193	1.52502	1.6563
X(5)	0.05998	0.047	0.047	0.047
X(6)	1.99636	1.33659	1.8651	1.44168
X(7)	0.047	0.047	0.047	0.047
X(8)	1.79754	1.04661	1.5998	0.6388
X(9)	0.047	0.047	0.047	0.047
X(10)	1.9969	1.9866	1.9866	1.9866
X(11)	0.047	0.04744	0.04745	0.04741
X(12)	0.99857	1.0	0.8117	1.00
X(13)	3.94854	4.0	3.81187	4.0
X(14)	0.047	0.047	0.047	0.047
X(15)	1.9975	0.43151	1.82318	0.42335
X(16)	0.047	0.047	0.047	0.047
X(17)	1.4022	1.50	1.5	1.5
X(18)	1.3969	0.69784	1.25563	0.64425
X(19)	0.05157	0.05725	0.04851	0.05857
Volume	71.455	56.69	65.1284	57.97

Optimization Path	Topology	Volume
Initial Optimization	Initial	71.455
First Topological Optimization	Add Beams Element 72 (node 6 - node 4) Element 73 (node 7 - node 5)	56.69 (final topology)
Second Topological Optimization	Add Beams Element 72 (node 6 - node 4) Element 73 (node 7 - node 5) Element 74 (node 22 - node 12) Element 75 (node 23 - node 13)	65.1284
Third Topological Optimization	Replace Beams Element 72 (node 6 - node 8) Element 73 (node 7 - node 9)	57.97

Fig.6-24 Topological Change for the Car Seat Frame Structure

Table 6-28 Optimum Result Under Loading Case Four at the Nonsymmetry Boundary Condition

Design Variable	Sizing Change	Sizing & Configurational Change
X(1)	3.71136	3.74034
X(2)	1.4114	1.44047
X(3)	0.047	0.047
X(4)	2.00	2.0
X(5)	0.08147	0.076904
X(6)	2.0	2.0
X(7)	0.047	0.047
X(8)	1.80735	1.832
X(9)	0.047	0.047
X(10)	2.0	2.0
X(11)	0.058643	0.0574
X(12)	1.01211	1.04244
X(13)	3.96214	3.99252
X(14)	0.047	0.047
X(15)	2.0	2.0
X(16)	0.047	0.047
X(17)	1.49994	1.5
X(18)	1.49994	1.40272
X(19)	0.077592	0.07168
Y coordinate at node 3		-0.277652
X coordinate at node 26		6.80486
Z coordinate at node 26		2.16098
X coordinate at node 27		6.96767
Z coordinate at node 27		2.54845
Y coordinate at node 28		-8.00341
Y coordinate at node 1		0.675662
Volume	84.478	81.094

Table 6-29 Result of Topological Optimization Process Under the Nonsymmetry Boundary Condition

Design Variable	Initial	First Step	Second Step	Third Step
X(1)	3.77034	3.71558	3.78369	3.69881
X(2)	1.44047	1.41556	1.48268	1.39881
X(3)	0.047	0.05	0.047	0.156617
X(4)	2.0	1.99984	1.99974	1.98634
X(5)	0.076904	0.0750603	0.0728034	0.0493944
X(6)	2.0	1.99997	1.42066	1.99704
X(7)	0.047	0.047	0.047	0.047
X(8)	1.832	1.81425	1.47246	1.79812
X(9)	0.047	0.0478361	0.0478361	0.047426
X(10)	2.0	1.9998	1.9996	1.99797
X(11)	0.0574	0.059643	0.060206	0.0580206
X(12)	1.04244	1.01785	0.897015	0.998821
X(13)	3.99252	3.81284	3.69082	3.79382
X(14)	0.047	0.047	0.047	0.047
X(15)	2.0	1.9998	1.61733	1.99803
X(16)	0.047	0.047	0.047	0.047
X(17)	1.5	1.49992	1.49987	1.49986
X(18)	1.40272	1.42891	1.5	1.40084
X(19)	0.07168	0.074618	0.07227	0.0751006
Y coordinate at node 3	-0.277652	0.151154	0.34	-0.760185
coordinate at node 26	6.80486	7.32426	7.6108	7.39983
Z coordinate at node 26	2.16098	2.52321	2.69551	2.30011
X coordinate at node 27	6.96767	7.46305	7.66854	7.29968
Z coordinate at node 27	2.54845	2.94394	3.16944	2.60019
Y coordinate at node 28	-8.0034	-8.12678	-7.94588	-7.50011
Y coordinate at node 1	0.67566	-0.123123	0.306309	0.229946
Volume	81.094	85.16	78.75	88.64

6.4 References

[1]Bhatt, P., "Programming the Matrix Analysis of Skeletal Structures," Ellis Horwood Limited, 1986

[2]Haug, Edward J. and Jasbir S. Arora, "Applied Optimal Design", John Wiley & Sons, New York, 1979.

[3]Peterson, R. E., "Stress Concentration Design Factors", John Wiley & Sons, New York, 1953.

[4]Mill-curran, W. C., R. V. Lust, and L. A. Schmit, "Approximations Method for Space Frame Synthesis," AIAA Journal, Vol. 21, No.11, November 1983.

CHAPTER VII

SUMMARY AND FUTURE RESEARCH

7.1 Summary

In the previous chapters of this dissertation, the research which was undertaken, has been described in some detail. The conclusions which have been previously drawn will now be summarized.

A systematic approach to the sizing optimization, geometric optimization, and topological optimization in beam structures based on finite element analysis and mathematical programming has been developed. In addition, the strategies for enhancing the optimization algorithm and the method for implementing geometric and topological optimization have been presented. It is shown by numerical examples that this approach performs very well and the methodology is a powerful design tool in the area of structural optimization. Also it is verified in this research that the application of design optimization is not limited only to the area of the maximum structural behavior, but also in the greatest aesthetic interest and topology requirements.

The previous examples have indicated that the linear sequence of the explicit approximate method and design sensitivity methods provide an effective way to improve

optimization efficiency. Also the constraint deletion strategy, worst case design, and design variable linking further enhance the performance of the optimization algorithm.

In principle, the present approach can be extended to treat problems in other kinds of structures. This, of course, would require a more sophisticated main searching algorithm for topological design and consequently a more complicated computer program in order to retain the efficiency of the method. Basically, the method seems to be extremely promising in practical application.

7.2 Future Research

The first aspect of the future research could be in the incorporation of more requirements, such as fatigue life, fracture mechanics, and dynamic stability, into the optimization scheme. This involves translating these requirements into concise and coherent stress, displacement, buckling, and frequency constraints. In addition, it is worthwhile investigating the possibility of incorporating hypothetical damage models into the optimization. Specification of all these requirement sounds quite ominous, but the resulting benefits can more than compensate for the effort by producing reliable, efficient and safe structures.

The next aspect of future research could be in

implementing the structural optimization algorithm in a parallel computing environment. Matrix manipulation constitutes a major portion of computation time in structural optimization. Hence the parallel programming of matrix manipulation should yield an improvement in the computational speed. The computations in the structural optimization have inherent parallelism which can be exploited to achieve enhanced speed in computation.

The final aspect of future research could be in developing a method which is closely aligned with the automated structural design in the topological design with the application of artificial intelligence. The potential of effective learning algorithms for artificial intelligence[1] could handle the problem of manipulating system graphs in a sophisticated manner. In addition, graph theory[2] could be applied to structural topological design in actual practical application.

7.3 References

[1]Davis, Randall and Douglas B. Lenat, "Knowledge-based Systems in Artifical Intelligence," McGraw-Hill, Inc., 1982.

[2]Chachra, Vinod, Prabhakar M. Ghare and James M. Moore, "Applications of Graph Theory Algorithms," Elsevier North Holland, Inc., 1979

Vita

Hsiender Lee, the eldest son of Mr. and Mrs. Fu-Yuan Lee, was born [redacted] in Chia-I, Taiwan, Republic of China. After attending Tainan First Senior High School in Tainan, he received the following degrees: Bachelor of Engineering in Marine Engineering from Taiwan National College of Marine Science and Technology at Keelung, Taiwan, R.O.C.(1974); Master of Science in Mechanical Engineering from the University of Missouri at Columbia(1983); Doctor of Philosophy in Mechanical Engineering from the University of Missouri at Columbia(1988).

He was a second Lieutenant in the ROC army during the ROTC service from 1974 to 1976; employed by Air Asia Company as a Mechanical Engineer from 1976 to 1979; employed by Taiwan Power Company as a Mechanical Engineer from 1979 to 1981. Married to the former Sheng-Mei Liang, he has three children, Irene, Tiffany and Jonathan.

The undersigned, appointed by the Dean of the Graduate Faculty, have examined a dissertation entitled

SHAPE OPTIMIZATION FOR BEAM STRUCTURAL DESIGN

Presented by Hsiender Lee

a candidate for the degree of Doctor of Philosophy

and hereby certify that in their opinion it is worthy of acceptance.

Signatures redacted–
MU Libraries Digital Initiatives

[redacted]
Dr. Eric Sandgren, Supervisor

[redacted]
Dr. Paul W. Braisted

[redacted]
Dr. Roger C. Duffield

[redacted]
Dr. Uee Wan Cho

[redacted]
Dr. Mohamed E. M. El-Sayed

[redacted]
Dr. Harold J. Salane

University Libraries
University of Missouri

Digitization Information Page

Local identifier Lee1988

Source information

Format	Book
Content type	Text
Source ID	Gift copy from department; not added to MU collection.
Notes	

Capture information

Date captured	Apr 2024
Scanner manufacturer	Fujitsu
Scanner model	fi-7460
Scanning system software	ScandAll Pro v. 2.1.5 Premium
Optical resolution	600 dpi
Color settings	8 bit grayscale
File types	tiff
Notes	

Derivatives - Access copy

Compression	Tiff: LZW compression
Editing software	Adobe Photoshop
Resolution	600 dpi
Color	grayscale
File types	pdf created from tiffs
Notes	Images cropped, straightened, brightened